An investigation of the "Orange Peel" Phenomenon

A thesis submitted to Cardiff University

for the degree of Doctor of Philosophy by

Wan Ahmad Yusmawiza Wan Yusoff

Manufacturing Engineering Centre

Cardiff University

April 2007

UMI Number: U584935

UMI

Dissertation Publishing

ProQuest

Abstract

Selective Laser Sintering (SLS) or Laser Sintering (LS) allows functional parts to be produced in a wide range of powdered materials using a dedicated machine, and is thus gaining popularity within the field of rapid prototyping. Two current manufacturers of LS equipment and materials are EOS GmbH and 3D Systems. The PA2200 semi-crystalline polyamide powder studied here was developed by EOS and was processed using the 3D Systems Sinterstation 2500 HiQ LS machine. One of the advantages of employing LS is that the loose powder of the building chamber can be recycled. However, the properties of some recycled powders such as polyamide 12 (PA12) deteriorate by comparison to those of fresh powder. Fabricating parts using only new powder, although providing the best quality, is considerably more expensive than using recycled powder. On the other hand, using recycled powder creates the problem of the coarse, rough, and uneven surface texture. This thesis examines LS fabricated parts which are affected by the "orange peel" phenomenon due to the usage of recycled PA12 powder. This problem must be addressed before the technology can be widely accepted.

This thesis presents the problematic areas and proposes solutions to manage and utilise the recycled powder. Further, the thesis discusses experimental work on the deterioration or ageing of PA12 powder properties in the LS process, the microstructure of "orange peel" texture and the improvement of part surface finish to avoid the "orange peel" problem.

Acknowledgements

DECLARATION

This work has not previously been accepted in substance for any degree and is not concurrently being submitted in candidature for any other degree.

Signed:........................ (Wan Ahmad Yusmawiza)   Date :..07 April 07..
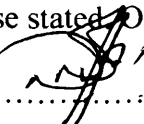
STATEMENT 1

This thesis is being submitted in partial fulfilment of the requirements for the degree of PhD.

Signed:........................ (Wan Ahmad Yusmawiza)   Date :..07 April 07..
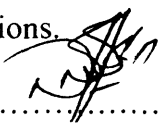
STATEMENT 2

This thesis is the result of my own independent work/investigation, except where otherwise stated. Other sources are acknowledged by explicit references.

Signed:........................ (Wan Ahmad Yusmawiza)   Date :..07 April 07..

STATEMENT 3

I hereby give consent for my thesis, if accepted, to be available for photocopying and for inter-library loan and for the title and summary to be available to outside organisations.

Signed:........................ (Wan Ahmad Yusmawiza)   Date :..07 April 07..

Contents

CHAPTER 1:

INTRODUCTION

CHAPTER 2:

THE TECHNOLOGY AND APPLICATIONS OF LASER SINTERING

CHAPTER 3:

EXPLANATIONS OF THE "ORANGE PEEL" PHENOMENON IN THE

LASER SINTERING PROCESS

CHAPTER 4:

DETERIORATION OF POLYAMIDE 12 POWDER PROPERTIES IN THE LASER SINTERING PROCESS

CHAPTER 5:

IMPROVEMENT OF THE PART SURFACE FINISHING IN LASER

SINTERING BY EXPERIMENTAL DESIGN OPTIMISATION

CHAPTER 6:

IMPROVEMENT OF POWDER MANAGEMENT AND RECYCLING IN

LASER SINTERING

CHAPTER 7:

CONCLUSION AND FURTHER WORK

LIST OF FIGURES

CHAPTER 4

CHAPTER 5

CHAPTER 5

CHAPTER 6

LIST OF SYMBOLS

Symbol	Description	SI Unit
A	constant specific to a molecules mobility	sec^{-1}
Dc	the degree of crystallinity	%
$M_{\bar{n}}$	the number average molecular weight	A.U
$M_{\bar{w}}$	the average molecular weight	g/mol
R	Boltzmann and gas constants	$\text{kJ mol}^{-1}\text{K}^{-1}$
T	the absolute temperature	Kelvin
T_b	part bed temperature	°C
T_c	crystalline temperature	°C
T_g	glass transition temperature	°C
T_m	melting point	°C
T_m^o	equilibrium melting point	°C
ΔE	the activation energy	kJ/mol
Δh_c	heat of fusion of purely crystalline material	J/g
Δh_f	heat of fusion of the test sample	J/g
ΔT	degree of super cooling	°C
η_0	the viscosity	Pa.s
r	spherulite radius	μm
t	cooling time	hours
v	growth rate	μm/hour
ED	energy density	J/mm^2

LP	laser powder	Watt
LSp	laser scan speed	mm/sec
MFR	melt flow rate	g/10min
P	laser power	Watt
SCSP	Scan spacing	mm

List of Abbreviations

ANOVA	Analysis of variance
CAD	Computer aided design
DOE	Design of experiment
DSC	Differential Scanning Calorimetric
DM	Direct manufacturing
DF ™	DuraForm™
EOS	Electro optical systems
GPC	Gel permeation chromatography
GF	Glass filled
IPCM	Integrated process chain management
LS	Laser Sintering
LF	LaserForm
MWD	Molecular weight distribution
PA12	Polyamide 12
DI	Polydispersity
PRM	Powder recycling method
Rv	Response variable

RM	Rapid manufacturing
RP	Rapid prototyping
RS	Rapid steel
SSt	Scanning strategy
SLS	Selective laser sintering

CHAPTER 1

INTRODUCTION

1.1 Background

In manufacturing, many products need to undergo increasing customisation, and a shortening of the manufacturing cycle time. This makes the time needed to produce prototypes one of the most important contributors to product development cycles. Because of the development and pre-production stages of rapid prototyping (*RP*), it is often necessary to have small batches of parts for testing and evaluation purposes. However, today's trend is for various companies, across different market sectors, to adopt RP, not only to produce test parts, prototypes and models but also to fabricate (non-mass production) functional parts. *RP* is also known as *solid-free form* or *layered manufacturing*. RP offers the user the ability to optimise part design in order to meet customer requirements with few manufacturing restrictions.

One of the most common RP processes is Laser Sintering (LS). A problem with LS is that sometimes the surface of the parts produced displays a texture similar to that of the skin of an orange (the so-called "orange peel" texture). This problem must be addressed before the technology can gain wider acceptance.

1.2 Aims and objectives

The aim of this research was to study the "orange peel" phenomenon related to RP material deterioration in LS. This problem can adversely affect the quality of prototypes and functional parts.

The objectives of the research were:

a) To conduct an investigation into the degree to which the properties of the LS material (Polyamide PA2200 powder) deteriorate, or 'age', during the LS process;

b) To study how the properties of the powder influence the surface finish of the fabricated part;

c) To develop a methodology of controlling the input material properties in order to provide consistency in quality;

d) To improve the surface quality of the fabricated parts by reducing or eliminating the "orange peel" texture through optimisation of the LS process parameters;

e) To introduce a recycled powder management practice.

1.3 Outline of the thesis

Chapter 2 reviews the technology and applications of Laser Sintering with emphasis given to describing the process parameters which influence the quality of the fabricated part. The chapter presents the common powder materials used in LS. Their applications and the related previous studies of the "orange peel" phenomenon are reviewed. The material utilised in this work is PA2200 (polyamide 12). The microstructures of parts fabricated in PA2200 and showing

the "orange peel" texture are examined and qualitative models for this problem are presented in chapter 3.

In chapter 4, the effects of LS process time and temperature which cause the loose powder to deteriorate are studied and the methods of measuring powder deterioration which affects the thermal properties and melt viscosity are presented. Melt Flow Rate (MFR) indexing, Differential Scanning Calorimetry, and Gel Permeation Chromatography approaches are discussed in chapters 3, 4, 5 and 6. Chapter 5 presents the application of fractional factorial design of experiments (DOE) to optimise the LS process. Recycled PA2200 powder with 18-19 MFR (twice-used material) was employed in the experiments. It was of interest to recycle powder in order to avoid wasting material.

Chapter 6 identifies the limitations of present powder management methods. To overcome those limitations, a new powder recycling method (PRM) is introduced. This involves classifying the quality of powders based on flow ability and experimentally determining optimal refresh rates.

Finally, chapter 7 presents the contributions of this research and its conclusions. This is followed by the identification of further work on this research topic.

CHAPTER 2

THE TECHNOLOGY AND APPLICATIONS OF LASER SINTERING

2.1 Preliminaries

There are many different RP technologies available today which differ in terms of speed, materials, and overall technique [Usher, 2000]. RP refers to the physical modelling of a design using a special class of machine technology which allows manufacturers to improve product quality and reduce both times to market and cost. Due to its tremendous impact on design and manufacturing, the global demand for RP technology has shown dramatic growth since it was introduced in 1988, as shown in Figure 2.1 [Pham et al., 1997; Gale, 1997; Dickens and Keane, 1998; Hopkinson, 2006].

One of the most effective and versatile RP techniques available is Selective Laser Sintering (SLS) or the Laser Sintering (LS) process. In this technology, an object is created layer by layer from heat-fusible solid fine powdered materials with heat generated from a CO_2 laser [Wholers, 1999; Naim, 2000; Wohlers, 2002]. It is capable of producing very complex part geometry directly from three-dimensional CAD software by a quick, highly automated and high-process, flexible manufacturing process. [Stacey, 1993; Kai, 1998; Pham et, al, 2000; King, 2003; Shi Y et. al., 2004]. It was originally developed by Carl Deckard at the University of Texas. It was then patented in 1989 and commercialised by DTM Corporation,

with support from B.F Goodrich. The first LS system was shipped in 1992, and there are currently several systems in use worldwide [Kai et al., 1997; Lauwers et al.,1998; Pham, 2000; Cooper, 2001, and Mazzoli et al., 2007].

RP systems have been sold worldwide. RP has gradually matured. As illustrated in Figure 2.2, this technology offers a unique, versatile process that can be used for a broad range of applications in different fields including the electronic, aerospace, and biomedical areas [Pham and Dimov., 2003; Salmoria et al., 2007; Mazzoli et al., 2007].

LS differs from conventional manufacturing processes in that it is an additive process which is able to produce a high degree of accuracy. In addition, no tooling, fixing, and reorientation is required during the process. In contrast, traditional machining methods involve removal of material from the final object geometry. [Pham et al., 1998; King, 2003; Mercelis and Kurth, 2006]. The advantages associated with this technique are as follows [Theodore, 1996; Effier, 1997; Potts, 1998; Usher et al., 2000; Steve and Richard, 2003]:

- a wide range of build materials, self-supporting build envelope and high output rate;

- high design flexibility and capability of producing complex shapes with internal features in a few days compared to conventional methods;

- the LS functional parts can be mechanically tested and fitted for application;

- time and cost-saving, especially for the manufacture of high-value parts.
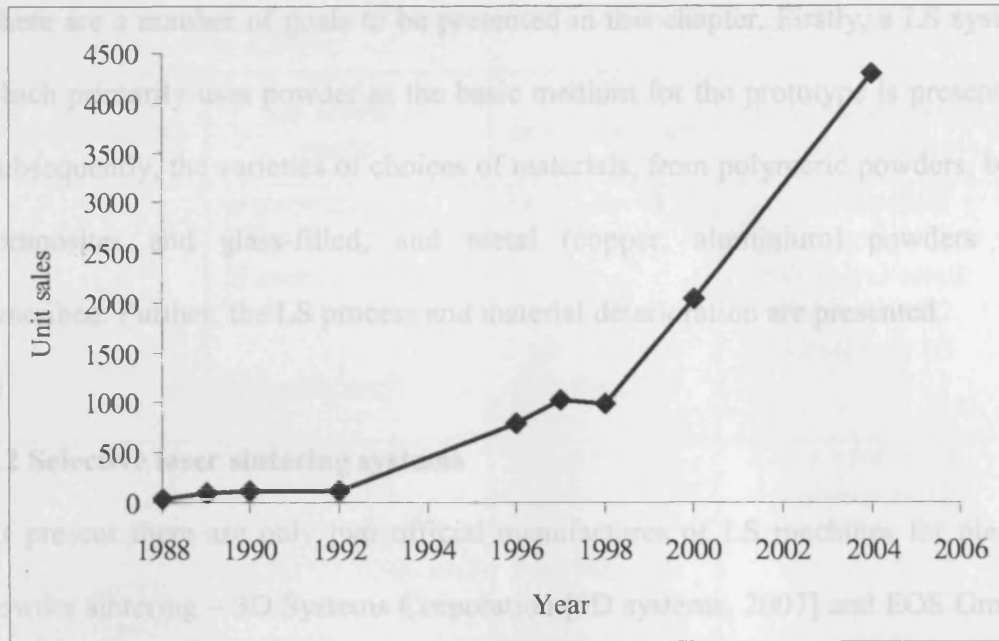
Figure 2.1 RP unit sales worldwide [Wholers, 2005]
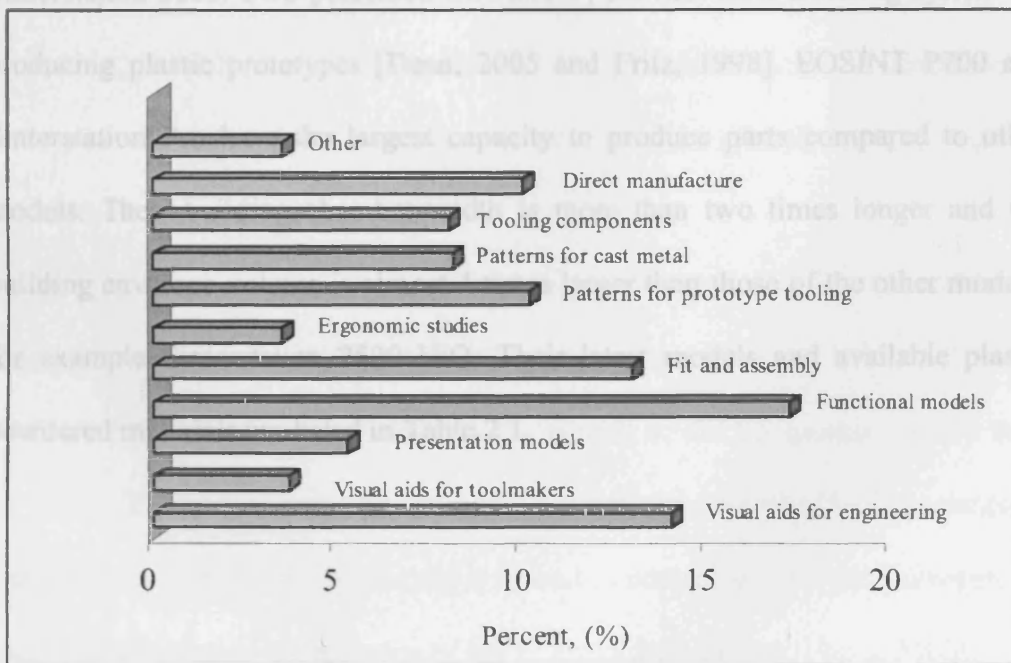
Figure 2.2 The use of RP systems in different applications [Wholers, 2005]

There are a number of goals to be presented in this chapter. Firstly, a LS system which primarily uses powder as the basic medium for the prototype is presented. Subsequently, the varieties of choices of materials, from polymeric powders, both composites and glass-filled, and metal (copper, aluminium) powders are described. Further, the LS process and material deterioration are presented.

2.2 Selective laser sintering systems

At present there are only two official manufactures of LS machines for plastic powder sintering – 3D Systems Corporation [3D systems, 2007] and EOS GmbH [EOS, 2007]. The current model of the 3D Systems Corporation is the Sinterstation 2500 HiQ, which has various improvements over its predecessor, the Sinterstation 2000. EOS presented EOSINT P, the first laser sintering system for producing plastic prototypes [Dean, 2005 and Fritz, 1998]. EOSINT P700 and Sinterstation Pro have the largest capacity to produce parts compared to other models. Their building chamber width is more than two times longer and the building envelope volume is almost 4 times larger than those of the other models, for example Sinterstation 2500 HiQ. Their latest models and available plastic powdered materials are listed in Table 2.1.

Table 2.1 Current LS machines manufacturers and available plastic powders

Manufacturers	LS machine models	Build envelope, mm	Plastic powdered materials
3D Systems Corp.	Sinterstation® HiQ (Sinterstation 2500 basic models) Sinterstation® Pro	381x330x457 550x550x460 550x550x750	DuraForm® Polyamide12, GF DuraForm® Polyamide 12, CastFrom PS
EOS Electro Optical Systems GmbH	FORMIGA P100 EOSINT P390 (EOSINT P360 and P380 basic models) EOSINT P730 (EOSINT P700 basic models)	200x250x330 340x340x620 700x380x580	PA2200 Fine Polyamide 12, PA3200 GF Polyamide 12, Aluminium filled Polyamide 12, Carbon fibre filled Polyamide 12, Flame retardant Polyamide 12

In general, the fabrication of a part using the LS machine can be described as having five main functional areas, as follows (Figure 2.3) [Neal, 1994; Mc Alea et al., 1995; Odonnchadha, et al., 2004]:

Computer system

CAD data files in STL file format are transferred to the LS machine where they are sliced. The computer system processes the data for control of build parameters and guidance of the laser. Moreover, it is used to control an inert gas (nitrogen) to prevent the oxidation or explosion of the fine powder particles [Pham, 2000].

Heaters

It heats the powder to a temperature just below the melting point of the material. The reason for this is to decrease the heat stress to the lowest degree and to prevent the fabrication part from warping. The temperature of the powder cartridge must be controlled to allow powder to be moved freely by the roller [Shi et al., 2004].

Roller mechanism

The roller spreads a very thin (between 100 μm to 125μm) layer across the part build cylinder [Pham et al., 1997 and Naim, 2002]. The roller transverse speed is an adjustable machine parameter. If the roller speed is set too slow, the processing time increases. Conversely, setting the roller speed relatively high may result in the powder being pushed in front of the roller [Naim, 2002].

CO_2 laser set

The mirrors cause the laser to scan specific areas of the powder corresponding to a slice thorough the object's design geometry. The interaction of the laser beam with the powder fuses the powder particles to produce the LS parts [Neal, 1994].

Build Cylinder

The part build cylinder lowers slightly and one of the feed cartridges rises. The sinter material forms the part while the unsintered powder remains in place to support the structure.

Powder supply cartridge

It supplies the powder to a part bed by a spreader roller for each build layer.
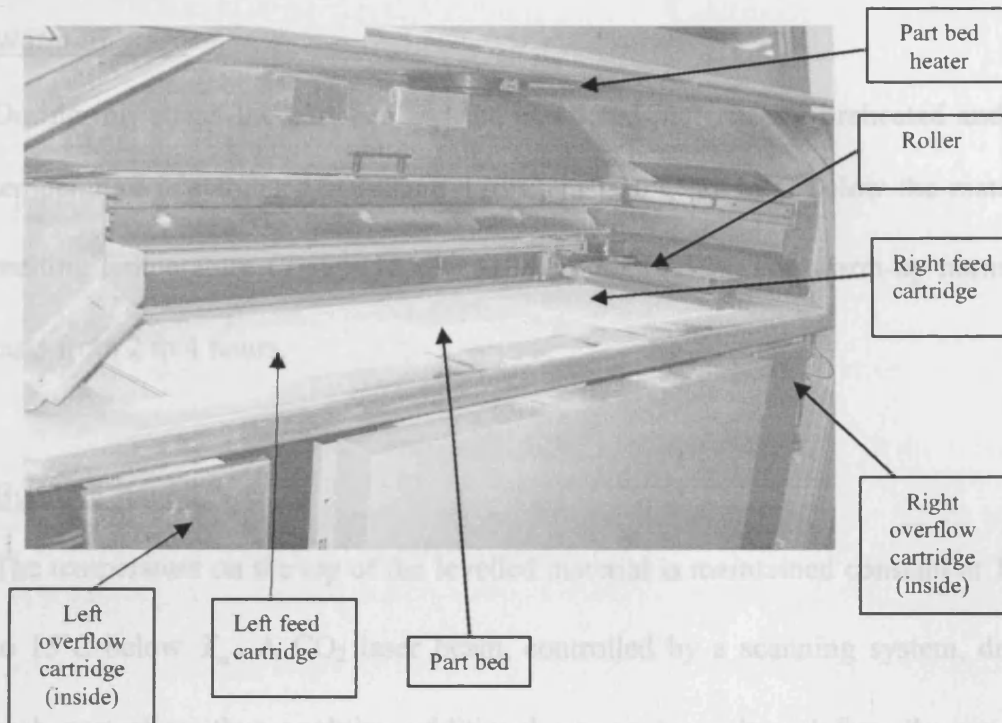
Figure 2.3 The major components parts of LS machine (Sinterstation 2500 HiQ)

In general, there are three processing stages common in the operation of any LS machine: warm-up, building (sintering), and cooling down.

Warm-up stage

During this stage, the part bed and the powdered material are preheated and the temperature is stabilised at around 170°C, just 10°C to 15°C below the material melting temperature (T_m) , (185 °C -188 °C for PA12). The warm-up normally lasts from 2 to 4 hours.

Building stage

The temperature on the top of the levelled material is maintained constant at 10°C to 15°C below T_m. A CO_2 laser beam, controlled by a scanning system, draws each part slice, thus applying additional energy to melt and fuse the powder particles into a layer. The build platform is then lowered and a new powder layer is spread on the top. These operations continue until the build is completed.

In addition, part cylinder heaters keep the temperature around the build at 130 °C to 150 °C in order to reduce the thermal gradient and prevent distortion.

In the Sinterstation 2500 HiQ design (Figure 2.8), the cylinder heaters maintain 130°C at approximately 200mm build height only. Once the piston is outside this area, the first half of a taller build starts to cool down while the other is still being processed. Thus, in full height builds, the un-sintered powder is not subjected to high temperature during the whole build time. If it were, the resulting shrinkage would disturb part accuracy. In contrast, in the EOSINT P700 models (Figure 2.9), the part cylinder heaters are integrated in the walls of the building chamber and maintain a temperature of 140°C throughout the whole build. This facilitates a

uniform temperature distribution and therefore uniform shrinkage but the un-

sintered material stays at higher temperature for much longer.

This stage could last from 10 hours to more than 100 hours depending on the LS

machine speed, build height, and volume of the parts in the build.

Cooling down stage

At the end of the process, the temperature in the build is very high, from 140°C to

180°C. The sintered parts can be removed only after their temperature falls below

that of material glass transition, 45°C - 60°C, otherwise they could warp or

deform. This could take from 10 hours (small builds) to more than 30-40 hours

(long builds) and therefore the un-sintered material is ageing further during this

stage. Generally, the larger the building volume, the longer is the cooling down

time.

In both technologies, the un-sintered PA12 powder in the build is subjected to

temperature close to T_m for a long period of time which affects significantly the

material properties and usability. It needs to be refreshed with a sufficient amount

of new powder in order to produce parts of good quality.

2.2.1 Sinterstation 2500 HiQ (3D Systems Corp)

The whole process of powder preparation and loading into the LS machine is manual. The recycled and new powders are measured and mixed with a mixer in a specified proportion (Figure 2.4). A rotating drum cement mixer is normally used for material blending.

"Recycled powder" "New powder" Mixer Blending LS Machines (Sinterstation 2500HiQ)
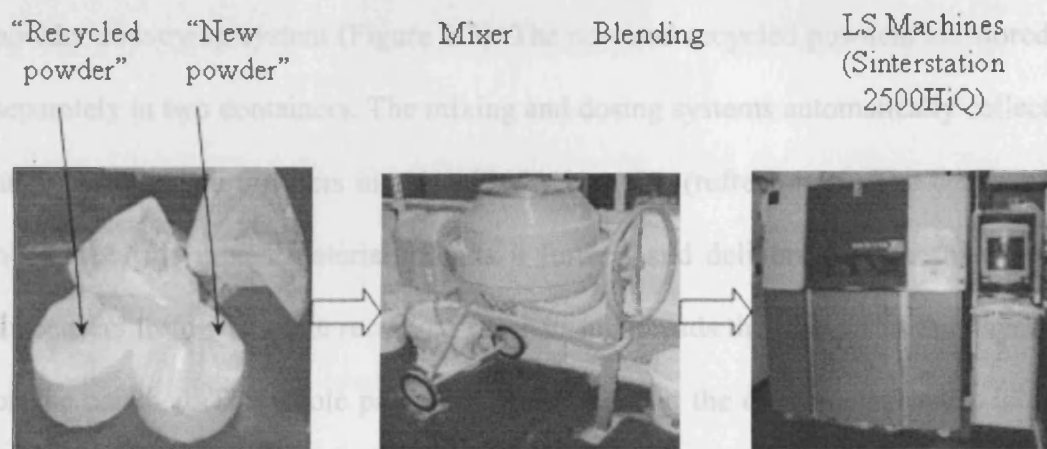
Figure 2.4 Powder management Sinterstation 2500HiQ (3D Systems)

The proportions recommended by the manufacturer are one part new material, one part recycled material from the part bed and one part recycled material from the overflow cartridges. The recycled material from the part bed is exposed to 170°C – 175°C temperature during the build. The powder from the overflow cartridges is less damaged by the heat because it is subjected to a lower temperature, typically 80°-90°C. These three types of powder are thoroughly blended for a period of time (normally 15-30 minutes) and then loaded into the LS machine. The disadvantage of this approach is that it is a manual process, with slow and messy preparation, and loading of the powders, dependent on operator's skills. The only advantage is

a better control of the quality of the powder loaded into the LS machine because each powder portion is prepared individually for each build.

2.2.2 EOSINT P700 (EOS GmbH)

For better productivity and powder recycling, the EOSINT P700 LS machine is equipped with an integrated process chain management (IPCM) system. This system consists of two containers, a mixing and dosing system, and automated powder conveying system (Figure 2.5). The new and recycled powders are stored separately in two containers. The mixing and dosing systems automatically collect and blend the two powders in a specified proportion (refresh rate). The conveyor hose takes the mixed material, blends it further, and delivers it to the machine dispensers from where the recoating mechanism spreads the powder in thin layers on the part bed. The whole process is automatic and the only manual work is to collect the recycled powder into bags, and keep the containers fully filled with powder. The advantage of the IPCM system is that dosing, blending, and loading of the powder are automated, fast, and less dependent on the operator's skills. However, it is impossible to control and achieve a consistent powder quality in the recycled powder container. It normally contains layers of powder collected from different builds and therefore having different grades. In order to compensate for the variation of the properties of the used powder and achieve good quality for the produced parts, the refresh rate should be kept high (Table 6.2).

"Recycled powder"   "New powder"   "Recycled powder" container   "New powder" container   Blending   LS Machines (EOSINT P700)
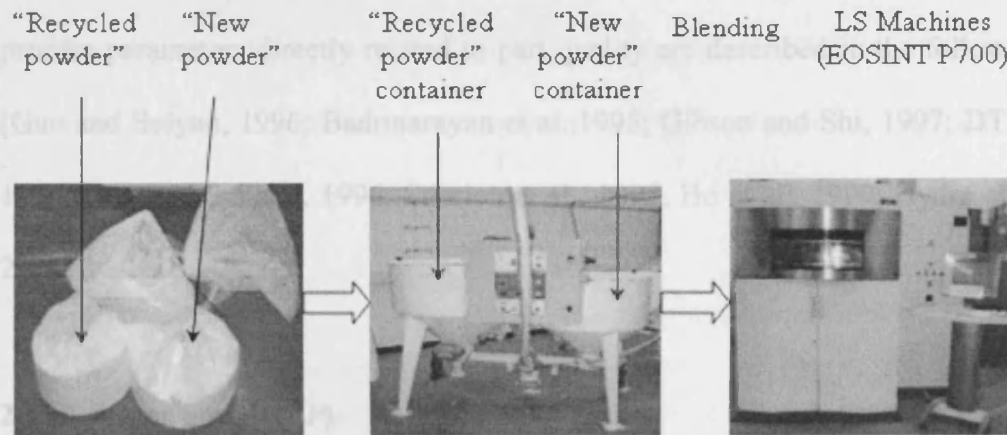
Figure 2.5 integrated powder management system and the EOSINT P700 LS machine (EOS GmbH).

2.3 Laser sintering (LS) process parameters

The quality of sintered parts produced by the LS process is highly influenced by its process parameters. These are the variables that influence and control the LS process, which directly affect the quality of the part fabricated, such as geometric problems and physical properties. The issues of LS parts' qualities have been studied by some researchers [DTMa, 1996; Kochan, 1999; Ho and Cheung, 2000; Naim , 2002; Salmoria et al., 2007]. The common problems related to fabricated LS parts are as follows:

- Growth and bonus Z

- Warp and curl

- Shrinkage

To produce a high LS part quality, the process parameters are set differently according to powder properties and the requirements of application. For this reason, the LS manufactures such as DTM and EOS have specified the default

values for all process parameters based on the material used in the process. Some process parameters directly related to part quality are described in the following: [Guo and Suiyan, 1996; Badrinarayan et al.,1995; Gibson and Shi, 1997; DTMa, 1996; Gou and Suiyan , 1996; Stierlen et al., 1997, Ho et al., 1999; Hydro et al., 2004].

2.3.1 Laser power (*LP*)

LP refers to the amount of energy applied by the CO_2 laser beam. Normally, relatively low *LP* is used to scan the powder because the T_b is close to the material melting temperature. Too high *LP* causes part growth and "bonus z" and too low laser power may cause delamination.

2.3.2 Laser scan speed (*LSp*)

LSp is the speed of the laser beam movement. A correct combination of *LSp* and other process parameters, such as *SCSP* and *LP*, gives better powder fusion due to low melt viscosity and better flow. As a result, low part porosity, good surface finish, high part density, and good mechanical performance can be achieved.

These factors are not independent of each other. It is common knowledge that the factors have interactions. Interaction means a situation in which the effect that a factor has on the response may depend on the levels of some of the other factors.

2.3.3 Scan spacing (*SCSP*)

SCSP is the distance between two nearest overlapping parallel scan vectors, as shown in Figure 2.6. The parts are fragile if the *SCSP* value is too high and part surface may be rough if the *SCSP* is too low.
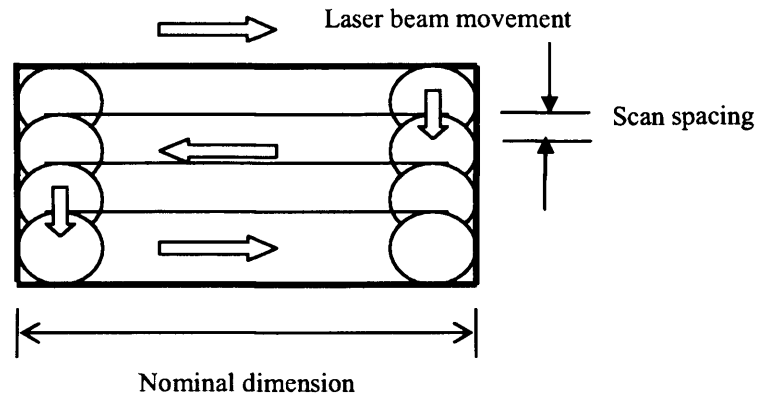
Figure 2.6 The laser beam movement in the LS process

2.3.4 Part bed temperature (T_b)

T_b refers to the powder temperature at the top of the build cylinder during the LS process. Normally, this temperature is 10°C to 15°C below the PA12 material melting point.

2.3.5 Scanning strategy (*SSt*)

In the LS process, the user can select the scanning strategy, which could be a "fill" only or a "fill" and "outline" one. In the most recently developed strategy, the laser beam does not only scan the entire cross section but also outlines its contour as shown in Figure 2.7.
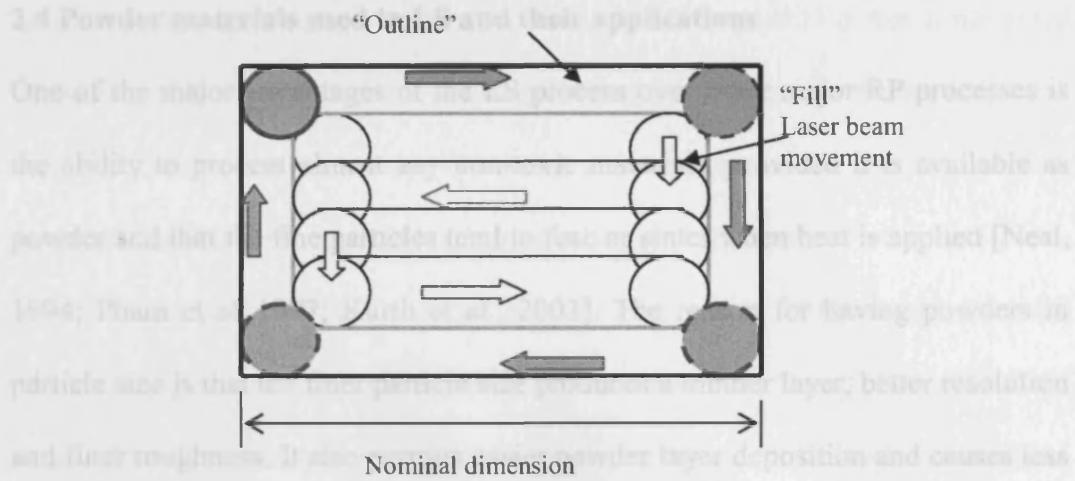
Figure 2.7 Laser scanning strategies

2.3.6 The influence of energy density (*ED*) on the LS fabricated part

In order to produce good functional LS parts, it is important that the powder on the part bed surface receives a sufficient amount of power energy through the laser sintering process. The reason is that sufficient energy density is produced when the energy input increases and is applied to the part bed surface, which causes a higher temperature, and thus better melt flow. However, too high an energy density causes hard part cake, difficulty in taking parts out of the build, roughness, and a light brown colour part surface due to overheating. The energy density is calculated by using the following equation [Badrinarayan, 1995; Gibson and Shi., 1997; Ho et al., 1999; Ho et al, 2000].

$$\text{Energy density (J/mm}^2) = \frac{P}{LS * SCSP}$$

Where *P* is a laser power, *LS*-laser speed, and *SCSP* - scan spacing.

2.4 Powder materials used in LS and their applications

One of the major advantages of the LS process over other major RP processes is the ability to process almost any non-toxic materials, provided it is available as powder and that the fine particles tend to fuse or sinter when heat is applied [Neal, 1994; Pham et al.,1997; Kurth et al., 2003]. The reason for having powders in particle size is that the finer particle size produces a thinner layer, better resolution and finer roughness. It also permits easier powder layer deposition and causes less shrinkage during the laser sintering process [Kurth et al., 2003]. To fulfil the demands of different applications, more materials with a wide spectrum of properties have been developed. Some of the materials available for the LS process are as follows [Kimble, 1992; Kai et al., 1997; Pham et al., 2000; Cooper, 2001; Kurth et al, 2003; EOS, 2007]:

2.4.7.1 Polyamide PA2200 (Nylon 12)

Polymer powders were the first, and are still the most widely employed, materials in LS [Kurth et al., 2003 and Wahab, 2006]. The use of polymeric materials in the LS process offers some advantages which are related to the low processing temperatures, melting flow control and ease of production [Salmoria et al.,2007].Currently, polyamide materials such as PA2200 of EOS and Duraform of DTM are the most common materials used in the LS process [Fritz, 1998; Shi et al., 2004; Mazzoli et al., 2007]. They are employed to produce prototypes and functional parts, and especially suitable for the part which has fine feature detail design and which is required to be durable, with good heat and chemical resistance properties [Forderhase et al.,1993; Kai, 1997; Shi.et al., 2004; Odonnchadha et al., 2004]

The advantage of using PA semi-crystalline as an LS material is that it has good physical properties with a high melting temperature due to the strong hydrogen bonding. Due to the LS process involving a thermal stage, the part produced is associated with shrinkage and wraps [Naim, 2002]. Typically for the semi-crystalline polymers, shrinkage is 3-4 per cent [Pham et al., 2000 and Kurth et al., 2003]. An alternative to PA2200 is PA2210FR and PrimePart. PA2210FR. This is suitable for parts which require flame resistance with high mechanical properties. It contains a chemical flame retardant and a carbonating coating develops at the surface of the part in case of fire [Metalworking production, 2006; Desktop Engineering, 2006 and EOS, 2007]. PrimePart is new fine polyamide powder which is suitable for the rapid and cost-effective manufacture of functional prototypes and end products. It offers a balanced relationship between mechanical strength and elasticity over a wide temperature range [EOS, 2007].

2.4.7.2 Glass-filled Polyamide 3200 (Nylon 12)

The GF3200PA of EOS and LNC 7000 of 3D Systems are two types of nylon composite commonly used in the LS process. However, the crystalline nature of PA affects the properties significantly and highly crystalline types can be stiff and hard [Walter et al., 2006]. The use of glass fibre and other reinforcements can improve the mechanical properties (modulus and strength). The weight fraction glass reinforcement in the nylon composite is 0.50 [Mc.Alea et. al., 1995]. This provides increased strength and dimensional stability as well as cutting down expansion due to water absorption by about 0.3% compare to nylon 0.41%. Compared to nylon it offers greater rigidity; higher stability; increased stiffness;

and good heat resistance; which makes it a perfect material for extreme testing conditions [Michael, 1998 and Mazzoli, 2007].

2.4.7.3 Aluminium-filled Polyamide (Alumide™)

This is a new LS powder which is made of aluminium-filled polyamide by EOS GmbH in 2005. The Alumide™ parts have an excellent accuracy, high temperature resistance, and are extremely rigid, with a shiny metallic appearance that means it is a favourite among motor sport teams [Mazzoli, 2007]. In addition, it produces a superior surface finish for many functional prototypes such as manifolds, thermoforming moulds, tooling and aerodynamic wind tunnel test models [Materialise, 2006]. The surface of parts made of Alumide can be finished by grinding, polishing, or coating. This provides an alternative to the conventional materials such as polyamide, glass-filled polyamide, or polystyrene [EOS, 2007].

2.4.7.4 Composites /Cooper Polyamide (Cooper PA)

Copper polyamide (Cooper PA) is a metal-plastic composite which was put on the market in 1998 by DTM [DTM, 1998d.] It is a metal - plastic composite used for tooling plastic injection moulding. It consists of nylon (polyamide base filled with copper powder [Pham, 2000 and Dimov, 2001]. It can be built into mould tool inserts in the LS machine in the same way as other PA materials (e.g. PA2200 and DF™). It is suitable for injection moulded inserts when need to mould 100-400 parts in polyethylene, polypropylene, polystyrene, ABS and other common plastics [King, 2002]. The advantage is that inserts from copper PA are easy to machine and finish. Their heat resistance and thermal conductivity are better compared to the most common plastic tooling materials [DTM, 1998c;

DTM,1998d; Levy and Schindel, 2002]. The cycle times of moulds using Copper

PA inserts are similar to those for metal tooling [Pham, 2000 and King, 2002].

2.4.7.5 CarbonMide®-Carbon Fibre-filled Polyamide

The part built of CarbonMide® has outstanding mechanical properties

characterised by extreme stiffness and strength. It is suitable for the production of

fully functional prototypes with high end finish for wind tunnel tests or other

aerodynamic applications [EOS, 2007].

2.4.7.6 Prime Cast 101 (Polystyrene)/ Castform

This material is used to make complex investment casting patterns because of its

low ash content (<0.02%) and compatibility with standard foundry practice.

Patterns made with Castform material are low density (45% dense), and can be

infiltrated with foundry wax to create a pattern that is easy to handle [Pham et

al.,2000; Pham et al., 2001; Dochev and Soe, 2006]. Moreover, it is ideal for

making patterns for casting reactive metal such as titanium, and it has also been

used successfully with low-melt temperature metals such as aluminium,

magnesium, and zinc [Pham et al.,2000].

2.4.7.7 Alloy mixtures / LaserForm™ (LF™)

This is a stainless steel-based powder which is employed in the production of

durable metal prototypes, parts and as a tooling application, for mould inserts or

discrete parts. According to 3D systems, parts produced from LF™ enjoy cycle

times faster almost 20% to 40% than most tool steels due to its high thermal

conductivity. In addition, the parts are easily finished and polished. This means

that complex designs can be rapidly fabricated. Another advantage is that the parts are durable as concerns casting temperature, welding, or highly corrosive environments [Das and Bourell, 1998, Ghany, 2006; 3D systems, 2007].

2.4.7.8 Steel

This was the first steel powder-based material, introduced by EOS GmbH in 1995, to offer a low melting point. It has been employed for producing complex inserts for plastic injection. Since then, a new generation of steel and metal powders have been introduced, such as the well-known DirectSteelTM 50-V1 and DirectMetalTM 50-V2, which allow inserts with layer thickness of 50 μm to be built, facilitating reproduction of intricate structural detail. The latest generation of metal powder-base is DirectMetal™, which has a maximum particle size of 100μm and is employed to produce at higher building speeds [Fritz, 1998; Pham, 2000; Dewidar and Dalgarno, 2001].

Rapid Steel 1.0 (RS1) and Rapid Steel 2.0 (RS2)

The starting material for Rapid Steel 1.0 (RS1) is a ferrous alloy with low carbon content and a particle size of 55 μm which is coated with 1% weight polymer [Pham, 1999 and DTMb, 1999]. It is used to produce inserts for pre-production and production tools. It was made commercially available in 1998 by DTM after modifications over RS1. It is used in creating metal core-and cavity inserts for injection moulding and die-casting tools. The average particle size of 34μm and a smaller layer thickness of 75 μm lead to smoother surfaces by a reduction of stair-stepping effects and a shortening of the time required for finishing. RS2 has higher accuracy than RP1, which is closer to the ±0.1 mm, and it is usually required for production injection moulding tools [Lacan, 2000].

2.4.7.9 Green sand (SandForm™)

SandForm™ Zr & Si is used to fabricate pre-production moulds for manufacturing, verification and testing, and in order to reduce the costs associated with conventional core production using the core box. According to DTM, the manufacture of complex cores is a time-consuming process but LS machines can fabricate the sand casting cores in a number of hours. The sand moulds and cavities produced are of equivalent accuracy, and have properties that are identical to cores fabricated with conventional methods. It can be employed for low-pressure sand casting [DTM, 1998e].

2.5 The LS process and material deterioration

Figure 2.8 and 2.9 illustrate the design and Table 2.2 shows a comparison of the main specifications of two typical LS machine models that have been employed in this research: Sinterstation HiQ 3D Systems [3D systems, 2007] and EOSINT P700 EOS GmbH [EOS, 2007], currently used for RP and RM.

Table 2.2 LS machines' specifications [Dean, 2005]

	EOSINT P700	Sinterstation 2500HiQ
Building envelope, mm	700 X 380 X 580	320 X 280 X 457
Volume, cm^3	154,280	40950
Material weight, kg	69	19
Recommended PA Material	PA2200	DuraForm^{TM} PA
Laser spot diameter, mm	0.75	0.45
Layer thickness, mm	0.15	0.1
Laser type	2 x CO_2 lasers	CO_2 laser

As illustrated in Table 2.2, the EOSINT P700 has a larger capacity to produce parts than the Sinterstation 2500 HiQ. The utilisation of the building envelope depends on the part size, volume, and the number of parts. It could vary from build to build but generally the total volume of parts in a build is relatively small and within 10% to 20% of the building chamber volume, which means that 80% to 90% of the material is not sintered and could be recycled and used in the next builds. However, this material deteriorates during the LS process and has to be discarded after being used several times.

In general, there are three processing stages common to any of the two LS technologies, which significantly influence the material ageing process.

Warm-up stage

In the Sinterstation 2500 HiQ design, the cylinder heater is set to maintain a temperature of 130°C while the piston heater is set to 150°C. A specific feature in this design is that the cylinder heater covers approximately a half of the total build height. Once the piston is outside the heater area, the first half of a full build starts to cool down while the other half is still being processed. By contrast, the building chamber or the frame in the EOSINT P700 design is removable and has heaters integrated in the frame walls and piston. The temperature is maintained at 140°C throughout the whole build. This facilitates a uniform temperature distribution and therefore uniform shrinkage distribution but the unsintered material is subjected to a higher temperature for much longer. In the Sinterstation 2500 HiQ design, the material stays at high temperature for a shorter time but the resulting non-uniform shrinkage disturbs the part accuracy in full height builds.

In both systems the part bed temperature is controlled in the region of 130°C to 150°C to prevent fast cooling rates and therefore excessive distortion and warping of the parts.

Build stage

During the whole build stage the powdered material is subjected to heat and the part bed temperature is constantly controlled to be 10°C to 15°C below the T_m with ±1 accuracy. It facilitates the LS process because only a small amount of energy is needed from the laser to melt and fuse the powder particles. This also prevents higher thermal gradients and part distortion. Based on the slice data obtained from the STL file, a CO_2 laser (or two lasers in the EOSINT P700 design) draws the part cross section and sinters the powder particles. Then the roller spreads a new layer on the part bed for the next laser scanning process.

Cooling-down stage

The already sintered parts and the powdered material, which is not sintered, stay in the building chamber for another period of time at relatively high temperature. Temperature measurements experimentally taken at the end of a full EOSINT P700 build in different places of the part bed show that the powder temperature in the middle area approximately 50mm from the frame walls is between 160°C and 180°C. Within 50mm distance from the walls, the temperature is between 140°C to 160°C.

The parts can be removed and cleaned only after the temperature reaches the material T_g or below 45°C to 60°C, otherwise they could warp or deform. The cooling-down time can vary depending on the building height, part volume and the LS machine design. For a typical build, it could be from 25 to 50 hours.

Generally, the LS process involves complex radiation, convection, and conduction of heat transfer as shown in Figure 2.10. The unsintered powder is exposed to a temperature close to T_m for a long period.
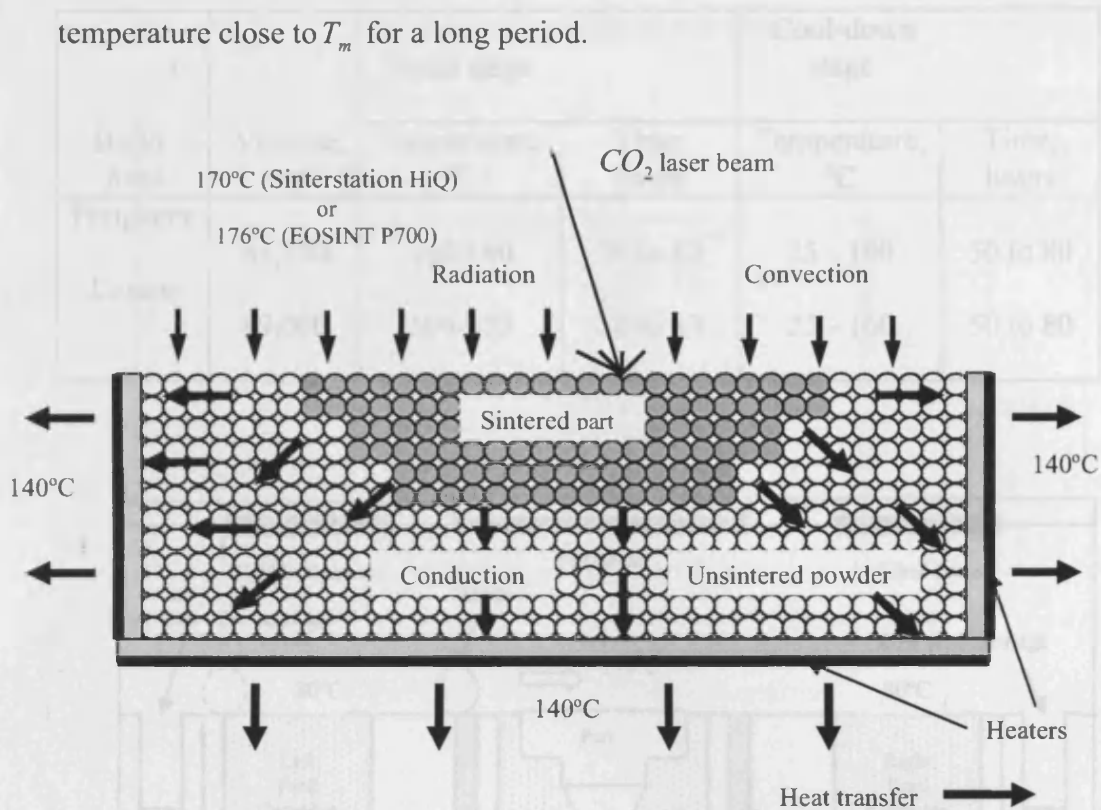
Figure 2.10 Heat transfer in the build cylinder during LS process

The centre of the building envelope, which is almost 60% of the total volume, is heated at a temperature of between 160°C and 175°C for almost 100 hours. The rest of the building volume is heated to 140°C to 160°C. This means that a vast amount of the powder is subjected to heat at temperatures between 140°C to 180°C for a long period. Taking into account the size of the EOSINT P700 building chamber, build time and cooling time, the approximate amounts of material required, the temperatures, and the duration can be calculated and summarised as shown in Table 2.3.

Table 2.3 The approximate amount of powder exposed at different temperature during the LS process (EOSINT P700).

Build Area	Volume, cm³	Build stage		Cool-down stage	
		Temperature, °C	Time, hours	Temperature, °C	Time, hours
Periphery	65,250	140-160	50 to 80	25 - 160	50 to 80
Centre	89,000	160-175	50 to 80	25 - 160	50 to 80
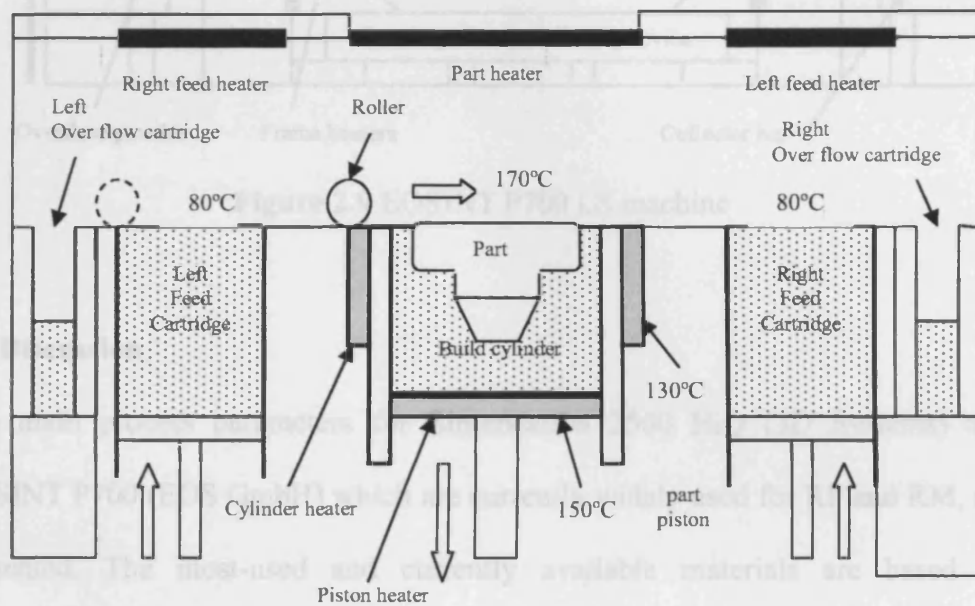
Figure 2.8 Sinterstation 2500 HiQ LS machine
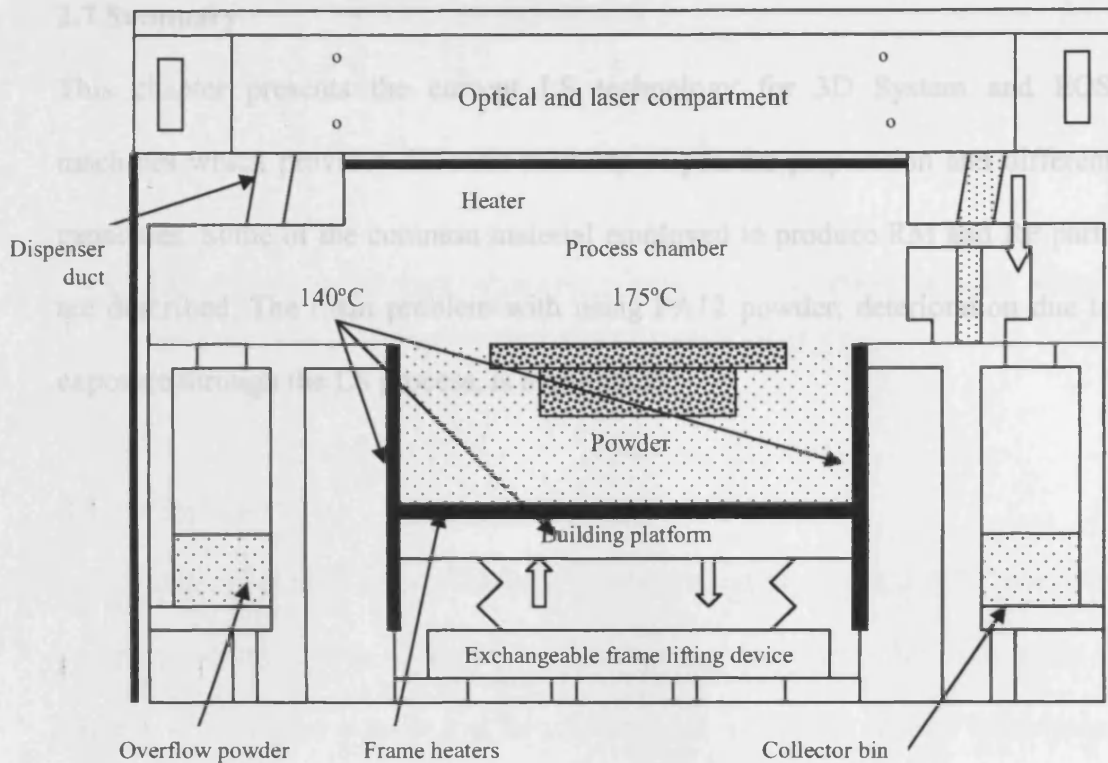
Figure 2.9 EOSINT P700 LS machine

2.6 Discussion

The main process parameters for Sinterstation 2500 HiQ (3D Systems) and

EOSINT P700 (EOS GmbH) which are currently widely used for RP and RM, are

presented. The most-used and currently available materials are based on

Polyamide 12 (PA12) or Nylon 12 powders. Some of them are composites and

filled with glass, metal (copper, aluminium), or carbon fibre powders. All of the

PA12 powders are processed in a similar way during the LS process. However,

the PA12 powder properties deteriorate due to the high temperature close to the

material melting temperature for a long period of time through the LS building

and cooling cycles.

2.7 Summary

This chapter presents the current LS technology for 3D System and EOS machines which provides different methods of powder preparation and different capacities. Some of the common material employed to produce RM and RP parts are described. The main problem with using PA12 powder, deterioration due to exposure through the LS process, is highlighted.

CHAPTER 3

EXPLANATIONS OF THE "ORANGE PEEL" PHENOMENON IN THE LASER SINTERING PROCESS (LS)

3.1 Preliminaries

Laser sintering (LS) is one of the most versatile rapid prototyping (RP) processes currently available. One of the main advantages of employing this technology is that the non-sintered powder can be recycled and reused for another fabrication. However, the fabricated part could be affected by rough and unacceptable surface texture. As a result, the parts may have to be scrapped and the build has to be repeated with a higher ratio of new material. This causes delays, customer disappointment, and additional expense. Sometimes, this could be avoided by adding plenty of new material. However, this would also raise the production cost due to the high proportion of the material cost within the total cost of the LS manufacture. The main aim of this chapter is to investigate the "orange peel" phenomenon which affects the LS part.

3.2 Previous studies of the "Orange Peel" phenomenon in the LS process

Prior to this study, the ageing of PA12 powder and more efficient recycling in the LS process had not been thoroughly investigated. Most previous research was carried out using PA12 as the focus for the study of the thermal, mechanical, and chemical properties which affect the part surface finish. Table 3.1 shows a summary of related research reviewed in this section.

Gornet [Gornet, 2002a,b] studied how the mechanical and thermal properties of LS parts from DuraForm (trade name of a PA12 powder produced by 3D Systems [DTM, 1996a and 3D system, 2006]) material were affected by the number of builds or the number of times the powder was used. In the Sinterstation 2000, the first LS machine available from DTM Corporation, the use of a plastometer, which is a commonly used tool in the injection-moulding industry, was suggested in order to measure the flow ability of the used DuraForm (DF™) powder. One of the conclusions was that after approximately 7-8 builds the properties of the processed material were so badly deteriorated that it should be fully discarded. However, the effect of the duration of each individual build, or the total LS processing time, on the powder and part properties was not investigated.

Table 3.1 Related previous work on the LS part quality

Researchers	Duraform™	PA2200	Tensile strength	Fracture Strength	Elongation	Young's Modulus	Impact strength	Toughness	Melting point	Melt Flow Rate	Molecular Weight	Crytallinity
Gornet et.al	X		X		X	X	X	X	X	X		
Chohen et.al	X					X		X				
Zarringhalam et.al	X	X	X		X	X			X		X	X
Caulfield et al	X		X	X	X	X						
Ajoku et al	X		X			X		X				
Shi.Y et al									X	X		X

Another author, Choren et al., [Choren et al., 2002], studied the effect of the LS process parameters, such as the laser power, on the surface quality and mechanical properties of parts sintered with used DF™ powder. The blended recycled 33% and 67% new DF™ powders was repeatedly employed up to 300 hours with different setting levels laser power (*LP*) parameters. In order to control the recycled powder quality, it was suggested that the recycled powders be stored in separate bins based on the number of hours spent on the machine.

A new PA12-based material, known as HPA, was developed by Y.Shi et al., [Y.Shi et al, 2004]. Shi et.al studied the effect of the properties of the polymer materials on the quality of LS parts by using an HRPS-III laser sintering system (developed by Huangzhong University). It is reported that the higher melt viscosity obtained was due to the increased M_w, which causes higher warp, part shrinkage and slightly less part density (about 1.8%). It is also suggested that a particle size of 75-100 μm is thought suitable in order to produce higher part density and accuracy. However, the properties of HPA (PA12-based) were not presented and it is important to compare them with those of PA2200 and DF™.

Zarringhalam, et al., studied thermal and, mechanical properties and microstructure of the test part fabricated from new and used DF™ and PA2200 produced by EOS (Electro-Optical Systems) GmbH [Zarringhalam et al., 2006]. The microstructure, which indicates the porosity of the LS parts, was studied. The mechanical and thermal properties of the test parts composed of both new and used powders were compared.

Ajoku et al [Ajoku et al., 2006] studied the comparison of mechanical properties of the LS test part produced by LS and injection moulding using the new DF™ powder. The LS part has higher strength and superior toughness than the injection moulded part. However, the cross-sectional test part made of LS was found to have high porosity due to uneven heat distribution, inadequate heat supply from the laser and insufficient process temperatures.

Caulfield et al [Caulfield et al, 2006] employed the new DF™ powder to investigate the influence of different levels of Energy Density (*ED*) and part build orientations to the part surface, as well as the mechanical properties of the sintered parts, using the Sinterstation 2500 HiQ. The increase in material property values found increased in *ED* correlate with the increase in material density.

Gornet et at, Chohen at el and Zarringhalam, et.al reported that the higher molecular weight and the melting point of the samples notably influenced the melt flow rate. They also reported that the mechanical properties of the sintered part do not significantly change depending on the LS part surface finish.

3.3 The "orange peel" texture study
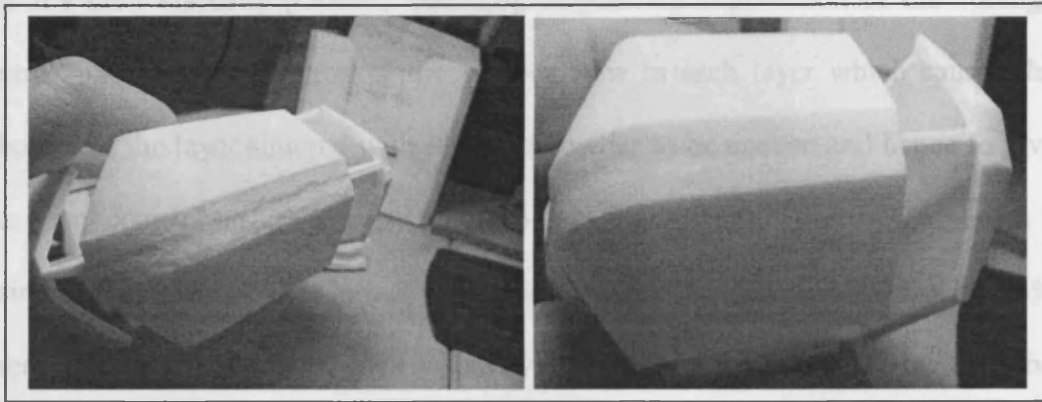
Figure 3.1a "Orange peel" texture   **Figure 3.1b** Good part surface

Figure 3.1a shows an example of an LS part affected by "orange peel" texture compared to a good LS part surface shown in Figure 3.1b. "Orange peel" texture is clearly a rough, uneven, and coarse texture observed on the part surface due to PA12 powder deterioration.
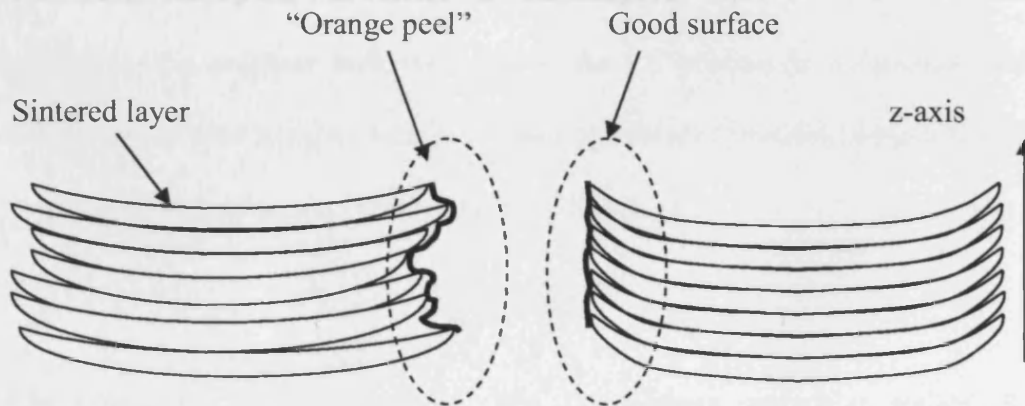
Figure 3.2a "Orange peel" sintered layers   **Figure 3.2b** Good surface sintered

layers

The "orange peel" texture affects part surfaces only along the z axis of the LS machine. The properties of recycled PA2200 powder significantly influence the

melt viscosity and sintering mechanism. The older the recycled PA12, the higher is it's melt viscosity [Gornet, 2002a,b]. A possible explanation of the "orange peel" texture is a variation of the viscous flow in each layer which causes the border of the layer sintered with recycled powder to be uneven and hence to give a poor, coarse, surface finish (Figure 3.2a). By contrast, Figure 3.2b shows a sintered layer employing less deteriorated powder (blended 35 % new with 65% recycled) which has lower melt viscosity. This causes better powder melting and fusion during the sintering process which results in a good surface finish.

The "orange peel" is a complex phenomenon and depends on not only on powder properties but also on part orientation. As noted earlier above (Figure 3.1a), it affects only surfaces along the vertical z axis but the "orange peel" affect varies depending on the angle of the sintered surface to the z axis. In order to study this relationship, a test part with surfaces at different angles and LS with recycled PA2200 powder were employed (Figure 3.7a and Figure 3.7b). Characterisation of the bench mark parts was carried out and analysed.

45° angled surface

90° angled surface

30° angled surface
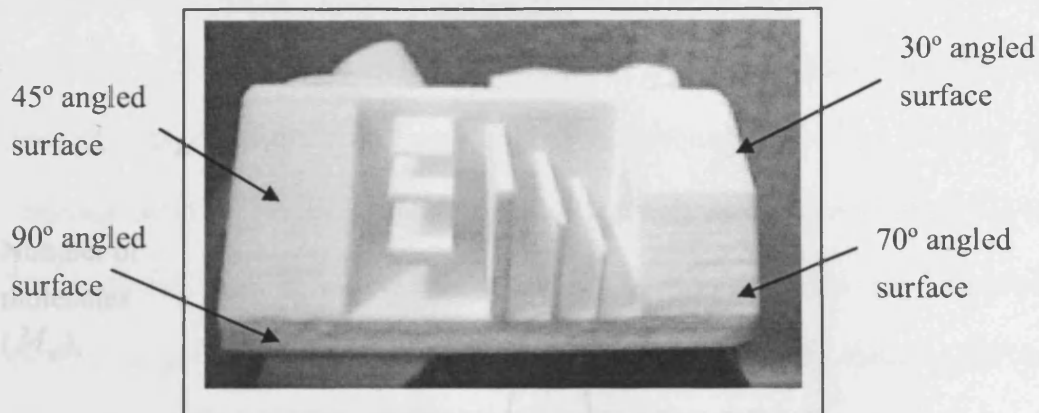
70° angled surface

Figure 3.3 Test part with surfaces at the different angles

As shown in Figure 3.3, the 90° angled parts exhibit the worst "orange peel" texture compared to all other surfaces. Signs of "orange peel" texture were observed also for the 45° angled surfaces. The surface at 30° was not affected by this phenomenon.

3.4 The significant of *MWD* to the melting viscosity in LS process

In general, the polymer melt viscosity in the LS process is a function of the average molecular weight, which follows the Mark-Houwink equation below [Cogswell, 1981; Brydson., 1999; Shi et al, 2004]:

$$\eta_0 = K \left(M_{\bar{w}} \right)^n$$

Where η_0 is the melting viscosity, $M_{\bar{w}}$ the average molecular weight, K a constant that depends upon the type of polymer and the exponent n, a function of polymer geometry, and which varies from 0.2 to 3.5. From this formula, the melt viscosity and $M_{\bar{w}}$ of the polymer are found to be closely related to the molecular weight distribution (*MWD*) which affects the LS part surface.
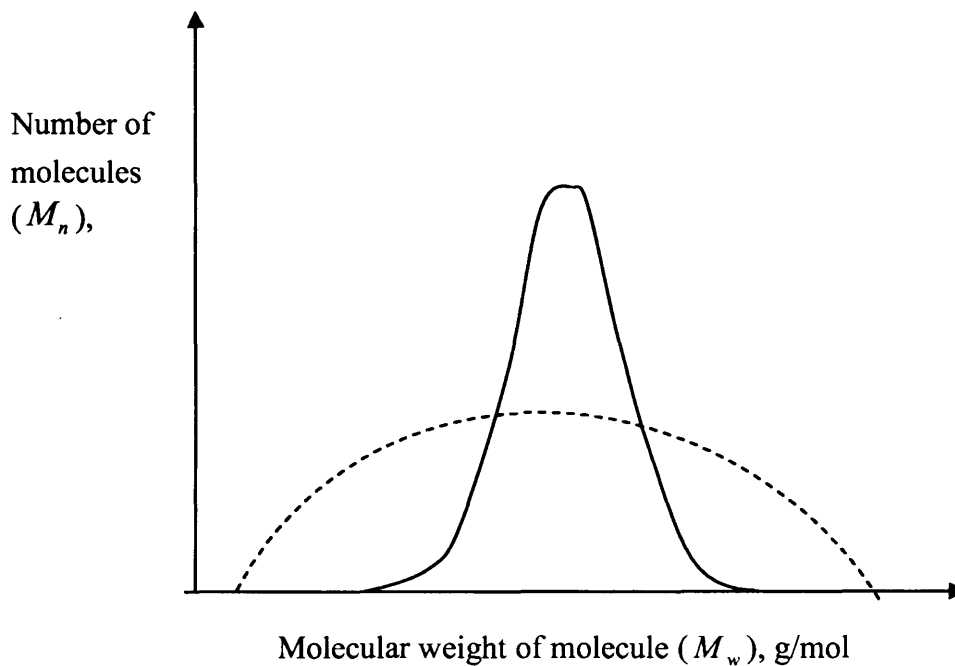
Figure 3.4 molecular weight distributions of polymers [Cogswell, 1981]

PA12 consists of very long chains, which are synthesised from smaller molecules during the polymerisation process. The longer the molecular chain, the higher the molecular weight. However, not all polyamide chains will grow to the same length, resulting in a different distribution of chain molecules [Callister ,2005 and Kohen, 1995]. As shown in Figure 3.4, M_w is known as the *molecular weight distribution* (*MWD*), which is usually represented by the polydispersity index (*DI*) as defined below [Callister ,2005]:

$$DI = \frac{M_{\overline{w}}}{M_{\overline{n}}}$$

Where $M_{\overline{w}}$ is the weight average molecular weight and $M_{\overline{n}}$ the number average molecular weight. In the LS process, the longer PA12 is exposed to high temperature, the higher is the chance that the powder will deteriorate.

At high temperatures, the 'chemical reactions', which involve the free radical molecules at the end of the chain segment of the polymer, begin to react and link up with other unstable molecules to form a repeating chain. As a result, the molecule chain becomes longer and has high entanglement (Figure 3.5b).

This causes changes in its molecular weight distribution and leads to changes in the thermal properties of the polymer and also to morphology changes. For this reason, recycled PA12 quality deteriorates in the LS process.

Molecular chain entanglements
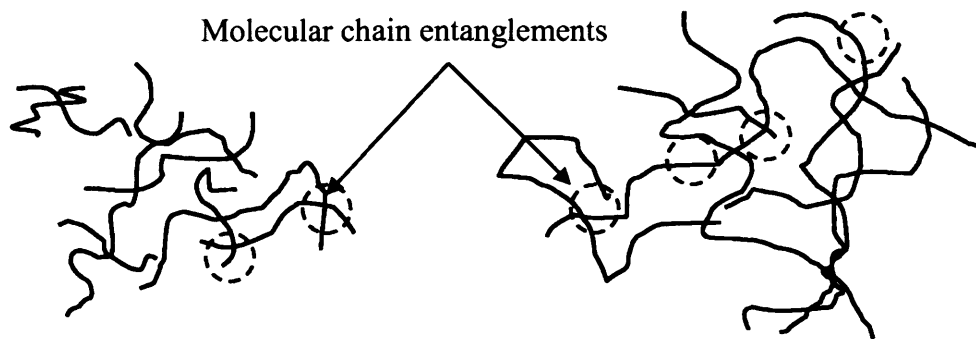
Figure 3.5a Narrow *MWD*   **Figure** 3.5b Broad *MWD*

As shown in Figure 3.5a [Cogswell, 1981], the polymer with narrow *MWD* has short molecular chains with an average of about 2 entanglements per chain. On the other hand, the polymer with broad *MWD* has long molecular chains with an average of about 4 entanglements per chain as shown in Figure 3.5b [Cogswell, 1981]. Therefore, the long chains of high molecular weight and more complex structure cause greater flow resistance.

3.5 Experimental results and discussion

3.5.1 Methodology and equipment used

The aim of this experiment is to study the relationship of *MWD*, melting heat or heat of fusion, to the external and internal microstructure of good parts and parts affected by an "orange peel" texture. DSC was employed to measure the *MWD* by using GPC [ISO16014]. The heat of fusion was measured using DSC [ISO 11357] and the PA2200 powder quality, which has been employed this experiment, was measured using the melt flow rate indexer [ISO1133]. These equipments are also used for the particular purposes of this research in succeeding chapters. The details of the procedures which relate to these equipments will be explained later in section 4.3.1.1, 4.3.1.2, and 4.3.2.3. For the purpose of "orange peel" texture study, refreshed and twice-used PA2200 is employed to produce the specially designed bench parts. As the average particle size of PA2200 is approximately 50μm, the microstructure of the "orange peel" texture of the sintered part may be studied using a Scanning Electron Microscope (SEM) [Tontowi and Childs, 2001].

3.5.1.1 Scanning Electron Microscope (SEM) examinations.

For all examinations, a thin layer of gold was sputtered on substrates using an auto sputter apparatus. Two pieces of equipment have been used consecutively. The first is a Bio-Rad SC500 for gold coating of the specimens and the second is an EMSCOPE SC500 for image capture. It is employed to characterise the individual powders and to analyse the surface morphology and microstructure of the sintered bench part. All LS fabricated bench parts were examined under high vacuum conditions. A low voltage (10kV) was chosen to minimise heat damage to the sample [Ho et al.,1999].

Powder

The LS material investigated in this study is PA12-based powder PA2200 supplied by EOS GmbH. In the preparation of the specimens for the SEM, a small amount of powder was stuck on a holder using glue. Then it is coated with gold in the Bio-Rad SC500. The specimen is now ready to be fixed in the EMSCOPE SC500 Cam Scan. Table 3.2 shows the melting viscosity of the two different powder grades in the experiment. These two powders were employed to produce the bench parts.

Table 3.2 PA2200 powder melt viscosities

Powder	Melt flow rate (MFR), g/10min
Refresh PA2200 (35% New + 65% once Recycled)	33.15
Twice used PA2200	17.41

3.5.2 Design and fabrication of bench part

The model of the sintering bench part test using Pro-ENGINEER is shown Figure 3.6a and Figure 3.6b. The special features incorporated in this model are shown in Table 3.3. The size of the benchmark part is 110mm (w) X 110mm (l) X 48mm (h) The file was then converted into STL format before it was transferred to the LS machine (Sinterstation 2500 HiQ).
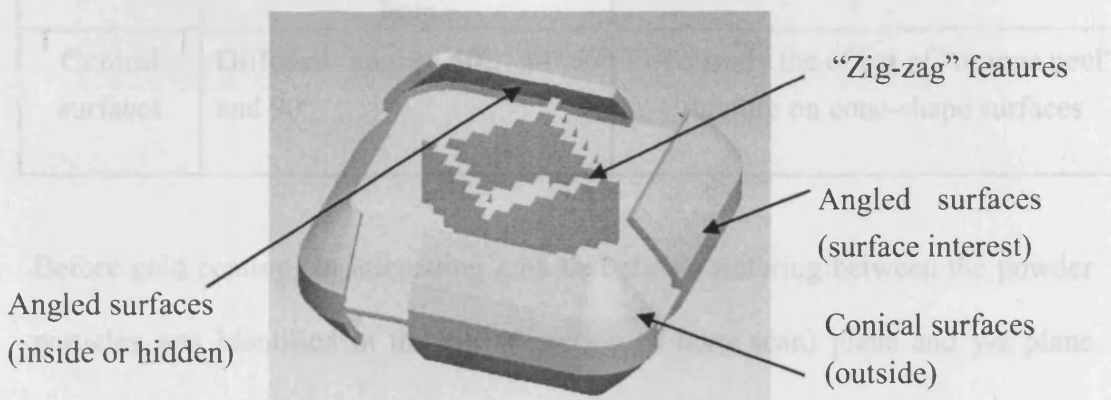
Figure 3.6a Benchmark part (top view)
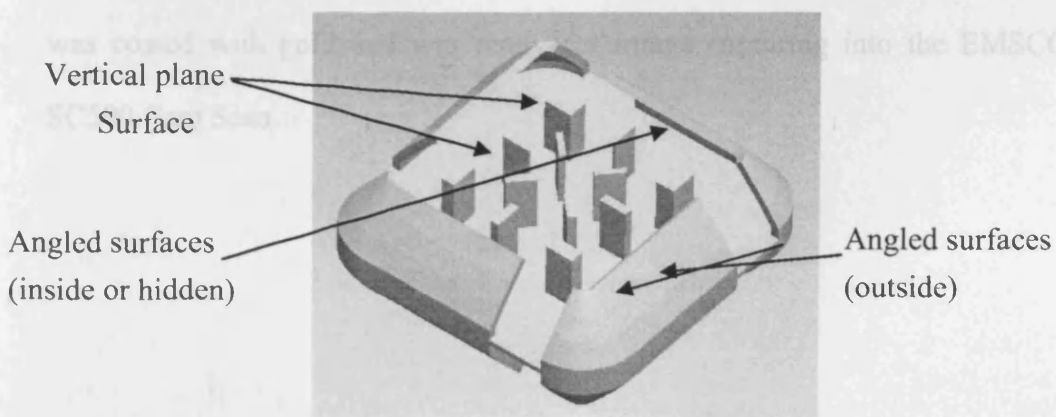
Figure 3.6b Benchmark part (bottom view)

Table 3.3 Benchmark part special features

Features	Description	Function
"Pyramid"	Located on top of benchmark part sample	Shrinkage measurement
Angled surfaces	Different angles 50°, 54°,57°and 90°	To study the effect of "orange peel" texture at different angles of surface
Vertical plain surfaces	Located at the bottom of bench part. Different size of 1mm, 2mm, 3mm, 5mm and 7mm	To study the effect of "orange peel" texture at different thicknesses and orientations
Conical surfaces	Different angles 50°, 54°,57° and 90°	To study the effect of "orange peel" texture on cone-shape surfaces

Before gold coating, an interesting area that shows sintering between the powder particles was identified in the x-y (direction of laser scan) plane and y-z plane (perpendicular direction of laser scan). To obtain access to these areas, the sintered part was cut by breaking it in the y-z plane and y-z plane. As a similar procedure was applied for the powder specimen preparation, a small part of the sintered part sample was stuck on the specimen holder using glue. Afterwards, it was coated with gold and was ready for image capturing into the EMSCOPE SC500 Cam Scan.

3.5.3 The study of the PA2200 powder sizes

The aim of this experiment is to study the effects of number of builds on the powder shape and size, which could affect the LS part surface.

Figure 3.7a Refreshed PA2200 powder	**Figure 3.7b** Twice recycled PA2200
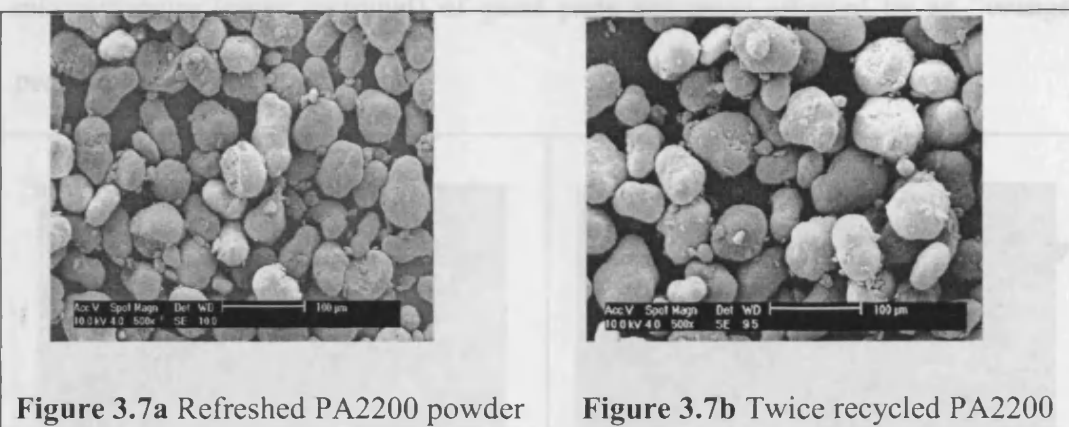
Figure 3.7a and 3.7b show a general view of the two different powder qualities that have been employed in the experiment. They provide a broad range of particle size, from 10 μm to 70 μm and an irregular shape with a rough surface. This result suggests that there is not much difference between the different particle sizes even when the powder was repeatedly used.

3.5.4 The microstructure of external surface and cross sectional of

benchmark parts

The objective of this experiment is to investigate the external and internal microstructure (cross sectional) of good parts and parts affected by an "orange peel" texture.

Figure 3.8a Smooth surface

Figure 3.8b Uneven and rough surface

Figure 3.9a Small voids

Figure 3.9b Bigger voids sizes
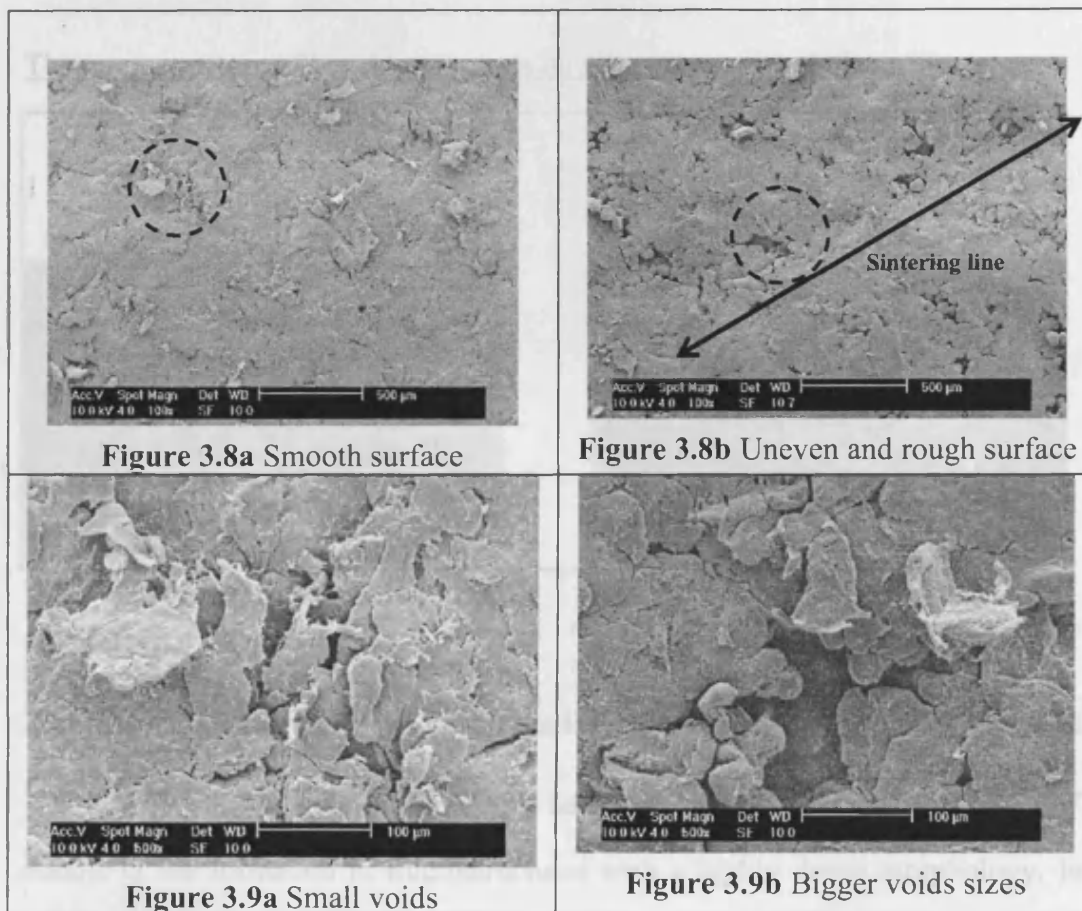
The external surfaces of good and "orange peel" parts are shown in Figure 3.8a and 3.8b, clearly differentiating the two surfaces finishes. It was found that the higher MFR used in the LS process, the lower the melting viscosity. This results in the polymer particles within the layers fusing easily which leads to a smooth surface. By contrast, employing the twice-times used powder, agglomerates of melted particles can be observed, which are in the direction of the laser scanning lines. Between the sintered lines, extended holes and cavities can be observed.

Figure 3.9a shows a close-up view of the good surfaces. They were most likely caused by the contact with unsintered particles while the surface was still molten. The formation of microstructures with highly dense morphology, and only small voids, can be observed. Figure 3.9b shows the region of high porosity and incomplete melting with the size approximately 100 µm found on the overall surface area.

The microstructure of bench mark parts on x-y cross sectional plane
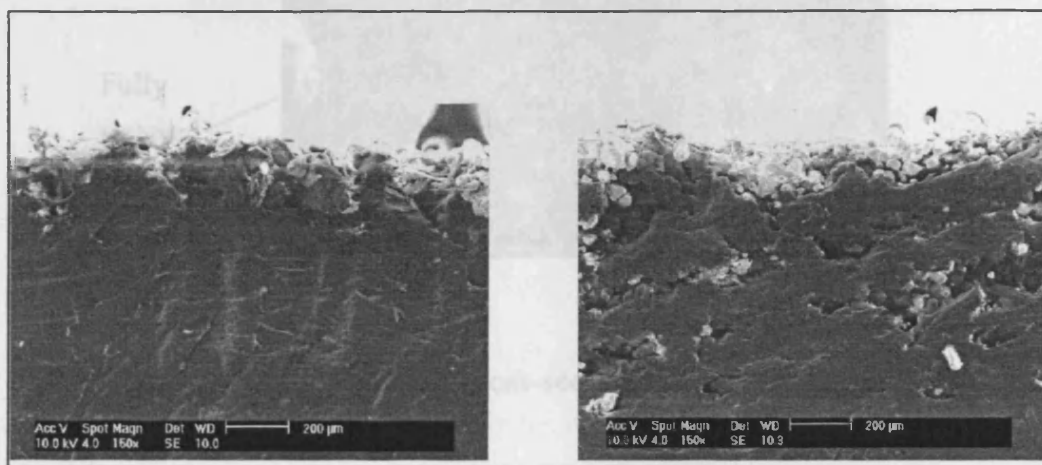
Figure 3.10a Dense microstructure structure

Figure 3.10b Inhomogeneous structure

The external microstructure of bench mark parts on the x-y plane are as shown in Figure 3.10a and 3.10b. This result suggests that the use of refreshed powder results in the formation of microstructures with a highly dense morphology. In contrast, the cross sectional of an "orange peel" texture exhibits a very inhomogeneous structure after laser sintering. It is observed that cavities have different shapes and sizes, the distance between voids when employing twice-used powder is as little as 100µm to 160µm and it may clearly be seen that the average cavity size is approximately 100µm to 200µm.

<u>The microstructure of bench mark parts on y-z cross sectional plane</u>

The microstructure of the cross-section of a good surface part and of an "orange peel" part are compared and shown in Figure 3.11 to Figure 3.14.
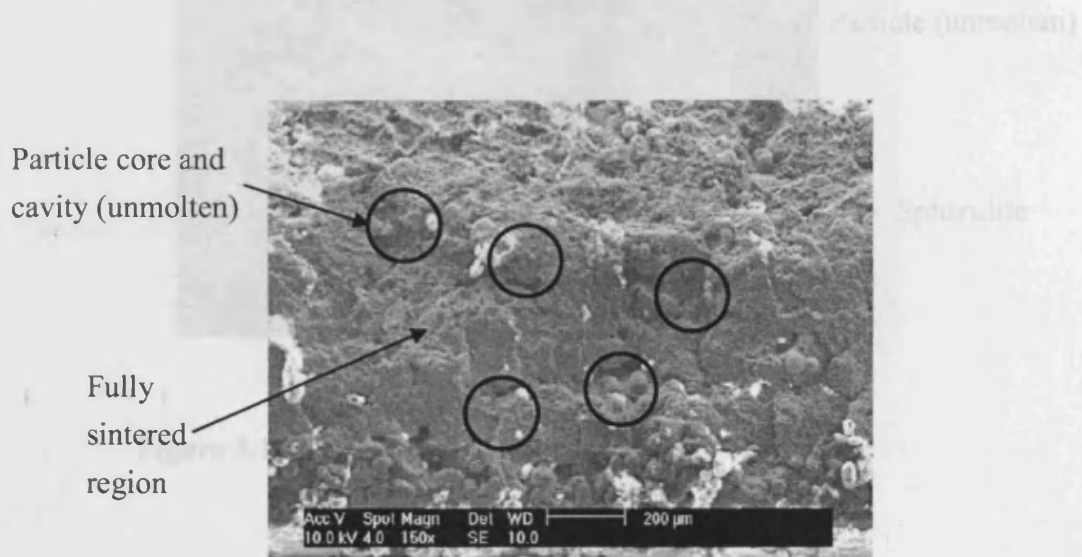
Figure 3.11 Microstructure cross-sectional of the "orange peel" part

The microstructure of the sintered twice-used PA2200 powder is shown in Figure 3.11. The cross sectional LS part affected by "orange peel" texture is shown with annotations on the left hand side. It can clearly be seen that there are a quantity of unmolten particles creating cavities in the sintered region.
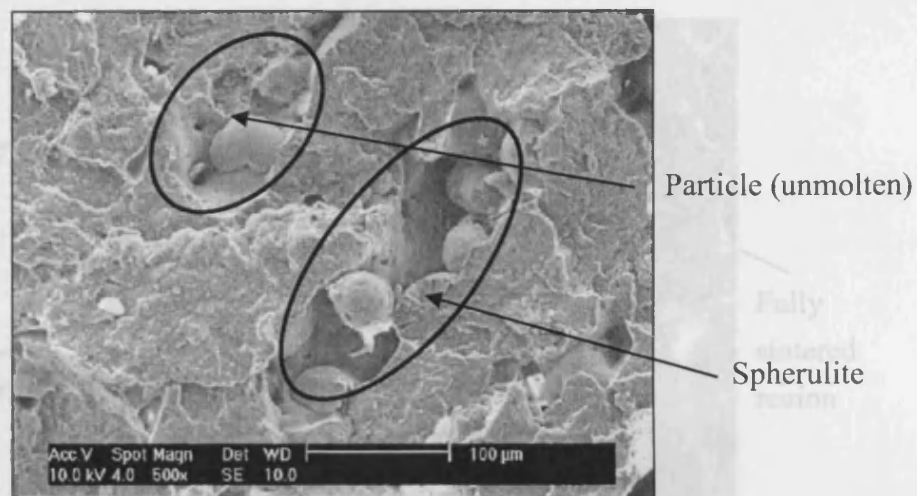
Figure 3.12 Particle core of "orange peel" microstructure

Figure 3.12 shows the SEM image of cross sectional of the "orange peel" microstructure at 500X magnification. It was assumed that the laser beam might penetrate through the gaps between the polymer particles and reach a deeper section between the layers. However, the presences of polymer crystallites, or spherulites, may be observed on the sintered regions, which indicate the high melt viscosity polymer during the LS process. The higher melt viscosity is related to a bigger spherulite size. In the centres of the single spherulites, the origins of crystallisation are clearly visible but nucleating particles cannot be detected. This is considered to be a sign of the deterioration of the polymer material. This means that it is not possible to seal off the voids due to inefficient melting of the polymer. It is observed that the cavities have different shapes and sizes and it is estimated that the average cavity size is approximately 100μm to 200μm, as may clearly be seen.

Cavities

Unmolten particle

Fully sintered region
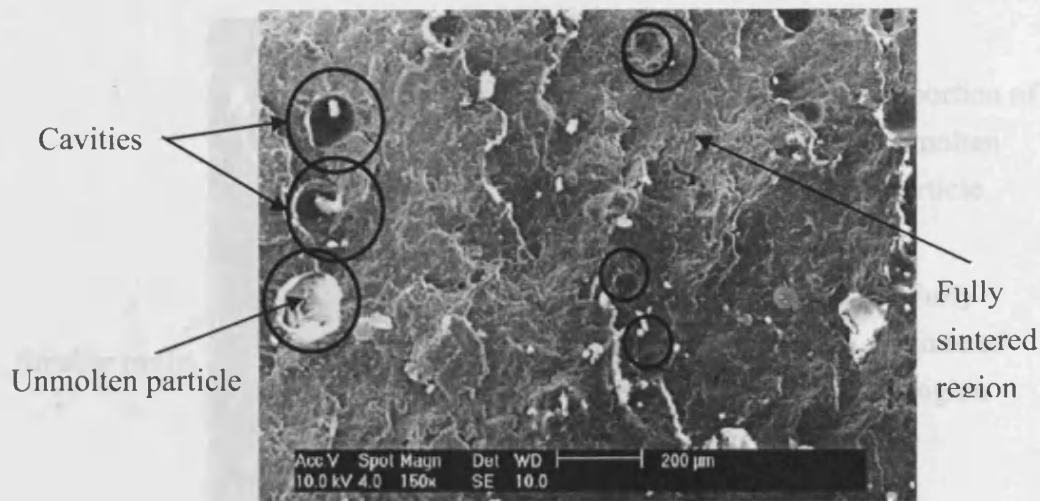
Figure 3.13 Microstructure cross-sectional of the good part

From the observation of Figure 3.13, sintering effects among the particles are clearly noticeable. It can be seen that the overall voids are smaller than those in Figure 3.11. The sizes of cavities are found approximately to be the size of a single particle (50μm to 80μm). However, a lot of partial core (unmolten) adheres to the surface, which leads to the formation of many small cavities. This could be because the particles do not receive sufficient heat during the sintering process.

A portion of unmolten particle

Fully sintered region

Smaller cavity

Figure 3.14 Particle core of good part microstructure

Figure 3.14 shows the cross-section microstructure of good part which still has some small cavities with larger fully sintered region compare to image shown in Figure 3.12. This because of less deteriorated powder was employed thus improves the sintering mechanism which causes the particles easily melted.

3.5.5 The relationship between *MWD* and MFR
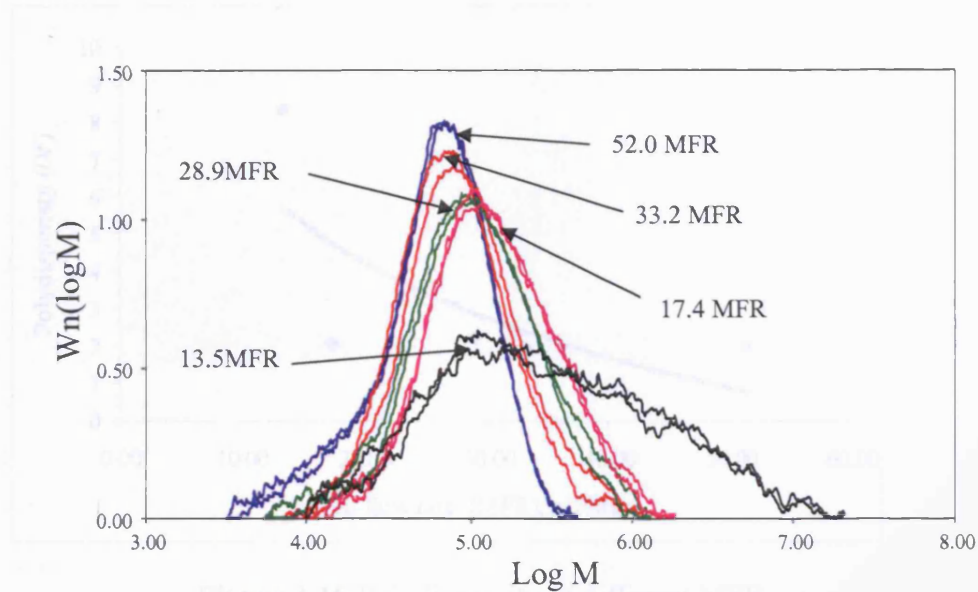
Figure 3.15 Molecular weight distributions (*MWD*) of different PA2200 quality grades.

In Figure 3.15, the x axis represents the molecular weight expressed as the log value. Therefore Log M =4.00 is a molecular weight of 10,000 and log M = 6.00 is a molecular weight of 1,000,000. The y axis is represented by *Wn* (log) M, which is the weight fraction per unit of log molecular weight. It is simply a frequency function.

As shown in Figure 3.15, the sample of new PA2200 powder stretches to the lowest log *M* and hence includes the lowest molecular weight. In contrast, the worst PA2200 powder quality has a broad molecular weight distribution because it has high molecular weight (Figure 3.4 and 3.5b). Therefore, the lower MFR value, the longer the chains. These long chains would be expected to become more entangled and hence melted at higher temperatures.

3.5.6 The effects of polydispersity on MFR
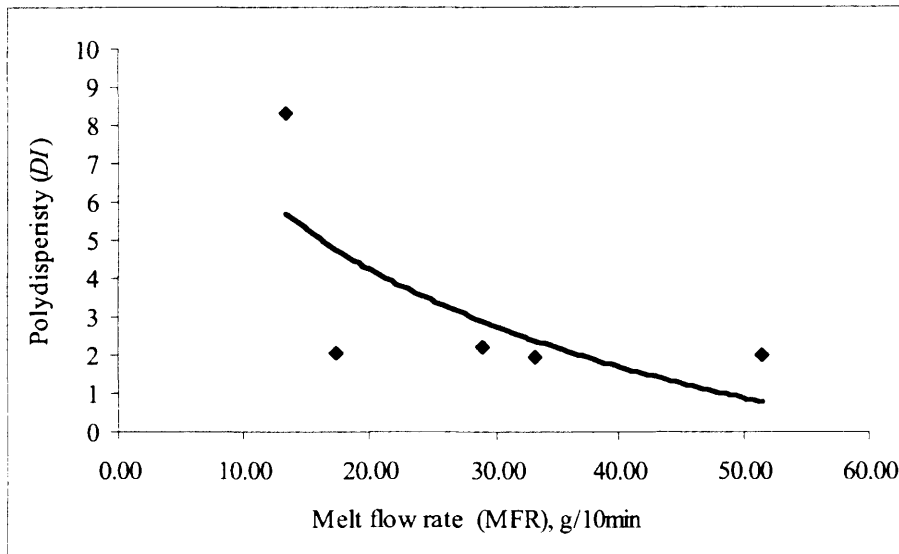
Figure 3.16 Polydispersity of different MFR

As shown in Figure 3.16, the better the PA2200 powder quality grades, the lower the *DI* value. This result proves that the higher quality MFR powder has shorter molecular chains. This causes it more easily to become liquid and to flow easily during the sintering process. The better PA2200 powder quality grades, the lower the $M_{\overline{w}}$ value. In contrast, the higher *DI* value makes the polymer have a higher viscosity.

3.5.7 The relationship between heat of fusion and recycled powder
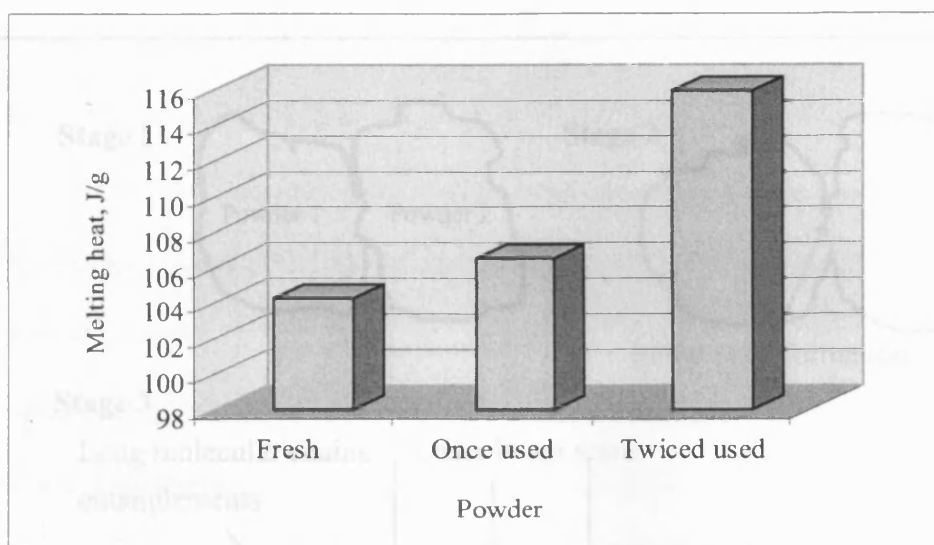
Figure 3.17 The melting heat of different powder usage

Figure 3.17 shows the amount of energy a sample absorbs while melting. It is clearly shown that the deteriorated powder (twiced-used PA2200) requires more energy to fuse the powder. This is associated with the stronger chain stiffness due to crystallites giving better packing of the polymer chains. This result supports the explanation of molecular weight distribution (*MWD*) and chain entanglement as explained in the earlier section 3.4.

3.5.8 Qualitative process model for the "orange peel" phenomenon
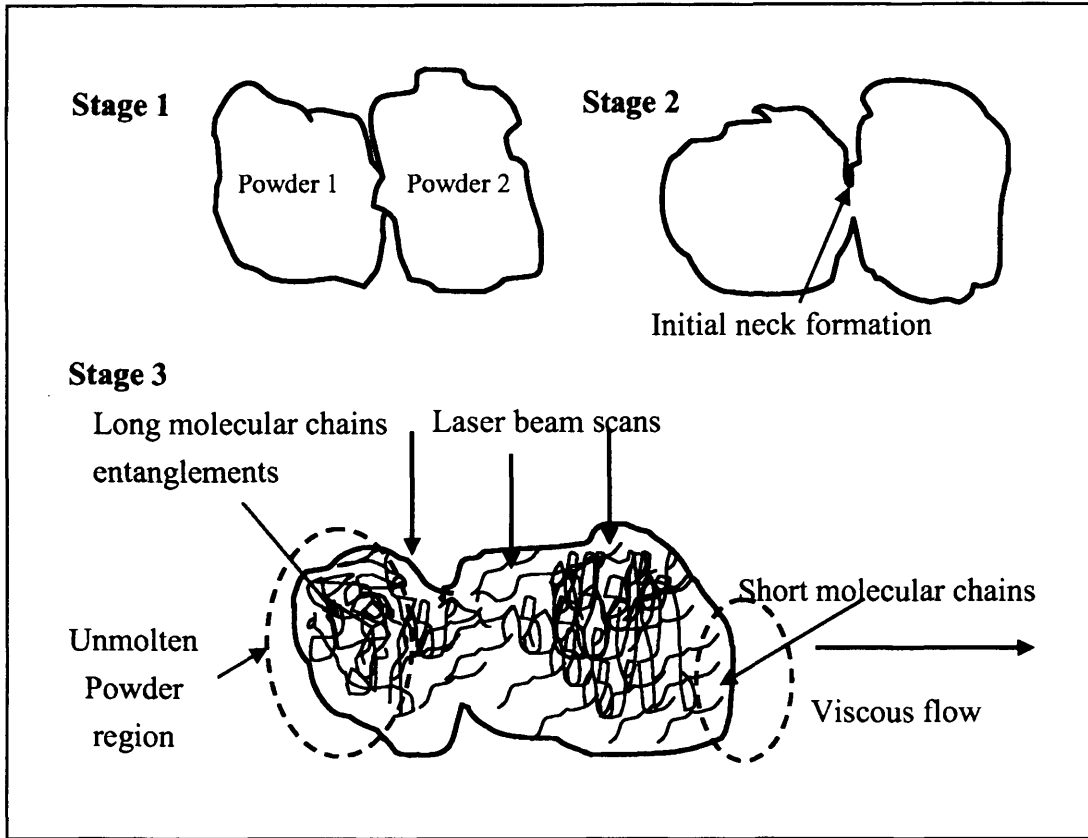
Figure 3.18 Qualitative processes model for the "orange peel" phenomenon

A qualitative sintering model is presented which estimates the sintering in a powder bed of viscous material.

Stage 1

The particles are packing close to each other in various sizes and shapes. Below the glass transition temperature they are in the solid state.

Stage 2

As explained in section 2.2, before the powder is sintered, the entire part bed is preheated 10°C to 12°C in the process chamber, or just below the melting point of the material, in order to stabilise the process chamber. This causes partial small region contact points between the particles starting to melt. This is due to the

breaking of the van der Waal chains which leads to the initial sintering neck formation developed during this stage.

Stage three: Viscous flow takes place at this stage. This is due to laser beam scans of the particles and laser energy absorption by the particles, leading to the significant growth of the neck formation between particles which then transforms into viscous flows. In liquids, an increase in temperature is associated with the weakening of bonds between molecules. Since these bonds contribute to viscosity, which decreases rapidly with an increase in temperature, it has been assumed that the amount of absorbed energy was large enough to melt the entire polymer and to form a stable sintering neck. Then, the polymers particles are completely melted and the fluid phase starts.

However, due to the limitation in the LS process, not all the powder particles are fused during the sintering process which still formed porosity as can be seen in Figure 3.13. This can be explained by the fact that the higher MFR value means a lower melting viscosity. This is strongly related to the shorter molecular chains and therefore to fewer entanglements. The sintering occurs by viscous flow. Then the material moves from large pores to smaller ones and dominates the vacancy. Also, employing deteriorated powder is influenced by its thermal history. This is associated with the higher *DI* and higher chains entanglements (Figure 3.5b). Moreover, the heat of fusion and the amount of heat absorbed to melt the polymers is affected by the variation in thickness of the lamella in the crystalline region (Figure 4.2 and Figure 4.5). This is the result of the mobility of the polymer molecules and is more restricted. Variations of the viscous flow may be expected, which lead to the formation of unmolten particle cores as clearly observed in the microstructure of the "orange peel" texture (Figure 3.1a).

3.6 Discussion

This research investigated the potential causes of the "orange peel" phenomenon which affects some LS fabricated parts. Refreshed and twice-used PA2200 powder with 33.15MFR and 17.41MFR respectively were employed to produce the bench parts. Visual inspection of an SEM micrograph showed that the overall particle powder sizes of these different melting viscosities were not influenced by the number of builds.

The experimental work shows that powder quality, melt viscosity, and part surface finish are correlated. The following main tendencies can be observed. A lower heat of fusion is required to melt the higher MFR value (33.15g/10min) powder. Lowering melting viscosity generally leads to a more highly dense microstructure and exhibits dimensional stability and is non-porous. The physically refreshed powders that were sintered exhibited good interconnectivity. Necking between the PA2200 particles indicated good sintering effects. This means that better sintering mechanism is achieved if a powder with lower melt viscosity is chosen. The explanation of the "orange peel" phenomenon can be understood by a multistage model. At first, nearly all laser energy is absorbed by particle powders, causing local heating. Then, a part of the particle is melted, which leads to complete melting of the surrounding polymer and the formation of sintering necks. At the build stage, the melt viscosity of the polymer is significantly influenced by the molecular chain entanglement (spherulites), the higher molecular weight, and longer molecular chains, leading to higher viscosity and to the formation of agglomerates of melted particles. This results in an inhomogeneous structure and a poor coherence sintered region.

3.7 Summary

The "orange peel" phenomenon is one of the main constrains in the LS process as it causes unacceptable LS parts' surface quality. It happens when deteriorated PA12 powder is employed in the LS process. This chapter reported on the effect of the properties of the PA12 polymer on the microstructure of the parts which are affected by the "orange peel" phenomenon.

CHAPTER 4

DETERIORATION OF POLYAMIDE 12 POWDER PROPERTIES IN

THE LASER SINTERING PROCESS

4.1 Preliminaries

LS with Polyamide 12 (PA12) or Nylon 12 powders is a widely used technology for the rapid prototyping of functional parts and recently has become very attractive for the rapid manufacturing of small batches of plastic parts. However, the plastic powder's properties deteriorate during the LS process, which requires new material to be mixed with the recycled one. An insufficient amount of new powder results in poor quality and rough surface finishing known as "orange peel" of the produced parts. This chapter presents an experimental study of the deterioration or ageing of PA12 powder properties in the LS process. The influence of temperature, time, and the number of exposures on these properties is investigated. The main aim of this research is to develop a methodology of controlling the input material properties that will ensure consistent and good quality of the fabricated parts.

4.2 The PA12 powder properties' deterioration during the LS process

The PA12 molecule structure is shown in Figure 4.1. It is a combination of carbon atoms and of the amide group. The presence of the amide group (COHN) increases the chain flexibility of semi-crystalline polymers (Appendix A) [William, 1993; Kohan, 1995; Mantia, 2005]. This is why the PA12 backbone is relatively flexible and the long irregular linear molecule chains can easily transform into a regular chain-folded structure through the crystallisation process.
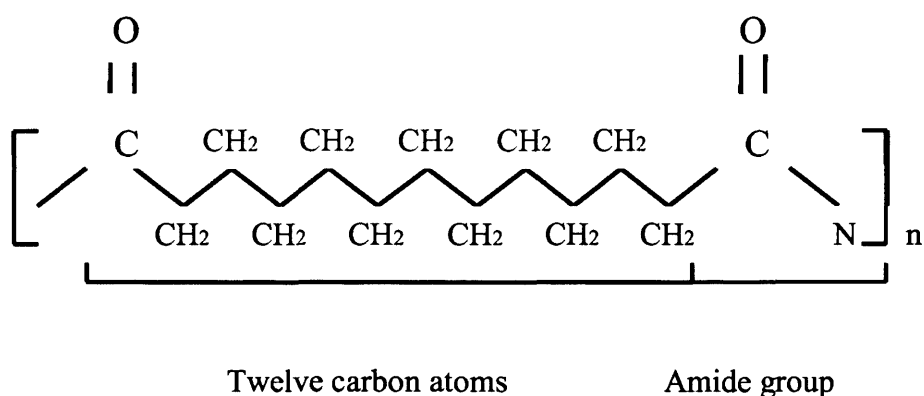
Figure 4.1 PA12 molecules chains structure [Kohen, 1995]

The strong bonds in the PA12 molecules determine their mechanical and thermal properties. A typical molecular structure of such a polymer is illustrated in Figure 4.2.
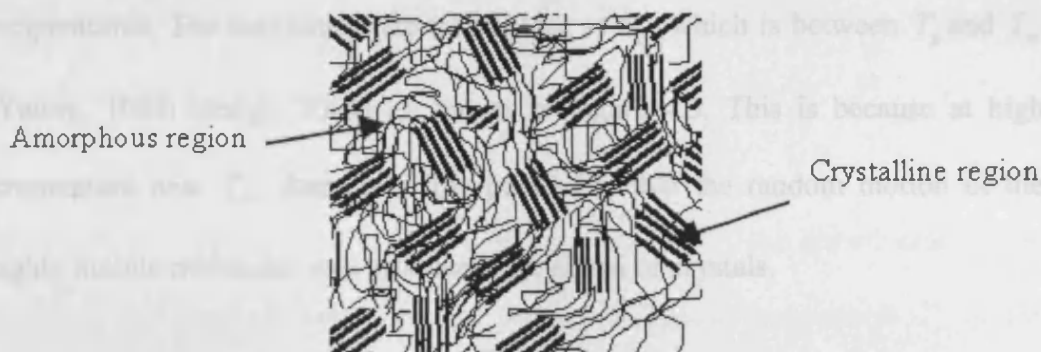
Figure 4.2 The molecular structure of a semi-crystalline polymer [Hedge, 2004]

The amorphous region determines the polymer toughness characteristics due to the irregular arrangement of the molecule chains [Dean, 1995; Mangono, 1999; Hedge, 2004]. This region is characterised by the glass transition temperature (T_g). The molecules in the crystalline region are arranged in a regular order known as lamellae and its properties are characterised by the melting temperature (T_m). This arrangement determines the material mechanical properties such as rigidity and brittleness. If the material is subjected to a temperature higher than T_g for a period of time, the molecules become highly mobile.

The first phase of crystallisation is known as nucleation and it takes place in the amorphous region when the temperature of the PA12 powder is just below T_m. It involves the ordering of chains into a parallel array by the stimulation of intermolecular forces, and thus creates stable nuclei from the initially entangled polymer melt. During cooling the addition of other chain segments to the nuclei leads to growth of this region, which constitutes the second phase of crystallisation [Ryan et al., 1999 and Callister, 2005].

This growth, or crystallisation rate, is influenced by the chain polymer structure and thermal history of the polymer. Therefore, growth can vary at different

temperatures. The maximum rate takes place at T_c, which is between T_g and T_m [Young, 1983; Hedge, 2004] as shown in Figure 4.3. This is because at high temperature near T_m, there is a low possibility that the random motion of the highly mobile molecules will produce large nuclei or crystals.
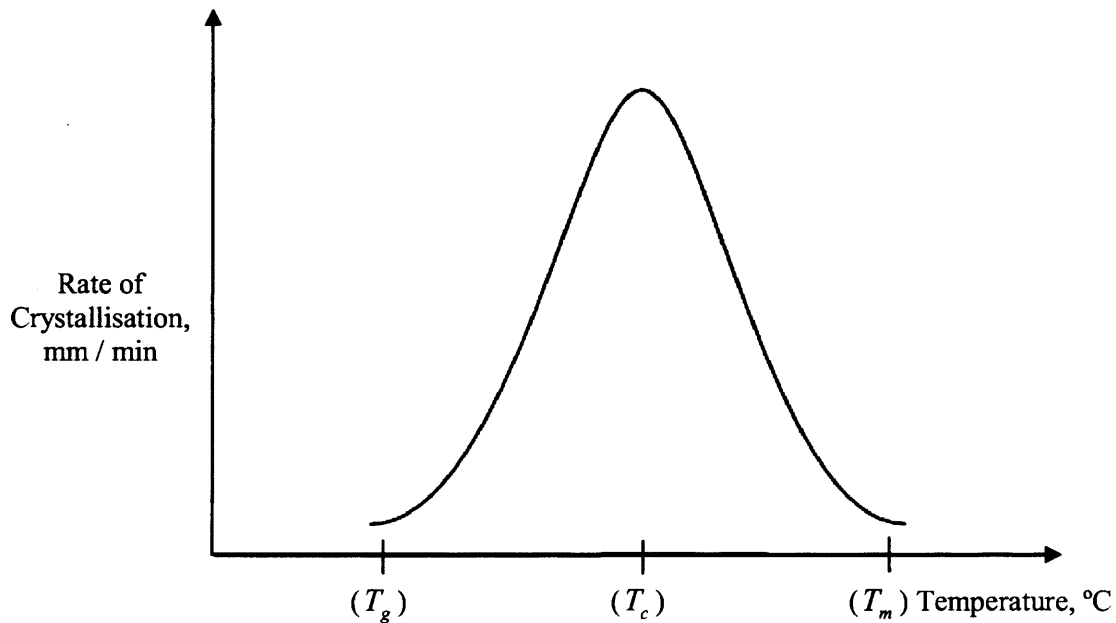
Figure 4.3 The rate of crystallisation and the temperature [Young, 1983]

Many bulk polymers crystallised from a melt create spherulites when the temperature decreases from T_m. Spherulites consist of an aggregate of chain-folded crystallites (lamellae) which radiate from the centre and can grow to be spherical in shape, as shown in Figure 4.3 [Young, 1983].

According to Young [Young, 1983], the spherulite radius is a function of time and the growth rate is written as:

$$r = vt$$

where r is the spherulite radius, t - the cooling time and v - the growth rate. In this equation, v is strongly dependent on the crystallisation temperature T_c of the polymer.

The crystallisation growth rate depends on the degree of supercooling, ΔT:

$$\Delta T = T_m^o - T_c$$

where ΔT is the degree of supercooling, T_c - the crystalline temperature of the PA12 powder, and T_m^o - the equilibrium melting point of a completely crystalline PA12 material.

During the LS process at a temperature higher then T_g, the PA12 molecule chain segments experience increased mobility known as *Brownian motion*. This encourages the unstable molecules of the side group, known as *free radicals,* to attract more molecules to be attached to the molecules' chain segments (Appendix A).

The higher the temperature and time at which the powder is exposed to heat, the higher the chance that the molecule chains will become larger. This means that the longer the unsintered PA12 powder stays in the LS machine build cylinder during the build and cooling-down stages, the more the molecular chains would become larger. Ultimately, this causes an increase of the molecular weight and, therefore, an increase of the melt viscosity.

The viscosity of the molten PA12 depends on the temperature, and follows the equation:

$$\eta_0 = A \exp^{(\Delta E / RT)}$$

where η_0 is the viscosity, ΔE - the activation energy for a viscous flow, A - a constant specific to molecules mobility, R - the universal gas constant, and T - the absolute temperature.

According to this equation, the increase of the temperature significantly reduces the PA12 viscosity [Beaman, 1997]. Also in the LS process, the temperature on the top of the part bed is constantly kept close to T_m and low laser power, therefore, is required to maintain low viscosity during the process [Bower, 2005].

The material deterioration takes place between T_g and T_m. Between these temperatures, nearly molten PA12 powder starts to crystallise. The crystallisation rate depends on the degree of supercooling [Hedge, 2004].

Due to the thermal processes explained earlier, the "New PA12" powder experiences morphology changes.

The relatively larger amorphous region of the "New PA12" powder has molecular chains most ready to become longer and entangle during the LS process, as illustrated in Figure 4.4.

"New PA 12" powder   "Recycled PA 12" powder
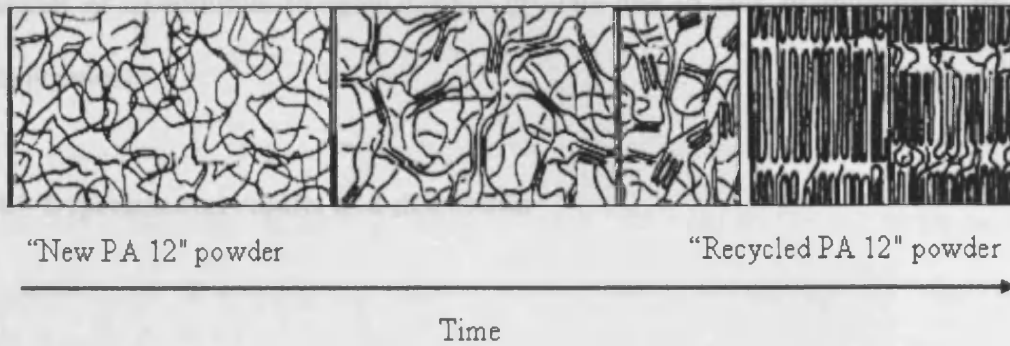
Time

Figure 4.4 Morphology changes "New PA12 " and "Recycled PA12" in time

Longer molecular chains in the "Recycled PA12" morphology means higher molecular weight and melt viscosity, which ultimately will affect the material sintering properties and part quality.

Spherulites growth

"New PA 12" powder   "Recycled PA 12" powder
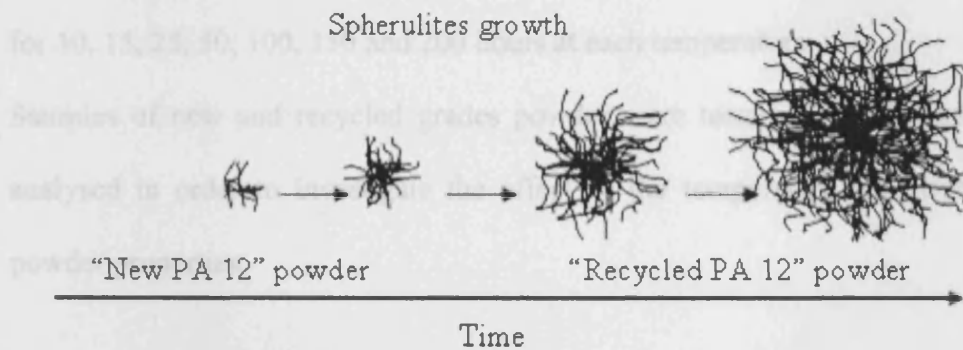
Time

Figure 4.5 Spherulite growths in "New PA12" and "Recycled PA12" powder in

time.

As schematically show in Figure 4.5, the crystal growth takes place by a chain folding mechanism that is influenced by the degree of supercooling and the time to form a bigger spherulite [Young, 1983]. At this phase, the growth process gradually slows down to temperatures close to T_g . During this stage, diffusion takes place, where the polymer chains are unable to move easily and to form

nuclei or to continue to grow further crystals due to lack of movement in the molecules.

4.3 Experimental results and discussion

4.3.1 Methodology and equipment used

The LS material investigated in this study is PA12-based powder PA2200 supplied by EOS GmbH. Samples of un-sintered (loose) powder were placed in a temperature controlled oven, *Heraeus Instruments* Vacutherm type 6060M, in a Nitrogen rich atmosphere. They were heated at a specified temperature for a period in order to simulate the conditions of the LS process. The samples were heated at temperatures 100°C, 120°C, 140°C, 150°C, 160°C and 180°C and kept for 10, 15, 25, 50, 100, 150 and 200 hours at each temperature.

Samples of new and recycled grades powder were tested, and the results were analysed in order to investigate the effect of the temperature and time on the powder properties.

4.3.1.1 Melt Flow Rate Indexer (MFR)

The Melt Flow Rate (MFR) measures the flow viscosity of a molten polymer when extruded through a capillary die under specific temperature and load conditions. The flow ability of any polymer depends on its chemical structure. Polymer chains with simple geometry and short length "slide" past one another relatively easily with low flow resistance. By contrast, long chains of high molecular weight and complex structure yield greater flow resistance or viscosity [Barnes, 1998; Martin et al., 2001; Martin, 2006].

The MFR was selected as a criterion because the flow characteristics of a molten polymer are very sensitive to changes in the basic polymer structure and its molecular weight [Van Waser, 1963; Shearman, 1970; Martinet al., 2002; Gornet, 2002a,b]. The basic polymer property which is measured by this test is the molten plastic flow at a particular shear stress (related to the applied load) and temperature as illustrated in Figure 4.6. In this case, the MFR test provides a relatively fast and inexpensive method of measuring the rate of PA12 powder degradation because of the LS process.

For each sample, 6 MFR measurements were taken to calculate the (average) result. The coefficient of variation of this experiment is about ± 3 %. The MFR experiments were performed according to ISO1133 standard [ISO1133, Thermo Haake, 2000]. A small amount of PA2200 material (8-10 grams) was extruded for 10 minutes, at a temperature of 235 °C under a weight of 2.16kg. The measured MFR units are in g/10 min.
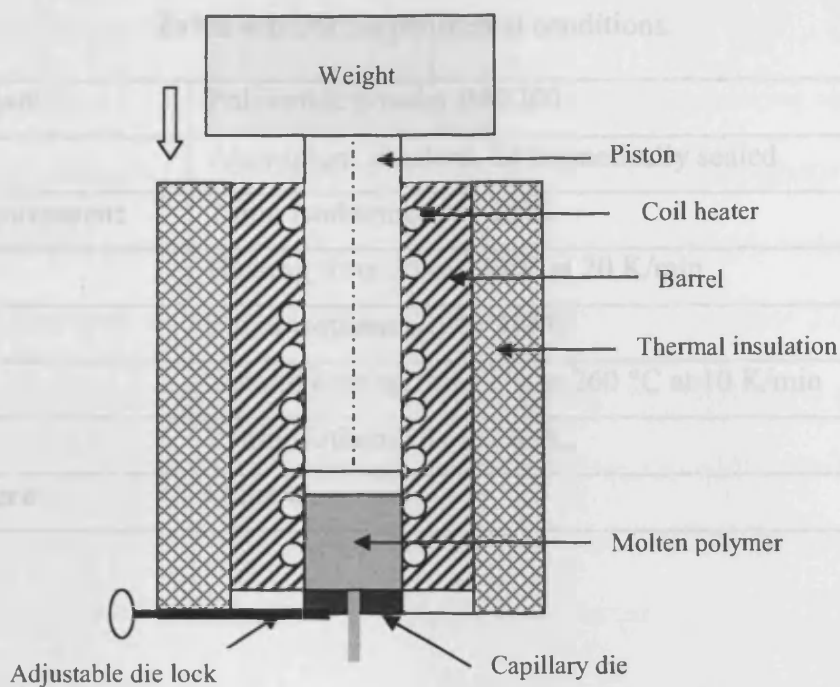
Figure 4.6 The cross sectional view of melt flow rate indexer measurement equipment [Crawford, 1990].

4.3.1.2 Differential Scanning Calorimetry (DSC)

DSC is a technique used to study the behaviour of polymers when they are heated. It can provide valuable information about the thermal transitions in the PA12 powder material corresponding to its behaviour during the LS process. A Mettler DSC 20 calorimeter from *Mettler Toledo* was used in this study. For the DSC, the temperature accuracy is +/- 0.2K and the heat flow accuracy is +/- 2% [ISO11357, Hatakeyama and Liu, 1999]. An example of DSC sample testing is shown in Figure 4.7, it measures respectively, the temperature difference and the heat flow difference between a sample and to an inert reference. The experimental conditions during the DSC analysis are summarised in Table 4.1.

Table 4.1 DSC experimental conditions.

Sample state	Polyamide powder PA2200
Crucible	Aluminium standard, lid hermetically sealed
DSC measurement	2 min isothermally to 25ºC
	Heating from 25 to 230°C at 20 K/min
	2 min isothermally to 230ºC
	Second heating from 230 to 260 °C at 10 K/min
	2 min isothermally to 260ºC
Atmosphere	Quiet air

Figure 4.7 DSC sample testing

4.3.1.3 Gel permeation chromatography (GPC)

GPC is a primary technique for characterising polymers and measuring molecular weight and molecular weight distributions [Shi et al., 2004; Zarringhalam et al., 2006; ISO16014]. In this experiment, the *DI* is measured using this technique. It separates polymers on the basis of their size relative to the polymer molecules. The GPC experiments were performed according to ISO16014 standard [ISO16014]. The chromatographic conditions during the GPC analysis are summarised in Table 4.2. As guideline, a 5% variation in molecular weight and 10% in the number of molecular weight should be expected.

Table 4.2 Chromatographic conditions

Sample state	Polyamide powder PA2200
Instrument	Polymer laboratories GPC 120. with PL GPC-AS MT heated autosampler
Columns	PL gel guard plus 2 X mixed bed-B, 30cm10μm
Solvent	1,3-cresol with anti-oxidant
Flow-rate	0.8 mL/min (nominal)
Temperature	PL GPC 120: 115°C (nominal) PL GPC-AS MT :80°C (nominal)
Detector	Refractive index

4.3.2 Thermal properties of new and recycled PA12 powders

The thermal properties of new and recycled grades PA12 powders were tested using DSC analysis (Appendix A). The purpose was to study the changes of the material thermal properties and morphology during the LS process. The assumption was that the deterioration of the PA12 material would lead to changes in the thermal properties (T_g, T_m, and T_c) and morphology (MFR) which ultimately would influence the LS process and fabricated part quality.
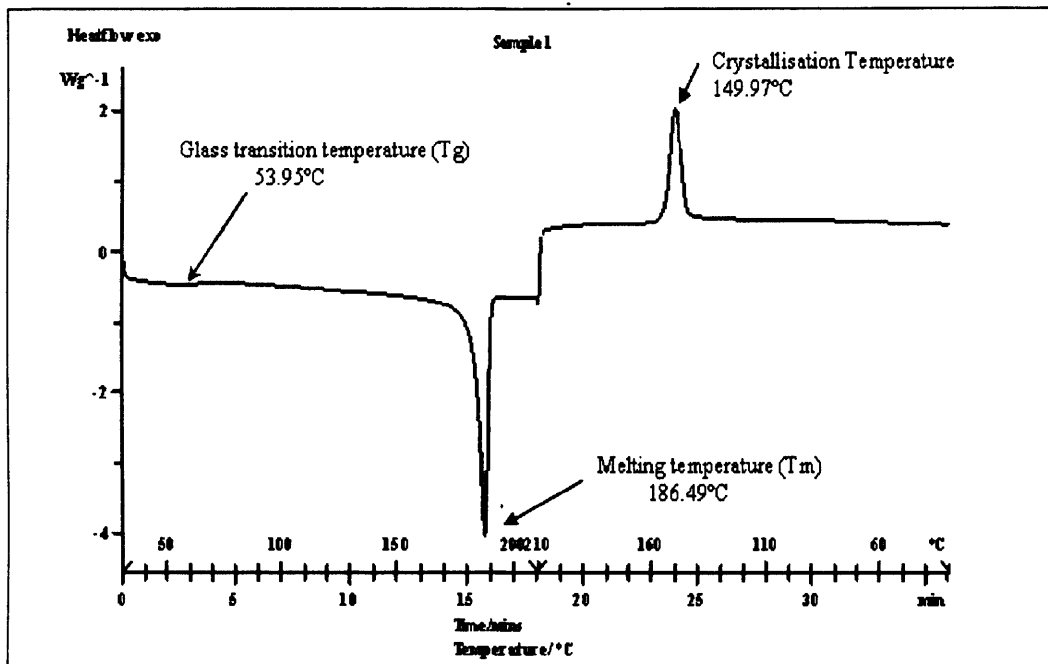
Figure 4.8 DSC plot of "New PA 2200" powder

Figure 4.8 is a DSC plot which illustrates the first and second order transitions of a "New PA2200" powder sample when heated from 25°C to 260°C and then back to 26°C. At glass transition temperature T_g, the polymer heat capacity increases and this can be observed as a slight curve sink as marked in Figure 4.8. The

melting temperature T_m and crystallisation temperature T_c can be determined

from the plot as "jumps" due to the latent heat involved (see marks in Figure 4.8).

The results of DSC analysis for samples of new PA12 and different grades of

recycled PA12 are summarised in Table 4.3.

Table 4.3 Comparison of different PA12 powder grades and their thermal

properties

PA12 powder	Melt Flow Rate (MFR) g/10min	Glass Transition Temperature (T_g),°C	Melting Temperature (T_m),°C	Crystallisation Temperature (T_c),°C
"New PA2200"	51.50	53.95	186.49	149.97
"35% New + 65% 1 x Recycled"	33.13	56.93	187.22	150.11
"1 x Recycled"	28.90	57.78	188.53	148.82
"2 x Recycled"	17.41	56.93	189.27	148.27
"3 x Recycled"	13.50	58.11	191.48	147.26

These results show that powder quality, thermal properties and melt viscosity are

correlated. The T_g and T_m increase for PA12 powders used many times, while the

MFR decreases. Although T_g and T_m change slightly, these changes are not very

sensitive to the changes in powder deterioration. Therefore, it would be difficult to

use any of these temperatures as a criterion for controlling the powder quality and

powder recycling process. In contrast, the MFR responds significantly to small

changes in PA12 powder quality due to deterioration. For instance, when 65%

"1X Recycled" material is mixed with 35% "New material", the MFR changes

from 28.9 to 33.13, while the T_g and T_m decrease by only 1°C. The higher MFR

means better PA powder quality. The lower the MFR and T_c, and the higher the

T_m and T_g the worse is the PA powder quality.

The relationship between T_g, T_m, T_c and MFR is shown in Figure 4.9, 4.10 and

4.11.
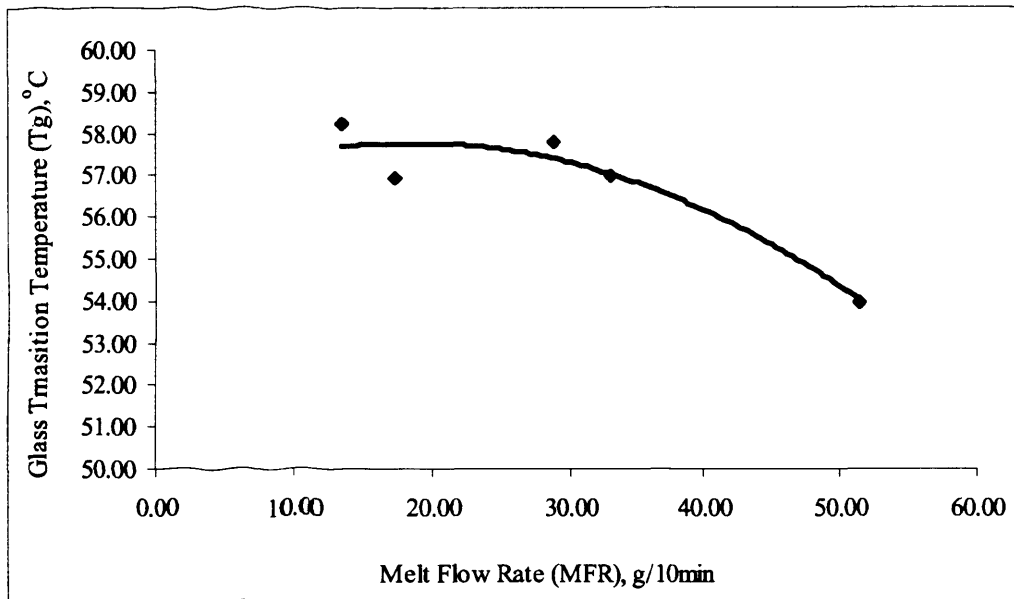
Figure 4.9 Glass transition temperatures (T_g) vs. melt flow rate (MFR)

In Figure 4.9, the lowest T_g is observed at the DSC plot of a "New PA2200"

sample. T_g increases from 54°C ("New PA2200") to 58°C ("3X Recycled"). This

is only a 4°C difference between T_g of new powder and very old powder used for

more than 200 hours ("3X Recycled").
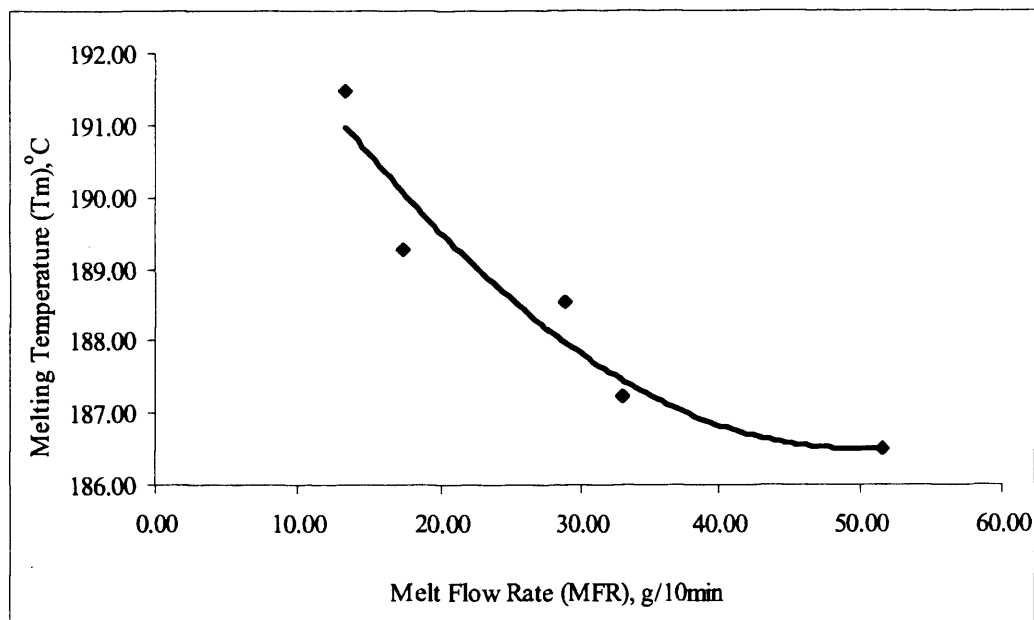
Figure 4.10 The melting temperature (T_m) and the melt flow rate (MFR).

In Figure 4.10, the T_m increases progressively with the decrease of the MFR. This is because a higher melt viscosity polymer has spherulites of a bigger size, as mentioned in section 4.2. In addition, a higher entanglement with a longer molecule chain causes a higher resistance to flow. T_m changes from 186.5°C ("New PA2200") to 191.5°C ("3X Recycled"), which is only a 5°C difference.
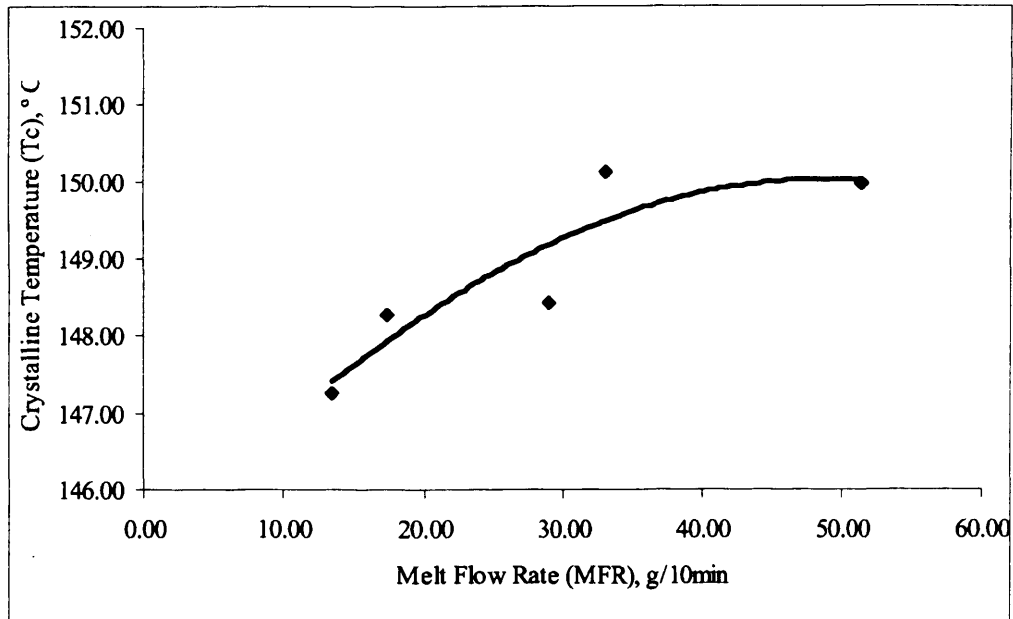
Figure 4.11 The correlation between crystallisation temperature (T_c) and the

MFR.

As shown in Figure 4.11, T_c increases for the samples with higher MFR. This is

because the PA12 polymer with higher MFR has a lower molecular weight

average ($M_{\bar{w}}$) and molecular number average ($M_{\bar{n}}$). In other words, "New

PA12" powder with shorter chain molecules and higher disorder region would

easily form chains with a parallel array structure.

4.3.3 The relationship between the Molecular weight and the MFR

As mentioned earlier in section 4.2, theoretically the polymer viscosity and $M_{\bar{w}}$ are closely related. In this experiment, $M_{\bar{w}}$ and $M_{\bar{n}}$ of different quality PA12 powder were measured using Gel Permeation Chromatography (GPC) [Shi et al., 2004; Zarringhalam et al., 2006; ISO16014].

Table 4.4 shows the relationship of the MFR, $M_{\bar{w}}$ and $M_{\bar{n}}$. The new PA12 powder with the highest MFR has the lowest viscosity, with less resistance to flow. This means that it is the readiest to enlarge the crystalline region. On the other hand, the more PA12 powder is recycled, the longer are the molecule chains and the higher the chain entanglement.

Table 4.4 The relationship of MFR, $M_{\bar{w}}$, and $M_{\bar{n}}$ of different grades PA12 powder

PA12 powder	Molecular weight average $(M_{\bar{w}})$	Molecular number average $(M_{\bar{n}})$	Melt Flow Rate (MFR), g/10min
"New PA"	76950	38800	50.1
"35% New + 65% 1 x Recycled"	122500	63100	33.15
"1 x Recycled"	157000	71500	28.90
"2 x Recycled"	201000	97100	17.41
"3 x Recycled"	926500	111000	13.50

It has been also found that there is a correlation between $M_{\bar{w}}$ and the degree of crystallinity *(Dc)* of the PA12 powder, where the higher $M_{\bar{w}}$ and $M_{\bar{n}}$ decrease the *Dc*.

A higher $M_{\overline{w}}$ causes chain folding to become less regular and the degree of crystallinity decreases. This is due to the freedom of chains to rearrange themselves during crystallinity decreases [Bower, 2002].

The Dc of the polymer can be calculated from the DSC plot. This requires T_m determination of the heat of fusion at T_m of the test sample and purely crystalline material. The Dc of the polymer sample is calculated as follows [Belofsky, 1995]:

$$Dc = \frac{\Delta h_f}{\Delta h_c} X100$$

Where Δh_f is the heat of fusion of the test sample, Δh_c - the heat of fusion of purely crystalline material. The heat of fusion for 100% crystalline material was taken as 209.3 J/g [Zarringhalam et al., 2006 and Gololewski et al.,1980].
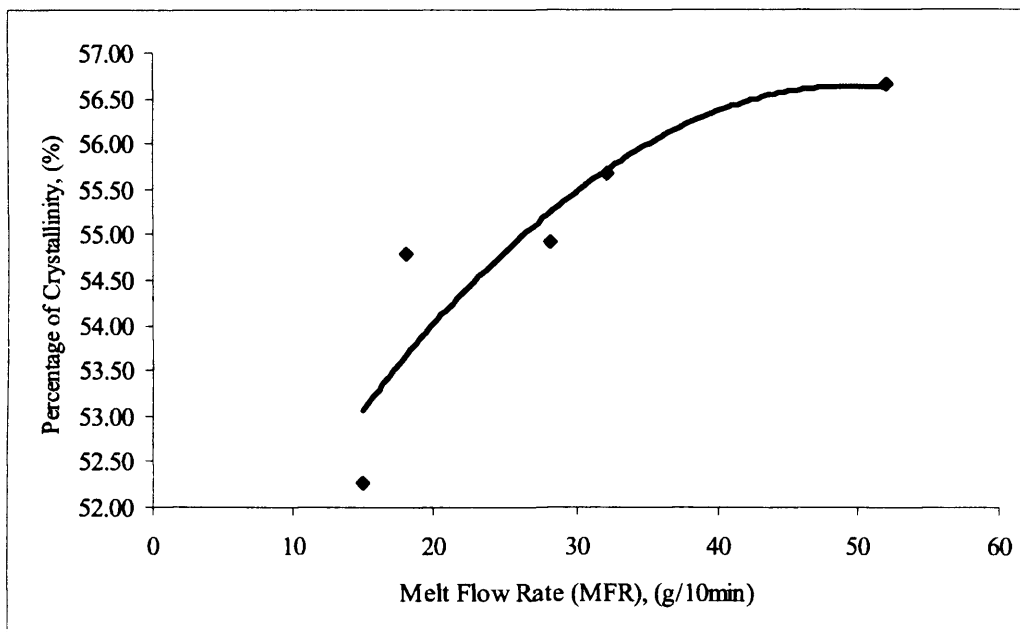
Figure 4.12 The percentage of crystallinity at different MFRs.

Figure 4.12 shows the relationship between the MFR and the Dc. The samples of "New PA2200" have larger Dc and higher MFR compared to the samples of the

older or recycled powder. These results support the analysis of the process of powder deterioration (section 4.2) and the hypothesis of the enlargement of the crystalline region in the new PA12 powder.
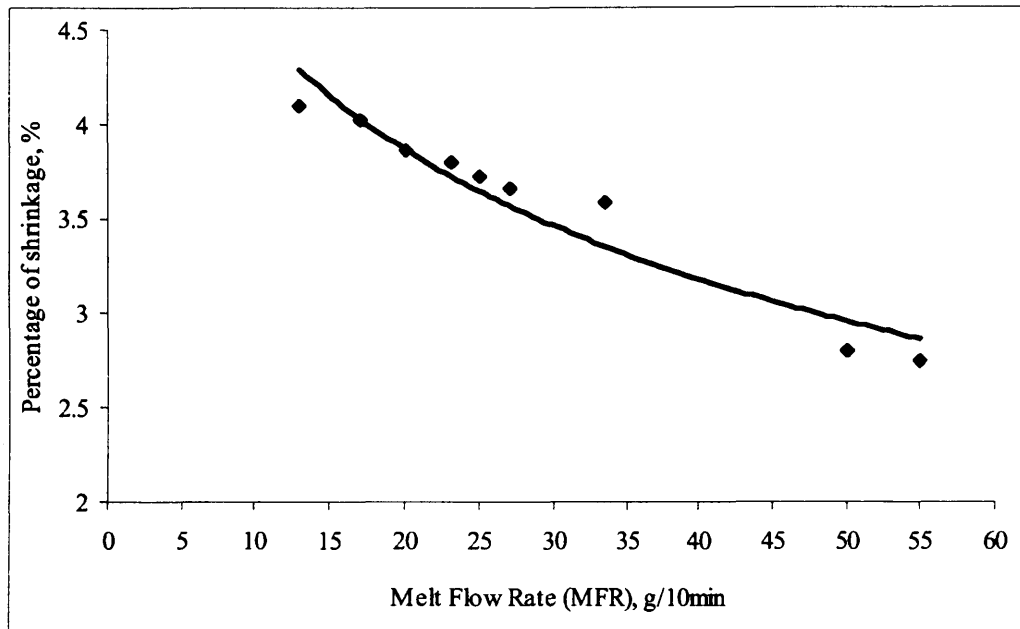
Figure 4.13 The shrinkage and MFR

Figure 4.13 depicts the average shrinkage of LS parts built from PA2200 powder with different grade and MFRs. As explained earlier in section 4.2 and Figure 4.4, more efficient packing of the PA12 polymer chains causes higher melt viscosity, which also leads to an increase in the LS part's shrinkage.

4.3.4 The effect of the time and temperature on the T_g and T_m

In this experiment, the "New PA2200" samples were exposed at 100°C to 160°C temperature in an oven with a nitrogen atmosphere. The purpose is to simulate the deterioration of the PA2200 powder in the build cylinder during the LS process.
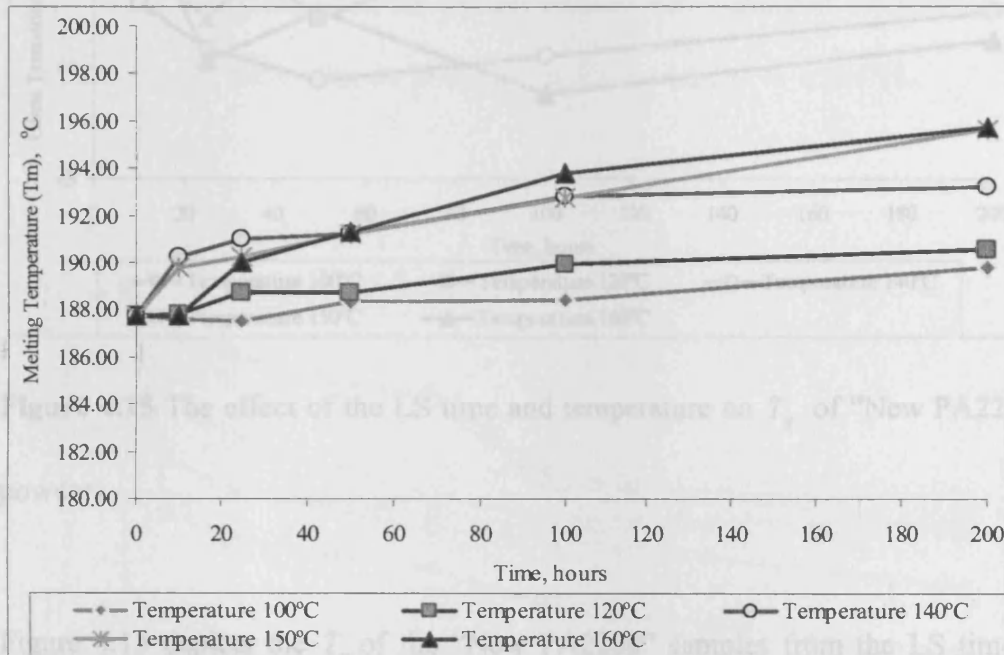
Figure 4.14 The effect of heating time and temperature to T_m of "New PA12" powder.

As shown in Figure 4.14, the melting temperature of PA12 samples is a function of the heating period. The samples heated at 140°C, 150°C and 160°C experience an increase of T_m of approximately 4°C to 7°C within 200 hours. However, the T_m of the samples heated at 100°C, and 120°C, increases just about 2°C to 3°C only for the same period. These results demonstrate that temperatures above

140°C are more damaging to the material properties that those below 140°C.
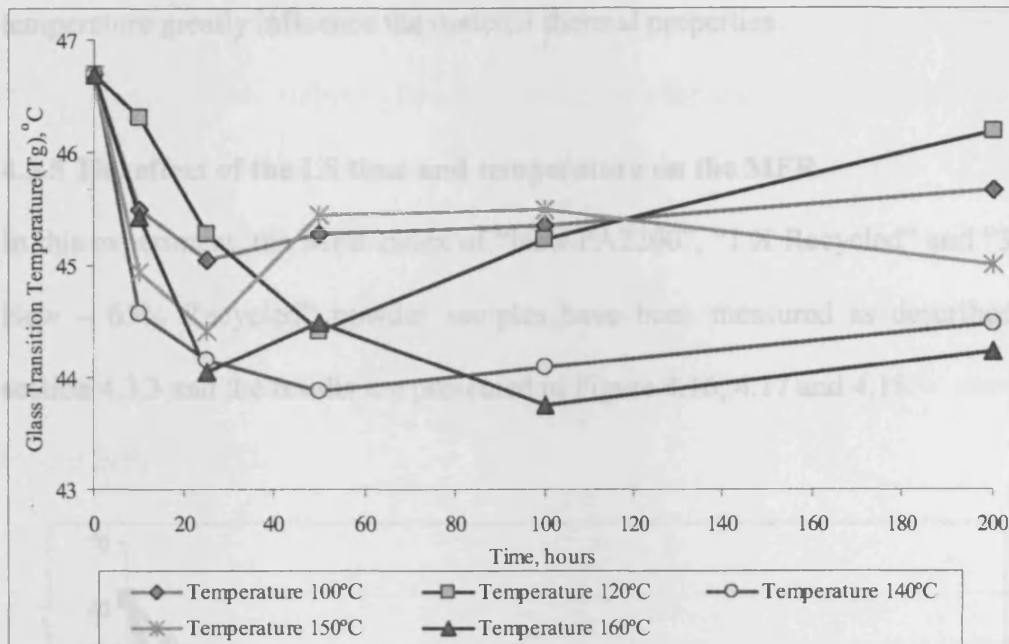
Figure 4.15 The effect of the LS time and temperature on T_g of "New PA2200" powder.

Figure 4.15 depicts the T_g of the "New PA2200" samples from the LS time at different temperatures. The main changes occur during the first 20-25 hours. Generally, the T_g reduces with the increase of the LS time, especially for samples heated at temperatures higher than 140°C. Only the samples heated at 100°C have a relatively stable T_g.

A limitation of DSC analysis is that the T_g is not clearly apparent from the DSC curve if the polymer has large crystalline region, as in our case. This is why the graph contains some inconsistencies.

The results presented in sections 4.3.2, 4.3.3, and 4.3.4 shows that the LS time and temperature greatly influence the material thermal properties.

4.3.5 The effect of the LS time and temperature on the MFR

In this experiment, the MFR index of "New PA2200", "1 X Recycled" and "35% New – 65% Recycled" powder samples have been measured as described in section 4.3.3 and the results are presented in Figure 4.16, 4.17 and 4.18.
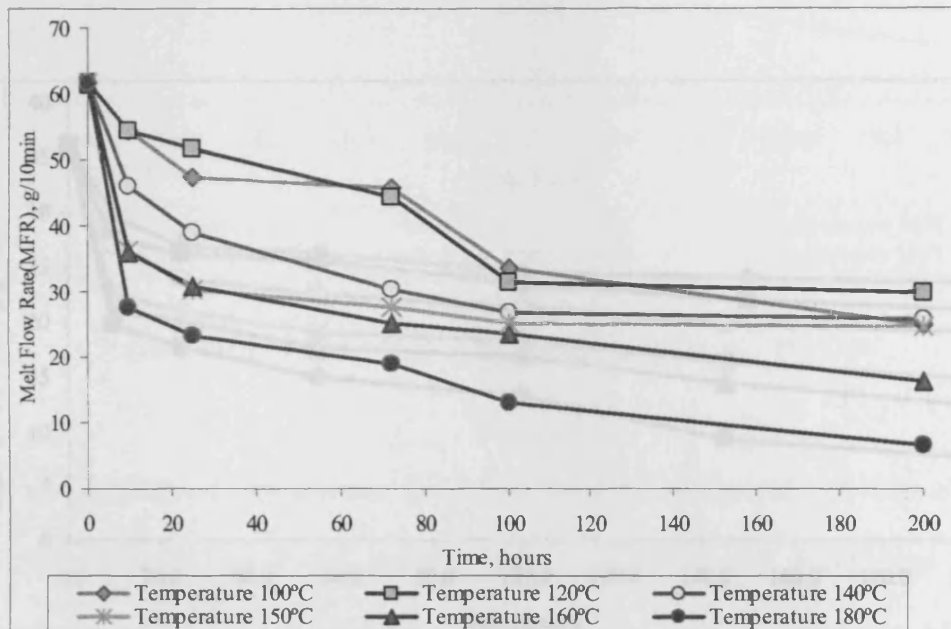
Figure 4.16 Melt flow rate (MFR) of "New PA2200" powder.

In all cases the powder heated at temperatures below 140 º C has a higher MFR and experiences less deterioration compared to the powder heated at a higher temperature. For instance, the fastest deterioration rate takes place at 180º and the MFR declines steeply in comparison to other samples heated at lower temperatures. The samples heated below 150 ºC represent the powder which is at the periphery of the build cylinder. The MFR of these samples is between 30

g/10min and 35 g/10min even after 200 hours of continuous heating. By contrast, those heated above 150 °C represent the material which is in the middle of the build cylinder. They experience much faster deterioration and their MFR drops from 60 g/10min to 25 g/10min after the first 10-15 hours. In general, all PA12 samples experience significant deterioration and MFR reduction after the first 25 hours. After that the deterioration is slower and the MFR declines gradually as shown in Figure 4.16. The slowest deterioration was experienced by the samples heated below 120°C.
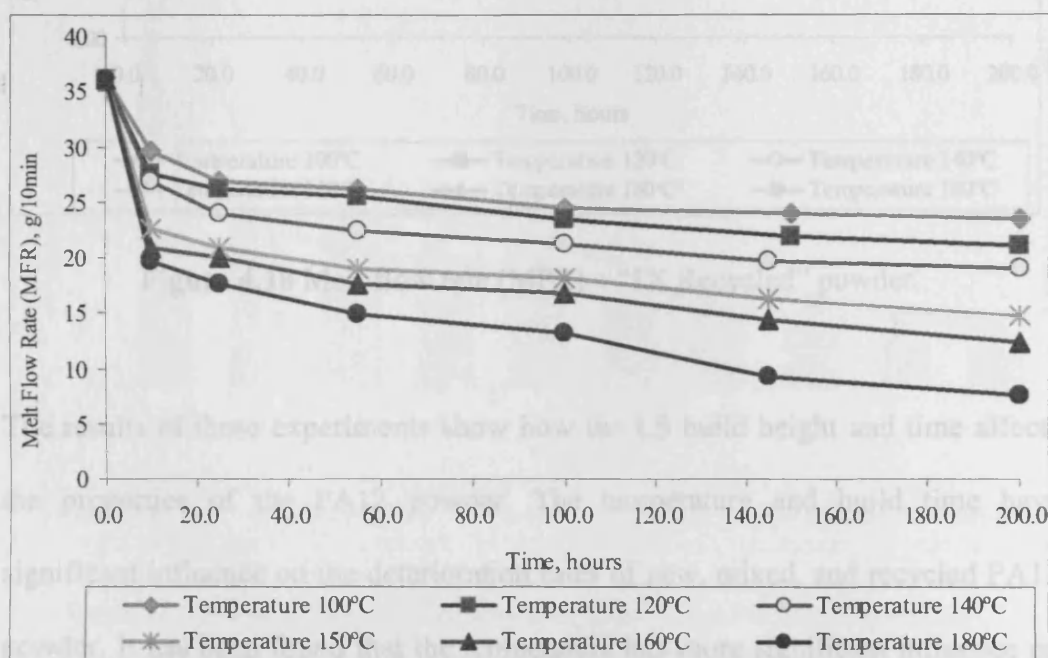
Figure 4.17 Melt flow rate (MFR) – "35% New PA with 65% Recycled" powder.

Figure 4.17 and Figure 4.18 show the results from the experiments with "35% New PA12 with 65% Recycled" and "1x Recycled" samples with initial MFRs of 36.31 g/10min and 28.16g/10min respectively. In both cases the MFR drops less drastically within the first 15-20 hours in comparison to 100% "new PA" samples.

However, after 50 hours of heating all samples experience a continuous decrease

in their MFR.
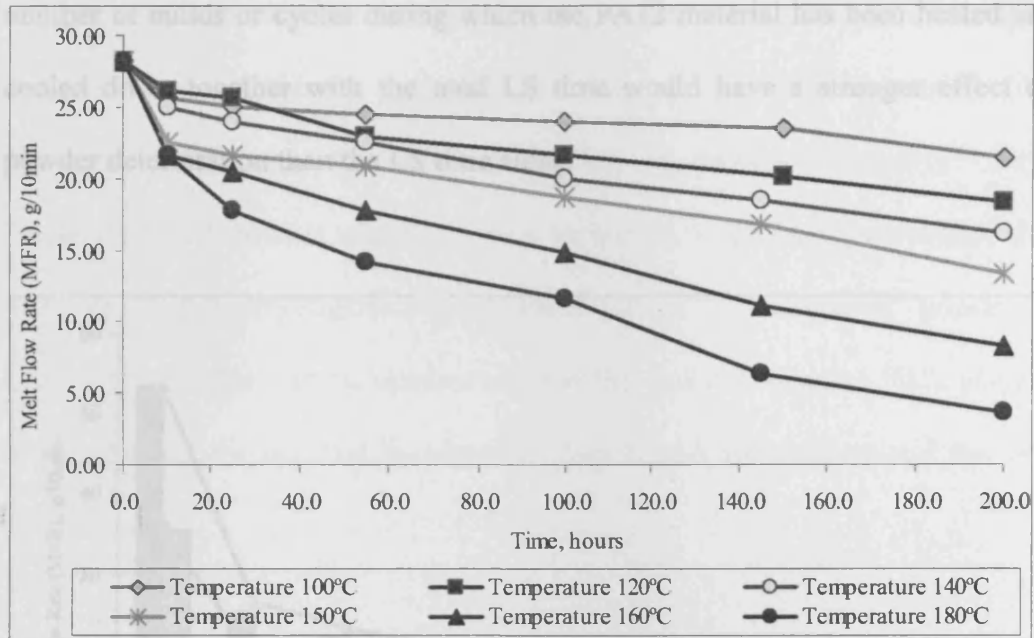
Figure 4.18 Melt flow rate (MFR) – "1X Recycled" powder.

The results of these experiments show how the LS build height and time affects

the properties of the PA12 powder. The temperature and build time have

significant influence on the deterioration rates of new, mixed, and recycled PA12

powder. It has been found that the temperature has more significant influence on

the powder deterioration rate than the LS time. The experiments also show that

the measurement of the powder MFR is a very accurate and efficient method of

investigating the deterioration of the PA12 powder and can be used to control the

quality of the input material in the LS process.

4.3.6 The effect of the number of builds on the MFR

In the experiments presented in section 4.3.5, the powder samples were subjected to continuous heating for up to 200 hours. However, it is not clear whether the number of builds or cycles during which the PA12 material has been heated and cooled down together with the total LS time would have a stronger effect on powder deterioration than the LS time alone.
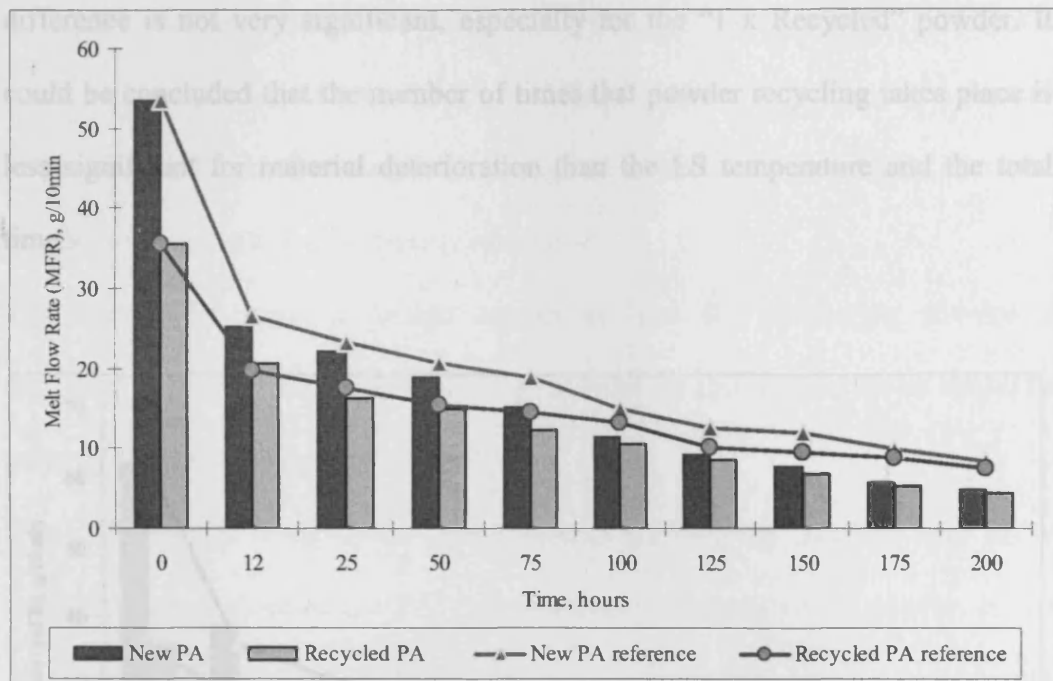
Figure 4.19 Two different conditions of simulating PA samples at 180°C.

In this experiment, "New PA2200" and "1X Recycled" PA12 powder samples were placed in the oven at temperatures 180°C and 160°C (section 4.3.6), and heated for 12 hours. Then they were taken out and cooled down to room temperature. After measuring and recording their MFR, they were returned back into the oven for another 12 hours. This procedure was repeated in 25 hour periods for up to 200 hours in total. The results of these experiments are shown in

a bar chart format in Figure 4.19 and 4.20. In parallel to this, a second set of samples were continuously heated without being cooled down. Their MFR was measured at the same intervals and plotted as reference points in Figure 4.19 and 4.20. These results show a clear trend of a higher deterioration rate of the samples subjected to cycle heating against those subjected to continuous heating. The maximum difference in the MFR occurs after 5-6 times of "recycling" of the "New PA2200" powder samples and it is within 3-5g/10min. Generally, this difference is not very significant, especially for the "1 x Recycled" powder. It could be concluded that the number of times that powder recycling takes place is less significant for material deterioration than the LS temperature and the total time.
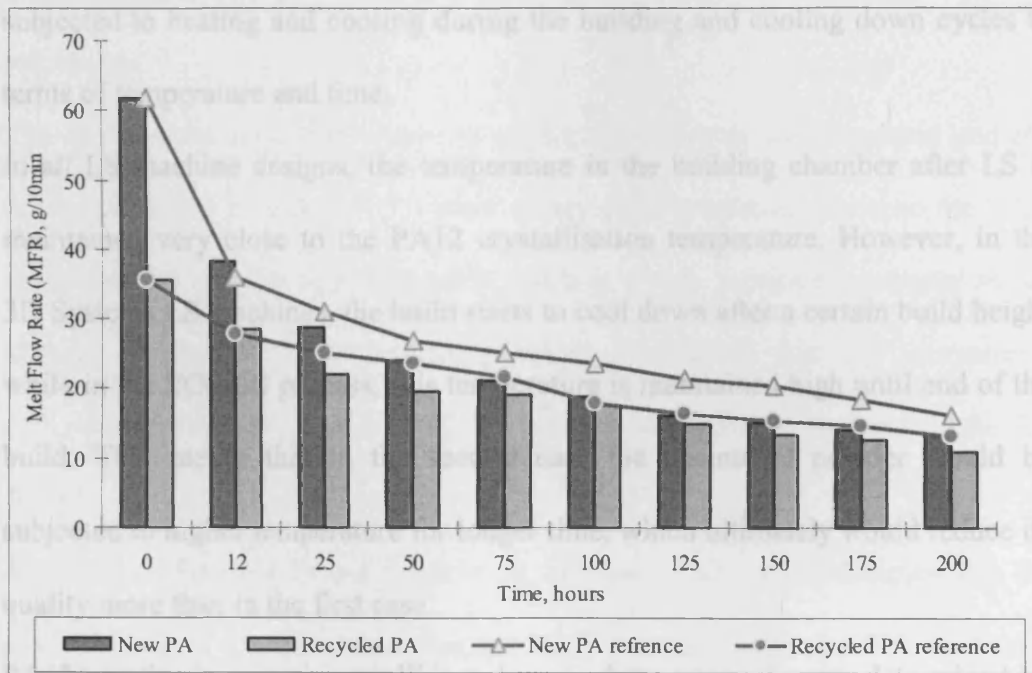
Figure 4.20 Two different conditions of simulating the PA12 samples at 160°C.

4.4 Discussion

PA12-based powders are the most used materials in the LS process for RP and RM of plastic parts. An average of 80% to 90% of the powdered material in the building chamber is not sintered during the LS and could be reused. However, the PA12 powder properties deteriorate due to the high temperature, close to the material melting temperature, for a long period of time through the LS building and cooling cycles. The recycled powder needs to be blended with a sufficient quantity of new material in order to produce parts with good quality. Adding too much new powder would increase the cost because of the high cost of the powder within the total manufacturing cost. Using too old recycled powder or less new powder would result in poor quality and waste.

The specific LS machine design determines how the unsintering powder is subjected to heating and cooling during the building and cooling down cycles in terms of temperature and time.

In all LS machine designs, the temperature in the building chamber after LS is maintained very close to the PA12 crystallisation temperature. However, in the 3D Systems LS machines, the build starts to cool down after a certain build height while in the EOS LS process, this temperature is maintained high until end of the build. This means that in the second case the unsintered powder would be subjected to higher temperature for longer time, which ultimately would reduce its quality more than in the first case.

PA12 powder is a semi-crystalline polymer whose properties are determined by the molecular morphology. After being repeatedly recycled during the LS process, the powder deteriorates and becomes less viscous, which ultimately affects the quality of the LS process and the part quality. It causes a decrease of the

crystalline region, enlargement of the chain molecule segments, more efficient packing, and ultimately larger molecular weight (M_w and M_n). Another consequence of the increased packing of the polymer chains is the higher material shrinkage and, as a result, poor dimensional accuracy.

Ultimately the powder ageing affects the PA12's thermal and mechanical properties. In order to understand this process, samples of PA2200 powder with different grades were artificially aged in a temperature-controlled oven by heating at different temperatures and held for different periods of time. DSC analysis was employed to determine T_m, T_g, and T_c of the samples. T_m and T_g increase by 4-5 °C with powder usage while T_c reduces insignificantly. Generally, DSC analysis is not a very practical method for measuring the powder deterioration because it is relatively slow and expensive and also that the error is compatible with the resolution.

The MFR or the melt flow viscosity of the samples was also measured and the results presented in section 4.3.3 show a very good correlation between the MFR index and the powder age. The MFR index is a very sensitive parameter to the changes in powder properties and provides a relatively fast and inexpensive method of measuring the rate of the powder degradation caused by the LS process.

As shown in Figure 4.19 and Figure 4.20, the new PA12 powder samples with the lowest viscosity experience the highest deterioration rate in the first 20 hours. After that, the deterioration rate gradually declines at a lower rate. The PA12 powder exposed at the higher temperature experienced a much higher deterioration rate. The temperature at which the unsintered PA12 material was exposed and the duration of this exposure are the most influential parameters for

powder aging and deterioration of material properties. Tests performed in section 4.3.6 proved that the number builds or the number of times powder recycling takes place is less significant than the LS temperature and total time of the process on material deterioration.

4.5 Summary

One of the challenges which LS faces is the RM of plastic parts with good consistent quality. This is due to the fact that plastic powder properties deteriorate during the long periods of time through the LS building and cooling cycles. The influences of temperature and time are found to be of significant influence on the deterioration of PA12 powder.

CHAPTER 5

IMPROVEMENT OF PART SURFACE FINISHING IN LASER

SINTERING BY EXPERIMENTAL DESIGN OPTIMISATION (DOE)

5.1 Preliminaries

The powder properties and process parameters have a great influence on the

mechanical properties and surface qualities of the LS parts. Therefore, it is

important to obtain a better understanding of the relationship between part quality,

powder properties, and LS process parameters [DTM, 1996a; Gibson and Shi,

1997]. The objectives of this research are to improve the surface quality of parts

produced by Laser Sintering (LS) and to reduce or eliminate the rough surface

texture known as "Orange Peel" by optimising the LS process parameters.

5.2 Fabrication of a part using LS

The details of the fabrication of a part using LS process have been explained in

detail in the previous section 2.2. All of the PA12 powders are processed in a

similar way during the LS process. They are exposed to long heating and cooling

cycles, at temperatures very close to the material melting temperature in a

Nitrogen rich atmosphere. These processing conditions cause physical and

chemical changes of the powdered material and deterioration of its mechanical

and thermal properties. As mentioned previously in section 2.5, the non-sintered

powder can be recycled and reused for another fabrication after being blended

with new material. If the amount of new powder is not sufficient or if only recycled material is used, then the fabricated parts experience variation in their quality, higher shrinkage, and a rough surface texture known as "orange peel". (section 3.1a).
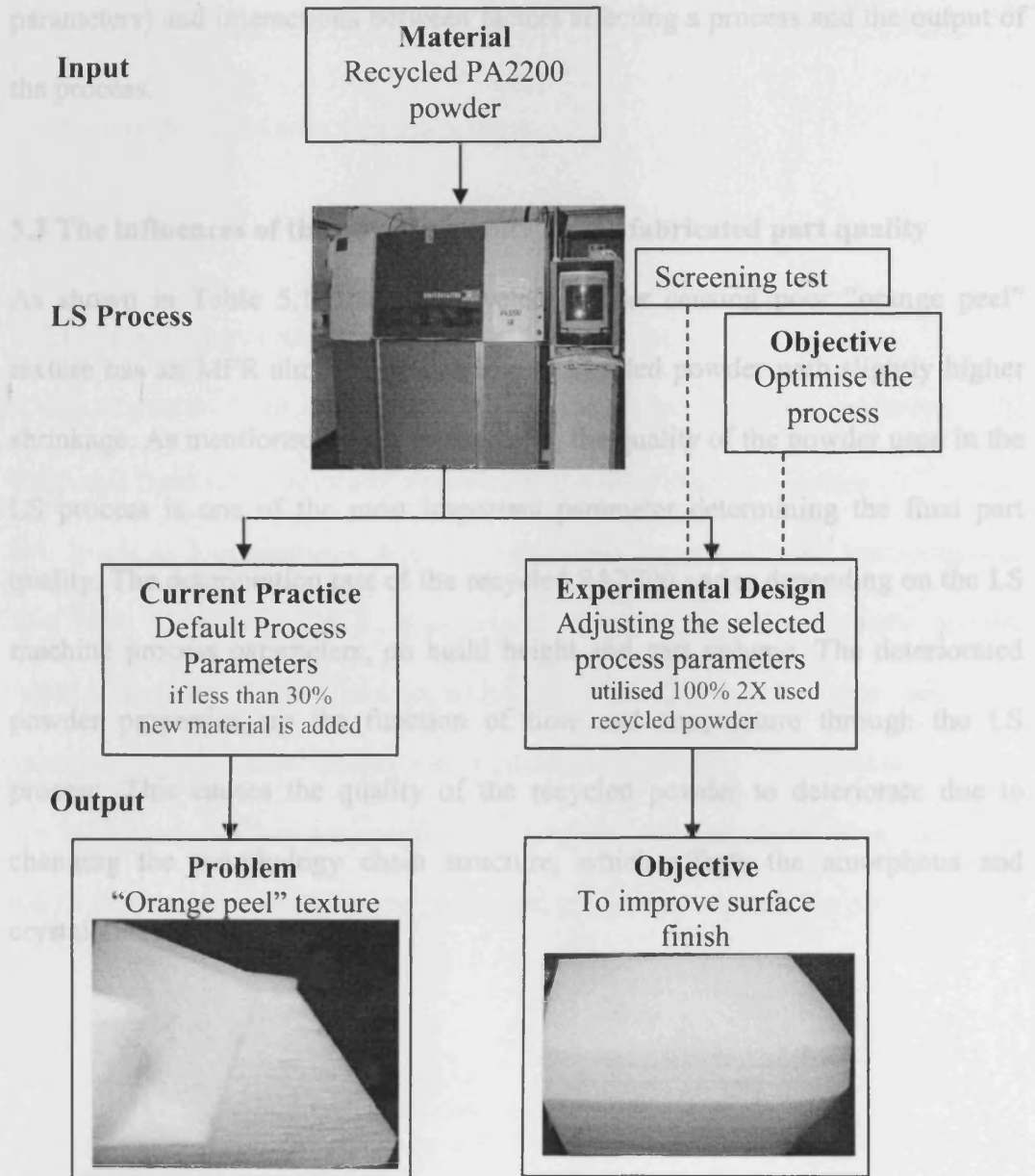
Figure 5.1 The problem identification of the current practice and DOE objective.

As shown in Figure 5.1, this study focuses on one of the major limitation of LS. Current practice, which utilises recycled PA12, causes poor texture known as "orange peel". This research aims to reduce or eliminate this problem by implanting a Design of Experiment (DOE) approach. It is a structured, organised method for determining the relationship between factors (selected process parameters) and interactions between factors affecting a process and the output of the process.

5.3 The influences of the powder quality on the fabricated part quality

As shown in Table 5.1, the old recycled powder causing poor "orange peel" texture has an MFR almost twice as low as blended powder with slightly higher shrinkage. As mentioned earlier in chapter 3, the quality of the powder used in the LS process is one of the most important parameter determining the final part quality. The deterioration rate of the recycled PA2200 varies depending on the LS machine process parameters, on build height and part volume. The deteriorated powder properties are the function of time and temperature through the LS process. This causes the quality of the recycled powder to deteriorate due to changing the morphology chain structure, which affects the amorphous and crystalline regions.

Table 5.1 The properties of different powders qualities affect the LS part quality.

	Melt Flow Rate (MFR), g/10min	Shrinkage (%)	Part Quality
35% New + 65% 1X recycled PA2200	33.13	3.5 to 3.7	Good
Twice recycled PA2200	18-19	3.8 <	Poor quality with "orange peel" texture

5.4 Experimental results and discussion

5.4.1 Methodology and equipment used

A Sinterstation 2500 HiQ machine was employed in the experiment. The fractional factorial of design of experiment (DOE) at half five factors (2^{5-1}), with two levels at 3 replications, were experimentally tested after the screening test. The Melt Flow Rate (MFR) was selected to determine the recycled powder quality. Recycled PA2200 powder with 18-19 MFR (2X recycled) was used in the experiments. The score system was introduced to evaluate the response variable. An individual part surface quality was justified through observation, feel, and touch. Optimisation actions were performed in order to improve the part quality.

5.4.1.1 DOE experimental approach to reduce/eliminate the "Orange Peel" texture

The idea of using DOE is to identify the optimal levels of the process parameters. It is an effective tool which is commonly used to identify the most important variables (material and process fabrications), and to select the conditions that result in lowest cost, highest quality and most reliable product [Nelson and Barlow, 1992; Ellekjear, 1998; Marit, 1998; Murphy et al., 2002]. The experimental approach used in this study is described in Figure 5.2.

```
┌─────────────────────────────┐
│ Recognise the problem and   │
│ objective of the experiment │
└─────────────────────────────┘
              │
              ▼
┌─────────────────────────────┐
│      Screening test         │
│ Identify the process         │
│ parameters                  │
│ and choose levels for each  │
│ factor                      │
└─────────────────────────────┘
              │
              ▼
┌─────────────────────────────┐
│ Select the amount of        │
│ replication                 │
└─────────────────────────────┘
              │
              ▼
┌───────────────────────────────────┐
│ Run the experimental design in     │
│ random order                       │
└───────────────────────────────────┘
              │
              ▼
┌──────────────────┐
│ Data collection  │
└──────────────────┘
              │
              ▼
┌──────────────────┐
│ Data Analysis    │
└──────────────────┘
              │
              ▼
┌──────────────────────────┐
│ Results and conclusion   │
└──────────────────────────┘
```
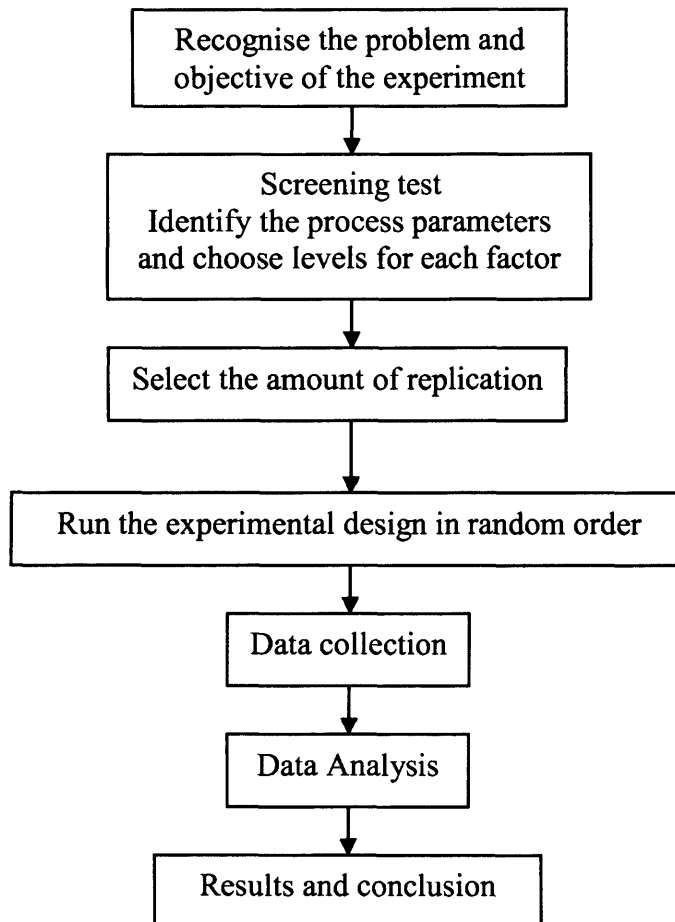
Figure 5.2 DOE experimental approach

PA2200 powder recycled several times was used in the experiment. The melt flow rate (MFR) of this powder is 18g/10min to 19g/10min. In normal LS practice, this material is mixed with 30% to 50% new powder (Table 6.2). The direct use of such material without blending with new powder would result in severe "orange peel" part texture (Figure 5.1).

5.4.1.2 Designing the benchmark part

The same benchmark part as used in the previous experiment in section 3.5.2 was designed to contain features with different thickness, shape, orientation, and surfaces with different orientation to the vertical z direction. (as shown in Figure 3.6 a and Figure 3.6b)

5.4.1.3 Selection of the Response variable (*Rv*)

The outcome of an experiment that can be observed and measured is known as a response variable (*Rv*). It is used to evaluate the resulting responses from different combinations of process parameters. In this investigation, the surface quality is measured and compared by feel and touch, and observation. The advantage of this method is that it is simple and quick because the "orange peel" texture can be easily seen.

5.4.1.4 The score system

As shown in Figure 5.3, the response score system is introduced in order to evaluate the *Rv*. Each part is individually inspected. The evaluation of the part quality from the point of view of the "orange peel" occurrence was done in accordance with a scoring system as described in Table 5.2.

Table 5.2 Scoring system for evaluation of the Rv

Description	Score	Quality
Good surface finish, NO "orange peel"	1	Acceptable
Slightly rougher surface finish, NO "orange peel"	0.5	Acceptable
Small signs of "orange peel"	0	Not Acceptable
"orange peel" texture	0	Not Acceptable

The three additional marks are given to any benchmark part which shows good surface finish and its features. For example, if all features at the bottom of the benchmark part are perfect (no defects), especially on the 1 mm thickness as shown in Table 3.3, an additional three points is given. The Rv is calculated based on the total number of scores divided by 96, which is the total number of surfaces.

```
┌─────────────────────────────────────────┐
│          Experimental design            │
│    Different setting process parameter   │
└─────────────────────────────────────────┘
                    │
                    ▼
        ┌───────────────────────┐
        │        Output         │
        │ Benchmark part sample │
        └───────────────────────┘
                    │
                    ▼
┌──────────────────────┐     ┌───────────────────┐
│    Evaluation of     │     │   Score system    │
│ part surface quality │- - -│   (Table 5.2)     │
│       through        │     └───────────────────┘
│ observation, feel and│
│        touch         │
└──────────────────────┘
```

Figure showing flowchart with Accept and Reject branches:

Accept
If good surface
and no "orange peel" texture
on the outside
benchmark part surface

Reject
If any defect and "orange
peel" texture on the outside
benchmark part surface

Response variable
$Rv_ = \dfrac{\text{No. of scores}}{\text{Total no.of outside surfaces}}$
(The accepted Rv target is 70%)

Part strength
If no features defect, 3
additional marks
are given

Figure 5.3 The response system

5.4.1.5 Screening Test

To set up the DOE, the investigator determines the factors to be studied and the levels for each of the factor. The screening test is conducted at the early stage of experimentation, when little information is known about the subject of study [Moen, 1991]. The purpose is to identify the most important factors and to determine the levels or range of the factors to be used in DOE optimisation. A factor or independent variable is a variable that is deliberately varied or changed in a controlled manner in an experiment to observe its effect on the *Rv*. In general,

the selection of the number of factors depends on many considerations such as; previous work, experience, cost, resources and time available [Moen, 1991; Deng et al., 1992; Badrinayaran 1995; Montgomery, 2000; Vinay, 2003; Ghanekar & Crawford, 2003].

The levels of a factor selected for study in an experiment may be fixed at certain values of interest. Choice of the interest-specific two levels used for each factor will be based on the knowledge of the process. Normally, the values used to set the levels of the factor for specific material come from configuration files that are developed by the LS manufacturers. These settings usually cannot be modified, except for small changes that are facilitated through part and build profiles [Hydro et al., 2004]. The default process parameters of the Sinterstation 2500 HiQ machine recommended by the manufactures of PA12 material are shown in Table 5.3.

Table 5.3 Default setting for the 2500 HiQ for PA12 powder-based material.

Laser sintering parameters	
Laser power (W)	12
Outline laser power (W)	5
Laser scans spacing (mm)	0.15
Layer thickness (mm)	0.1
Laser scan speed (mm/sec)	5080
Part bed temperature (°C)	172

Determination of important factors and estimation of the effects of these factors on the Rv is important in this experiment. The factors chosen for the experiment are usually those that the experimenter believes will have the greatest effect on the Rv. Through experience and the previous work done by other researchers [DTMa, 1996; Gibson and Shi; 1997; Kochan, 1999; Ho and Cheung, 2000; Hydro et al., 2004; Salmoria et al., 2007], the following factors are the main LS parameters which significantly influence the parts quality and the mechanical properties of parts sintered and were, therefore, selected for the DOE screening test:

- **Scan spacing (*SCSP*)**

- **Laser Power (*LP*)**

- **Scanning strategy (*SSt*)**

- **Laser scanning speed (*LSp*)**

- **Part Bed Temperature (T_b)**

The next step of planning DOE is selecting the number of replications. This means repeating an experimental trial at constant factor settings in order to determine the amount of experimental variability. It is also the primary way of studying the stability of the effects of the factors and increasing the degree of belief in the effects [Jiji, 1998; David, 2001; Ghanekar and Crawford, 2003; Hydro et al., 2004]. Effect means changes in the Rv that occur when a factor is changed from one level to another. The number of replications that is feasible depends partly on how difficult it is to change the levels of the factors [Moen, 1991; Murphy et al., 2002]. In this experiment, two levels at 3 replications were experimentally tested after the screening test.

Randomising the order of the test is important in DOE. It involves choosing the order of the test and assigns the combinations of the factors (process parameters). Figure 5.4 shows arrangements of benchmark parts with different process parameters in the build chamber that are built randomly.
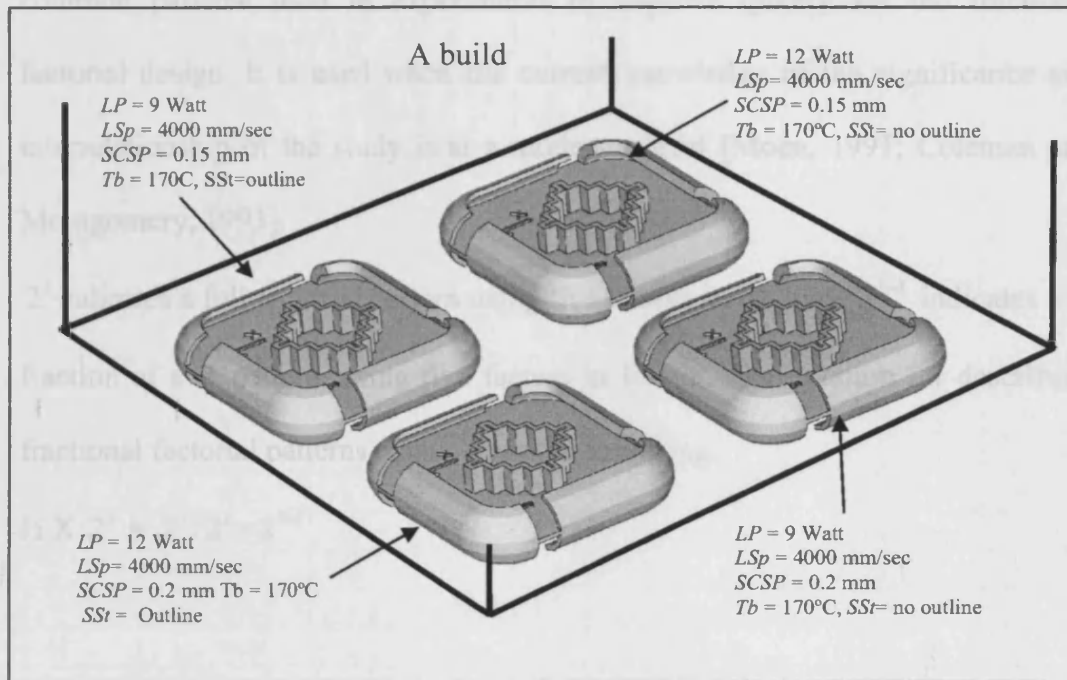
Figure 5.4 An arrangement of benchmark parts in the build chamber.

In any experimental design, variability occurs and a nuisance factor could influence the results. In this experiment, the nuisance factor can be defined as a design factor that would have an effect on the *Rv*. In our case it is assumed that no nuisance factors exist, and that therefore blocking will not be incorporated.

All parts built using 3000 mm/sec *LSp* with 9W, 12W and 15W *LP* were affected by severe "orange peel" texture. Parts built with 4000 mm/sec *LSp* with 15W *LP* had a slightly brown colour and rough surface. All these parts were built with *ED* higher than the default. For this reason, the 3000 mm/sec of *LS* and 15W of *LP* are

not included in the DOE. The benchmark parts built using 4000 mm/sec and 5080 mm/sec *LSp* with 9W and 12W *LP* had better *Rv*. In this experiment MINITAB 14 was used to develop the test plan.

The choice as to wether to use a full factorial design or a fractional factorial design depends on the level of the current knowledge of the process. The most common patterns used in experiments to improve quality are the fractional factorial design. It is used when the current knowledge of the significance and interrelationship of the study is at a moderate level [Moen, 1991; Coleman and Montgomery, 1993].

2^5 indicates a full factorial pattern using five factors in 64 runs, 2^{5-1} indicates a ½ fraction of a 2^5 pattern, using five factors in 16 run. The notation for describing fractional factorial patterns comes from the following:

$$½ \times 2^5 = 2^5/2^1 = 2^{5-1}$$

The structure of the DOE test plan allows all the data from the experiment to be used to study each factor.

Table 5.4 The matrix of DOE factional factorial of half five factors at two levels 2^{5-1}.

Benchmark part test	Run Order	Factors					Energy density *(ED)*, J/mm²	Response variable *(Rv)*				Build time (%)
		Laser power *(LP)*, W	Laser Speed *(LSp)*, mm/sec	Scan Spacing *(SCSP)*, mm	Part bed temperature *(Tb)*,°C	Scanning strategy *(SSt)*		Replication 1	Replication 2	Replication 3	Average *Rv*	
1	1	9	4000	0.15	170	Yes	0.022	58	52	59	56	1.23
2	5	12	5080	0.15	172	No	0.016	52	47	50	50	-0.04
3	9	9	4000	0.15	172	No	0.015	60	56	57	58	1.04
4	13	9	5080	0.2	170	Yes	0.014	34	41	40	38	-0.26
5	10	12	4000	0.2	172	No	0.015	20	23	22	22	1
6	6	12	5080	0.2	172	Yes	0.017	49	54	52	52	-0.26
7	2	12	4000	0.15	170	No	0.020	55	47	53	52	1.04
8	14	9	5080	0.15	170	No	0.012	44	48	45	46	-0.04
9	3	12	4000	0.2	170	Yes	0.020	41	37	42	40	1.25
10	15	12	5080	0.2	170	No	0.012	50	46	47	48	-0.22
11	11	9	4000	0.2	172	Yes	0.016	45	44	45	44	1.25
12	16	12	5080	0.15	170	Yes	0.022	62	60	59	60	default
13	4	9	4000	0.2	170	No	0.011	56	59	54	56	1
14	7	9	5080	0.15	172	Yes	0.018	37	35	37	36	default
15	12	12	4000	0.15	172	Yes	0.027	54	55	58	56	1.23
16	8	9	5080	0.2	172	No	0.009	50	53	48	50	-0.22

- (-) lower than default build time, (+) higher than default build time

Table 5.4 shows the matrix of DOE factional factorial of half five factors at two levels 2^{5-1}. The build time of each part was compared to the standard build time, which used the default setting LS process parameter. As shown in Table 5.4, the benchmark test part no.12 and benchmark test part no.5 were observed as being the best and the worst *Rv* results. The build time of benchmark parts (test) no. 12 and 14 were found to be the same standard build time, which is 4.56.23 hours

(default). It was found that the level of the factors determined the build time. For instance, the build time of all benchmark test parts which employed 4000 mm/sec *(LSp)* were slightly higher than the standard build time by increasing 1.04% to 1.23% due to lower *LSp*. However, the build time results of all benchmark test parts which used 5080 mm/sec *(LSp)* were found to be not much different compare to standard times (less than 1%).

5.4.2 Results and Analysis of DOE

As mentioned earlier in section 5.4.1, the DOE experiments were performed for 16 run fractional factorial designs with 3 replications. The average *Rv* was taken and further analysed using the Minitab 14.0 software.

The normal probability plot of the effects graph is used for assessing whether or not a data set is approximately distributed. The data are plotted against a theoretical normal distribution in such a way that the points form an approximately straight line. Departures from this straight line indicate departures from normality.
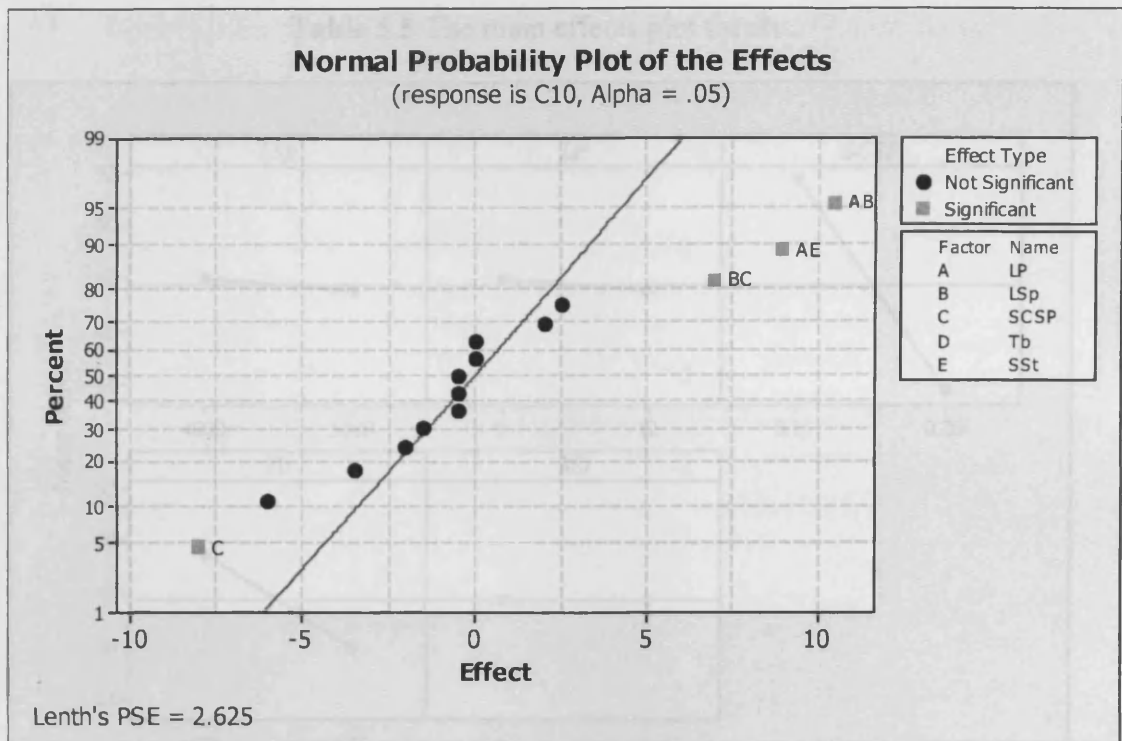
Figure 5.5 Normal probability plot of the effects.

The normal probability plot is used to highlight how the significant effects of the process parameters interact with each other as can be seen in Figure 5.5. Points AB, AE, and BC and C are significant.

Table 5.5 The main effects plot for *Rv*.
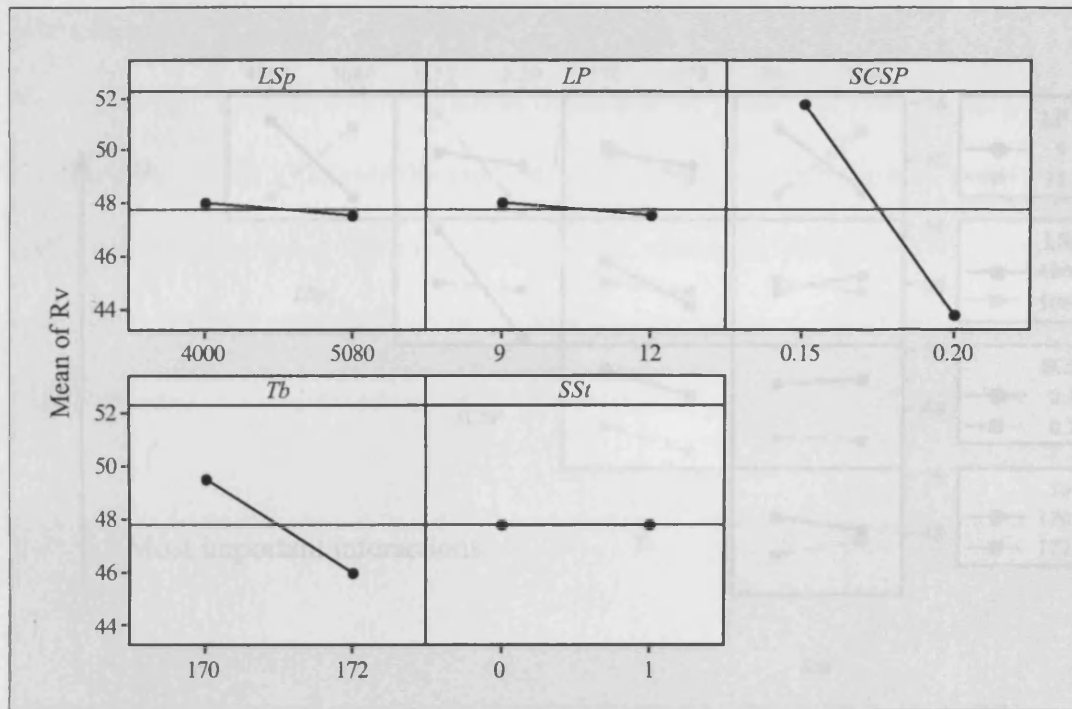
The effect of a single factor is known as a "main effect". As shown in Table 5.5, any changes of the *SSt* do not affect the *Rv*. The same results were observed for the *LSp* and *LP*. In contrast, a decrease of the *SCSP* or T_b results in significant improvement to the *Rv*. This means that the "orange peel" texture could be reduced or eliminated by optimising the T_b and *SCSP*. Therefore, the main factors to be considered are *SCSP* and T_b. This does not take into account the interactions between factors. Once the important effects have been identified and estimated, the relationships can be graphically summarised using simple interaction plots such as those in Table 5.6.

Table 5.6 Response plots illustrating various degrees of interactions.
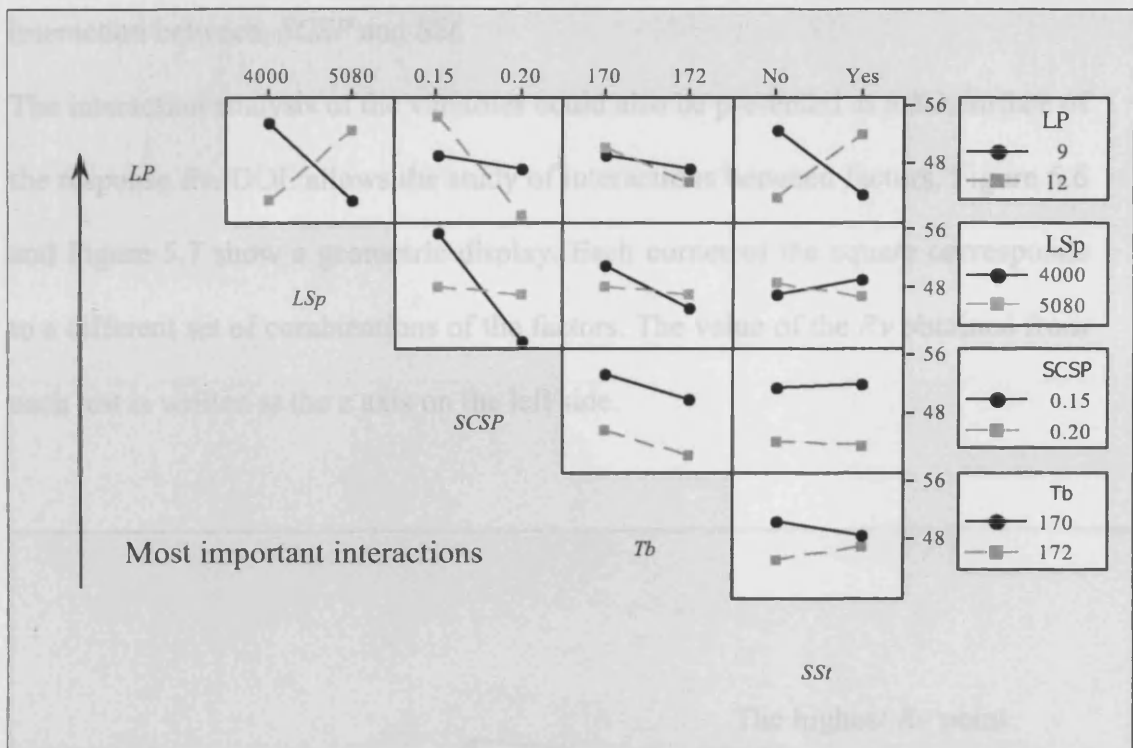
Each interaction plot displays the levels of one factor along the x-axis, the *Rv* on the y-axis, and the points corresponding to a particular level of a second factor connected by lines. This type of plot provides useful information for exploring or discovering interactions. For instance, the interactions could be ranked from most important to least important. As shown in Table 5.6, the results suggest that the strong interactions between *LP* *LSp*; *LP* * *SCSP*, and *LP*SSt* are significant. However, there are no interactions between *SCSP* T_b ; and *SCSP*SSt*.

The interactions of either 12W *LP* and 5080mm/sec or 9W and 4000 mm/sec *LSp* may also be clearly observed; and also another interaction of 0.15mm *SCSP* and 12 W *LP* which could raise the *Rv*. In contrast, the interactions both 12W *LP*, and 4000mm/sec *LSp* or 9W *LP* and 5080mm/sec *LSp* are the combination which could reduces the *Rv*. It is also found that there is no interaction between T_b and

SSt. A similar result may also be observed in Table 5.6, where there is no interaction between, *SCSP* and *SSt*.

The interaction analysis of the variables could also be presented as a 3D surface of the response *Rv*. DOE allows the study of interactions between factors. Figure 5.6 and Figure 5.7 show a geometric display. Each corner of the square corresponds to a different set of combinations of the factors. The value of the *Rv* obtained from each test is written at the z axis on the left side.

Figure 5.6 Surface plot of *Rv* vs *LP, LSp*.

As shown in Figure 5.6, the factor 1, *LP* is studied by comparing the data on the left side of the cube to the data on the right side. The factor 2, *LSp* is studied by comparing the front to the back, and the *Rv* of these two factors can be studied by comparing the bottom of the cube to the top. The results suggest that the

interaction of 12W *LP* and 5080mm/sec *LSp* can achieve the highest *Rv*. A lower

Rv is achieved by the interaction of 9W *LP* and 4000mm/sec *LS*.

The same results were observed on the interaction plot for the response shown in

Table 5.6. The interactions 9W *LP* and 5080mm/sec *LSp* or 12W *LP* and

4000mm/sec *LSp* may decrease the *Rv* (Figure 5.6).
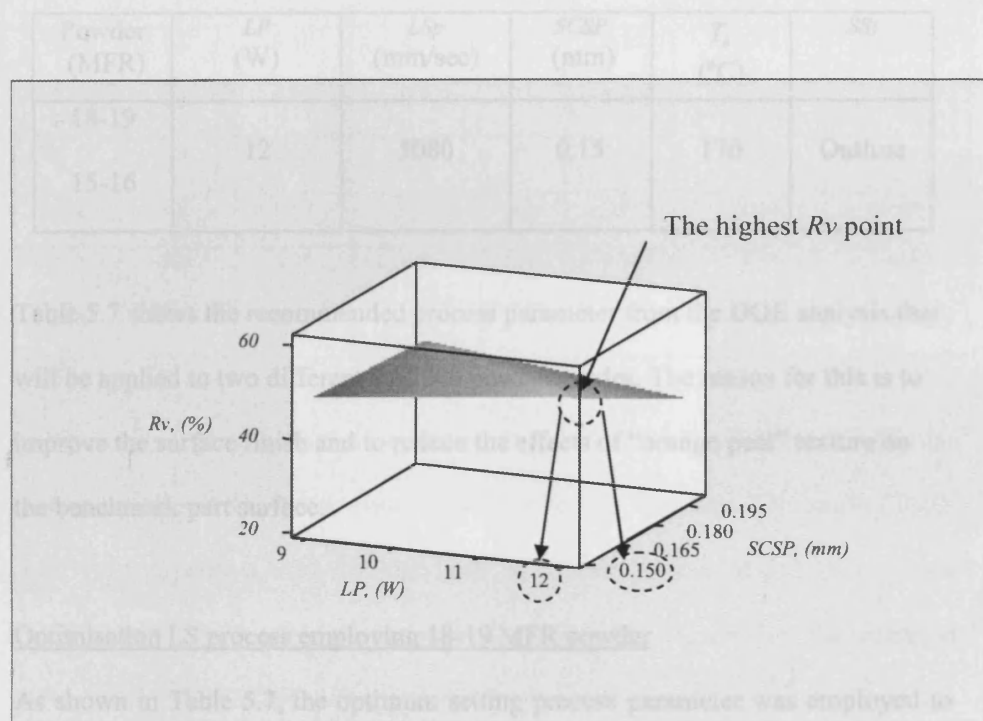
Figure 5.7 Surface plot of *Rv* vs *LP*, *SCSP*.

As shown in Figure 5.7, the interaction of 0.15mm *SCSP* and 12W *LP* produces

the highest *Rv*. In contrast, an interaction either 0.15mm or 0.2mm and 9W *SCSP*

produces the same *Rv*.

Optimisation of the LS process to reduce "orange peel" texture

Having considered the surface response analyses and interaction plot results, the optimum process parameters setup is shown in Table 5.7;

Table 5.7 The optimum LS process parameter

Powder (MFR)	*LP* (W)	*LSp* (mm/sec)	*SCSP* (mm)	T_b (°C)	*SSt*
18-19 15-16	12	5080	0.15	170	Outline

Table 5.7 shows the recommended process parameter from the DOE analysis that will be applied to two different PA2200 powder grades. The reason for this is to improve the surface finish and to reduce the effects of "orange peel" texture on the benchmark part surface.

Optimisation LS process employing 18-19 MFR powder

As shown in Table 5.7, the optimum setting process parameter was employed to improve the *Rv*. In this experiment, a 2500 HiQ plus machine with the default setting 0.225mm for X and Y beam offset and one time (1X) outline scanning was changed to 0.38 mm and one time (1X), two times, and three times outline scanning. The first powder quality was the 18-19 MFR which was used in this DOE test and the second powder was the older recycled grade with 15-16 MFR. The *Rv* benchmark parts of using these old recycled powders were compared.

Table 5.8 The optimisation experiment results of employing 18-19 MFR

Powder MFR	SSt (No.of times outline scan)	Beam offset Fill laser power X &Y ,(mm)	Beam offset Outline laser power X &Y ,(mm)	Rv (%)	Energy Density (ED), J/mm²	Shrinkage (%)	Build time (%)
18-19	1X	0.38	-0.1	21	0.022	Delamination	default
18-19	1X	0.38	0.1	62	0.022	3.72	default
18-19	2X	0.38	0.1	58	0.029	3.78	+0.82
18-19	3X	0.38	0.1	46	0.036	3.82	+0.98
18-19	1X	0.38	0.2	66	0.022	3.68	default
18-19	2X	0.38	0.2	78	0.029	3.65	+0.82
18-19	3X	0.38	0.2	65	0.036	3.76	+0.98

As shown in Table 5.8, changes of the setting level of beam offset fill to 0.38 mm and outline 0.1 & 0.2 better observed the Rv results than the DOE result (Table 5.4). Three repetition tests with one layer build were performed and the old used PA2200 with 18-19 MFR was employed. As noted in Figure 5.3, the accepted score of Rv is 70%. The average of Rv for this optimisation experiment is 78%. This means the Rv target is achieved.

The beam offset of the machine is 0.2 mm in the x and y axis. When the beam offset is set to a lower value, as it is in our experiments for trials with 0.1 and -0.1, the processed parts will be slightly bigger. In our case, the main reason was to study the effect of the beam offset on the "orange peel" texture regardless of the accuracy.

The results suggest that the overall Rv decreases with the number of iterations of outline scan. However, the build time and part shrinkage slightly increase. Due to the fact that only a small portion of "outline" laser beam overlaps into "fill" laser beam in the sintering process, benchmark parts which set the beam offset laser power at -0.1 setting level were found to be fragile and delaminated

Figure 5.8a, 5.8b, 5.8c, and 5.8d show the different surface finish position of the best Rv benchmark part (Table 5.8) after the optimisation process.
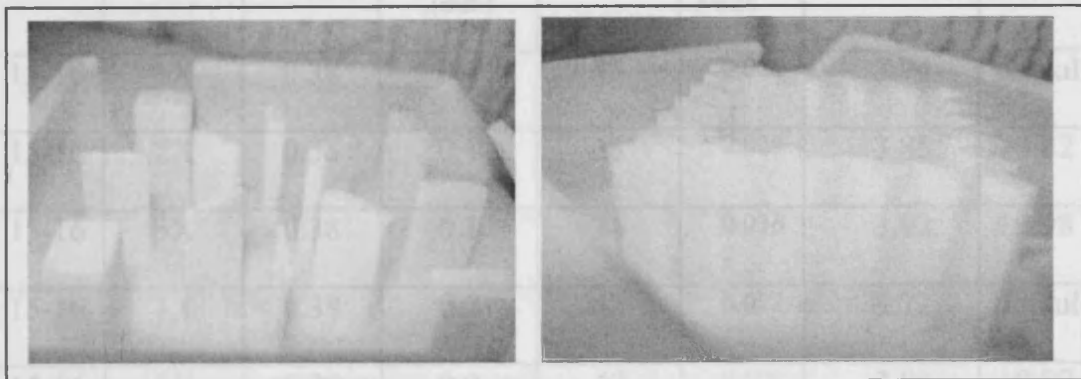
Figure 5.8a Different plain surfaces thickness **Figure 5.8b** Zig-zag surfaces
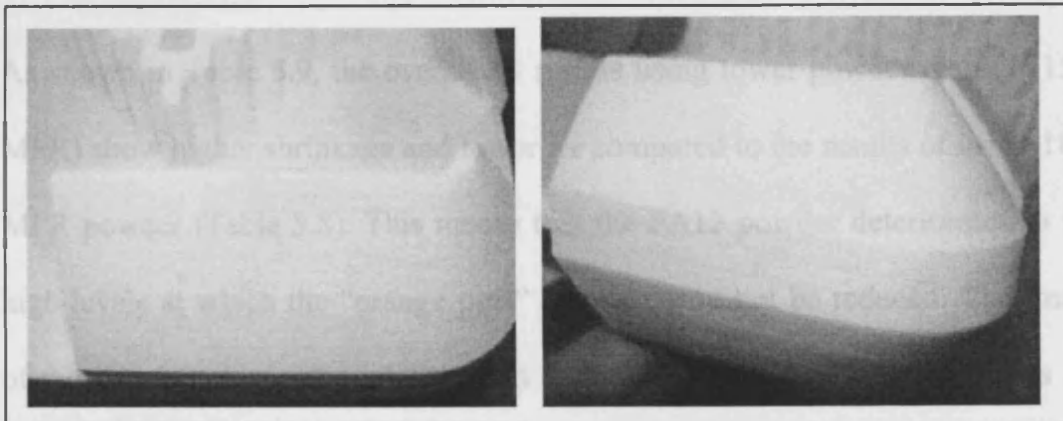
Figure 5.8c Angled surfaces   **Figure 5.8d** Vertical plain and cone surfaces

No "orange peel" found on all parts features, however the angled surfaces of the benchmark part shown in Figures 5.8c and 5.8d quite rough but still consider as acceptable quality.

Optimisation of the LS process of employing 15-16 MFR powder

The second optimisation LS process used the very old recycled PA2200 powder with 15-16 MFR powder quality.

Table 5.9 The optimisation experiment results of 15-16 MFR powder

Powder MFR	SSt (No.of times outline scan)	Beam offset Fill laser power X &Y ,(mm)	Beam offset Outline laser power X &Y ,(mm)	Rv (%)	Energy Density (ED), J/mm^2	Shrinkage (%)	Build time (%)
15-16	1X	0.38	0.1	45	0.022	3.74	default
15-16	2X	0.38	0.1	38	0.029	3.85	+0.82
15-16	3X	0.38	0.1	34	0.036	3.92	+0.98
15-16	1X	0.38	0.2	42	0.022	3.72	default
15-16	2X	0.38	0.2	40	0.029	3.80	+0.82
15-16	3X	0.38	0.2	39	0.036	3.86	+0.98

As shown in Table 5.9, the overall *Rv* results using lower powder quality (15-16 MFR) show higher shrinkage and lower *Rv* compared to the results of using 18-19 MFR powder (Table 5.8). This means that the PA12 powder deteriorates to very high levels at which the "orange peel" texture could not be reduced. The images of the benchmark part which obtained the highest *Rv* are shown in Figures 5.9a and 5.9b.
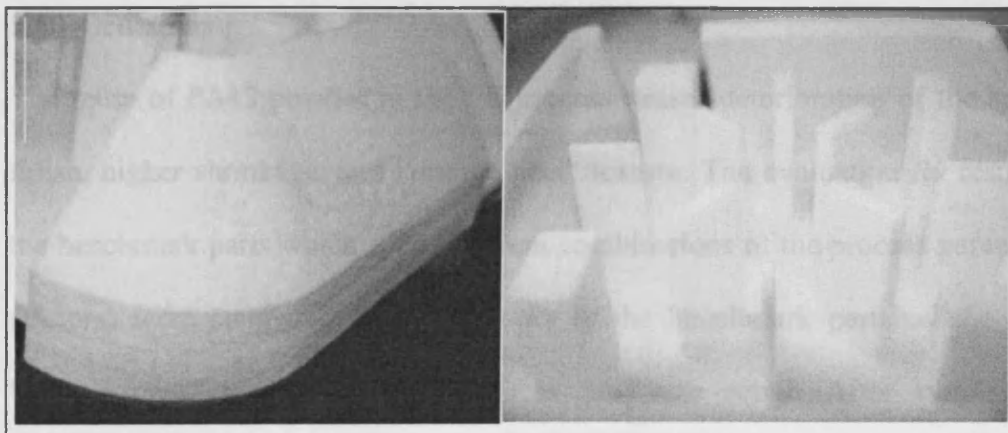
Figure 5.9a Cone and angled surfaces   **Figure 5.9b** Different plain surfaces

thicknesses

Figure 5.9a shows the conical and angled surfaces along the z axis at 90° and 57° affected by "orange peel" texture. The signs of "orange peel" and rough surfaces were observed along the z axis when angled at 50° and 55°. Figure 5.9b shows the different results for the different vertical plain thicknesses. For example, no "orange peel" texture was observed on the 1 mm and 2 mm thicknesses. At 3 mm vertical plain thickness, however, the signs of "orange peel" texture were noticed. The thicker vertical plain surfaces, such as 4 mm, 5 mm and 7 mm, displayed poorer "orange peel" texture. The surfaces of "Zigzag" features which were located on the top of the benchmark part were found to be rough.

5.5 Discussions

The reuse of PA12 powder in the LS process causes deterioration of the surface finish, higher shrinkage, and "orange peel" texture. The evaluation Rv results of the benchmark parts which used different combinations of the process parameters (factors) were compared. The lowest Rv *of* the benchmark part has the worst "orange peel" texture and its surfaces are very rough After running the experimental design, Minitab 14.0 was used to process data, conducting the statistical analysis, making the necessary assumptions, identifying significant effects and also identifying significant process parameter combinations. The practical problems this study set out to investigate have been addressed.

The result of the normal probability plot of the effects suggest that the interactions between $LP * LSp$, $LP * SSt$; $LSp * SCSP$ and one factor $SCSP$ are statistically significant. This means that the problem of "orange peel" texture is significantly correlated between the selected process parameters (factors) which influence the sintering mechanism through the LS process. That a sufficient amount of ED is applied in the LS process is important, but a slight variation of ED applied to benchmark parts shown in Table 5.4 seems not greatly to influence the Rv. This could be because the variation of melt viscosity still cannot much improve the sintering mechanism due to deteriorated powder properties.

The recommended optimum process parameters were found to be the same as the default setting. However, by slightly changing the fill and outside beam offset x and y (Table 5.8) and applying twice the number of outline scanning cycles, the Rv *of* the benchmark parts was found to be improved. In this case, the rough and coarse surfaces shown in Figures 5.8c and 5.8d were properly sintered. This means that applying the correct combination of the process parameters and ED

could significantly improve the viscous flow mechanisms and powder fusion which leads to a reduction in the "orange peel" texture. In contrast, the same optimum process parameters applied to the older PA2200 powder (15MFR-16MFR) could not overcome the "orange peel" texture problem. This could be due to the fact that the deteriorated powder has changed its thermal and sintering properties, which could not be easily improved. For instance, it could be due to the higher degree of chain molecules' entanglement which influences the viscous flow to become higher. As a result, more efficient packing of the polymer chains leads to significant shrinkage, as shown in Table 5.9.

These experiments suggest that the optimisation of process parameters could help the RP industry to reuse the recycled PA2200 powders at specific powder grades. The optimisation of the LS process parameters could improve the part surface quality if the MFR of the recycled powder is 18g/10min-19g/10min or higher. The proposed method does not lead to improvement of the surface quality when the PA2200 powder is deteriorated to very high levels (18-19 MFR or lower)

DOE can be employed to optimise the LS process parameters and MFR is the most suitable method for use as a quality control tool to determine the powder quality due to its effectiveness.

Summary

This chapter furthers the understanding of the LS process and in particular the relationship between the LS parameters and part quality. This methodology could be used to determine the optimum LS process parameters' setup in relation to the recycled powder PA12 properties and to improve the surface quality of the LS part.

CHAPTER 6

IMPROVEMENT OF POWDER MANAGEMENT AND RECYCLING IN LASER SINTERING

6.1 Preliminaries

Nowadays the utilisation of PA12 powders using the LS process has become very popular, not only for rapid prototyping but also for the direct manufacturing (DM) of bespoke parts. In order to fabricate parts with good quality and to avoid the "orange peel" occurrence, the users of LS machines apply a constant refresh rate with a higher portion of new powder. As a result, a huge amount of recycled powder has to be discarded.

This chapter reports on an experimental study of the deterioration of PA12 powder properties in the LS process. The main aim of this research is to develop a methodology for powder recycling and for controlling the input material properties that will ensure a good and consistent quality of the fabricated parts and a more efficient use of the LS material.

6.2 Powder utilisation

In the LS process a CO_2 laser controlled by a scanning system draws each slice of the model, thus applying enough energy to fuse the powder particles together and produce a solid part. As mentioned in section 2.5, the remaining volume of the building envelope is loose powder and its utilisation depends on the total number of build parts, their size, and volume. Although the LS process allows many parts to be packed in a single build, about 80% to 90% of the material is not sintered and could be recycled. Some examples of well packed builds for one of the largest LS machines available, EOSINT P700 [EOS,2007], are given in Table 6.1 .

Table 6.1 EOSINT P700 build envelope utilisation

Build	Z height (mm)	Parts volume (cm^3)	Unsintered powder volume (cm^3)	Parts weight (kg)	Unsintered powder weight (kg)	Utilisation by weight (%)
1	72	2082	20976	1.98	9.44	21
2	65	1206	18620	1.15	8.3	14.5
3	84	2214	38570	2.1	10.9	19.7

In Table 6.1 the build utilisation is given as the total weight of the sintered parts divided by the total weight of the powder used in the build. As shown in this table, the maximum utilisation is generally from 15% to 21%. In the general case, this proportion could be around 10%, which means that theoretically 90% of the powder is not sintered and could be recycled for the next builds. However, this is not quite true and the used material cannot be fully recycled.

PA12 powder properties deteriorate during the LS process [Gornet, 2002a,b]. As explained in section 4.3.6 above, the temperature, building time, cooling down time, and the number of times the powder have been used, affect its properties and

ability to be reused.

6.3 Current powder management practice and its limitations

The recommendation is to refresh the recycled powder by mixing it with portion of new material. However, if the amount of the new powder is not sufficient or if the recycled material is too "old", then the fabricated parts experience variation in their quality, higher shrinkage, and a rough surface texture known as "orange peel" (Figure 3.1a).

Table 6.2 Recommended refresh rates

Manufacturer / Material Name	Refresh rate new powder, %	Additional recommendations
EOS GmbH		
PA2200 fine polyamide	30% to 50%	Scrap the powder if there is severe "orange peel" texture
PA3200 GF polyamide	50% to 70%	
3D Systems Corp.		
Duraform^{TM} (polyamide)	30% + (30% overflow)	Scrap the powder if there is severe "orange peel" texture.

Current powder recycling practices are not able to determine the deterioration rate of the unsintered powder and the operator of the LS machine doesn't know exactly what is the quality of the material used in different builds and follows the manufacturer's recommendations (Table 6.2), using a constant refresh rate with very high portion of new material in order to keep good part quality. Normally, about 50% of the used material is recycled and the rest is scraped. In the case of RM this raises the production cost enormously due to the high portion of the material cost within the total cost of the LS manufacture, and creates huge amount

of scrapped PA12 powder with consequent environmental problems.

At present, powder recycling practices vary from user to user and are mostly based on supplier's recommendations (Table 6.2). A standard technique is to mix old powder with new powder in a fixed ratio and there are two main blending techniques.

Sinterstations HiQ (3D Systems Corp)

For the 3D System's machines (Figure 2.3) the recommendation is to mix new powder, used powder from the part bed, and powder from the overflow cartridges in proportion 1:1:1, and to blend it with a drum mixer (Figure 2.4).

EOSINT P700

For the EOS LS machines, the recommendation is to use 30% to 50% new PA2200 material and to blend it with 70% to 50% powder from the part bed.

The EOSINT P700 and P730 models are equipped with an automated powder blending system known as an "integrated process chain management" (IPCM) system. It combines an automatic powder feeding system, an unpacking station with an exchangeable frame docking system, with integrated powder recycling and sifting [Prototype, 2005; EOS, 2007] (Figure 2.5).

```
┌─────────────────┐        ┌─────────────────┐
│   New powder    │        │ Recycled powder │
└─────────────────┘        └─────────────────┘
         │                          │
         └──────────────┬───────────┘
                        │
                        ▼
        ┌───────────────┬───────────────┐
        │   EOS GmbH    │   3D System    │
        ├───────────────┼───────────────┤
        │   Table 6.2   │   Table 6.2    │
        └───────────────┴───────────────┘
                        │
                        ▼
              ┌───────────────────┐
              │    LS process     │
              └───────────────────┘
                        │
                        ▼
        ┌───────────────────────────────┐
        │    Remove parts from build     │
        └───────────────────────────────┘
                        │
                        ▼
   ┌──────────────────────────────────────────┐
   │ The loose powder is collected, sifted and │
   │        used for the next build            │
   └──────────────────────────────────────────┘
```
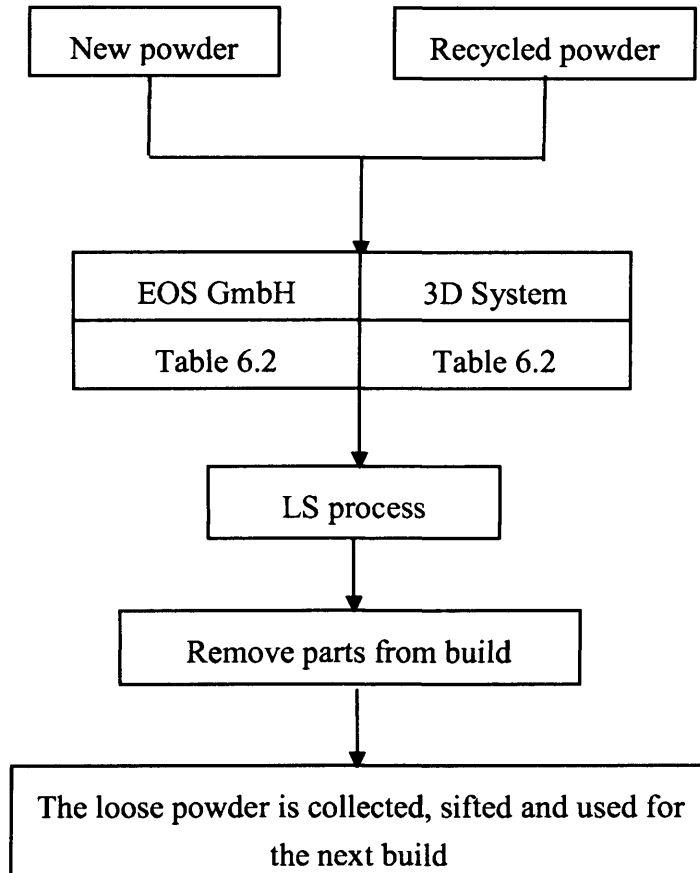
Figure 6.1 The current LS recycling practise

In all cases, the used powder quality is not tested (Figure 6.1). Often, despite the large portion of new powder added in the mix, the final part quality is not adequate. The reason is that the quality of the used powder could be so bad that even a higher portion of new material cannot make it usable. To maintain good part quality and prevent the "orange peel" texture, the users employ the highest recommended ratio of new powder, and discard huge quantities of used material. Even so, from time to time the sintered parts are of bad quality and the whole batch of mixed material is scrapped.

6.4 Powder recycling method (PRM)

A major constraint that limits the application of LS as a viable RM process is the inconsistency in the part quality due to variation of the powdered material properties. For this reason, the systematic new practice of recycling powder management takes into consideration all the limitations of the current practice that have been discussed above and seeks to minimise the usage of fresh powder in order to sustain parts quality.
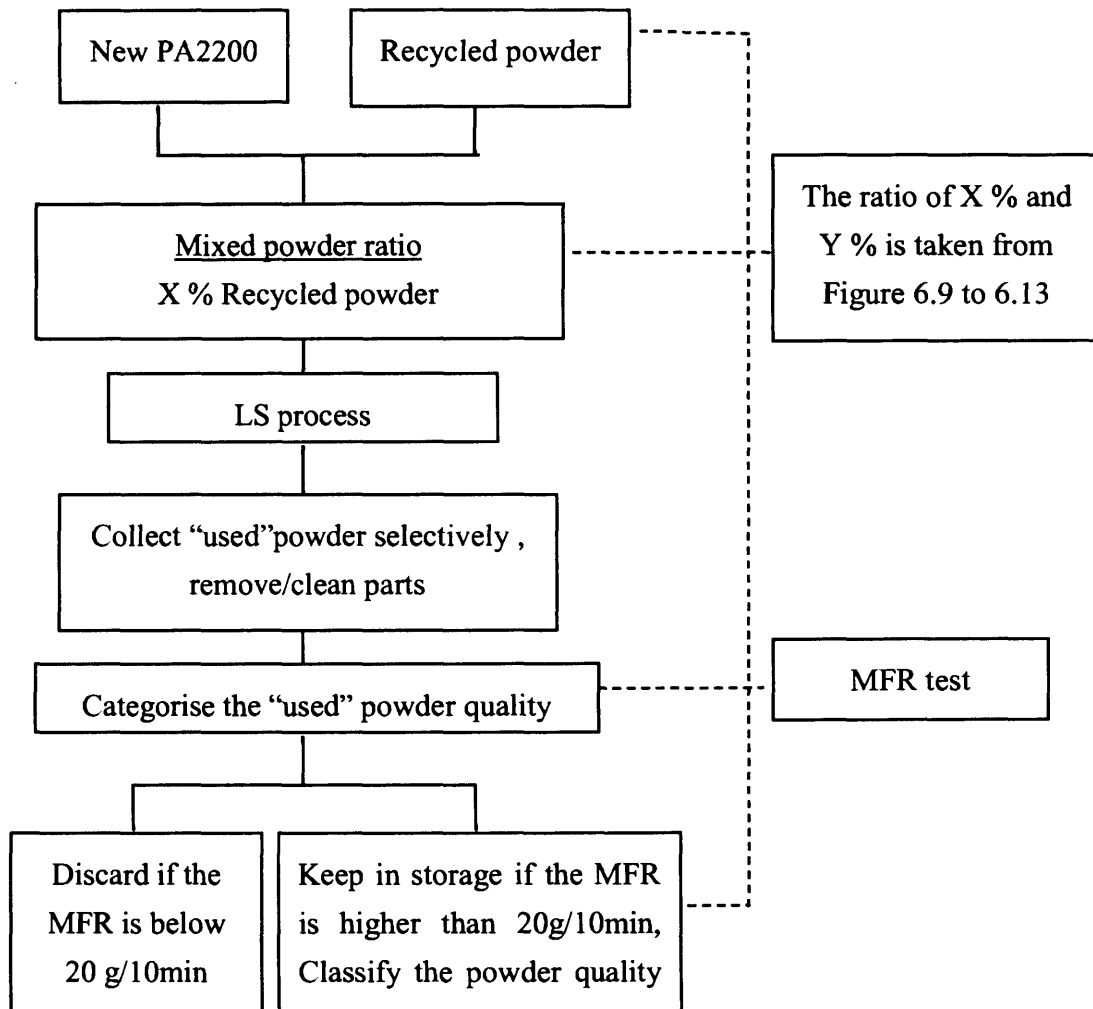
Figure 6.2 PRM is a new method of controlling PA2200 powder quality

PRM is a systematic approach to controlling the input material properties that will ensure consistent and good quality for the fabricated parts as shown in Figure 6.2. As mentioned earlier in section 2.5. The longer build stage period in the LS process increases the chances that loose powder in the build cylinder may become badly deteriorated due to exposure to high temperature. This is significantly influenced by the thermal history of the loose powder in the build cylinder.

The new recycled powder practice principles are as follows:

- It is assumed that the loose powder deteriorates at a different rate for every different build of the LS process.

- The quality of all the powders must be tested to determine the MFR.

- The method of collecting the loose powder from the build should be reviewed and its quality experimentally tested.

It is assumed that not all the loose powder in the build cylinder is badly deteriorated. This is because it is the loose powder located around and closer to the sintered part that is the hottest, and therefore exposed to the longest period of high temperature through the LS process.

The quality grade of the loose powder at the different locations in the build envelope must also be identified before it is discarded because there is a possibility it can be reused. Therefore, the PRM fundamental strategies for recycling the used powder are as follows:

- The mixed powder ratio, or the ratio of blending the new PA12 powder/ less deteriorated powder, should be varied and it must be based on the recycled powder quality grade itself.

- The key factor in improving the optimal refresh rate is to achieve the

specific melt viscosity target. All LS machine users must control the input

material quality and so ensure the consistent and good quality of the

fabricated parts.

6.5 Experimental results and discussion

6.5.1 Methodology and equipment used

The LS material investigated in this study is PA2200 fine polyamide supplied by

EOS. The MFR measurements were performed according to ISO1133 standard

[ISO1133]. The details of the MFR test procedure have already been mentioned

above (see section 4.3.1.1).

6.5.1.1 Variation of PA12 powder properties in the LS process

As mentioned earlier in section 6.4, the powder deteriorated at a different rate for

each different build of the LS process and there is a possibility that the less

deteriorated loose powder can be reused. In order to confirm these assumptions,

and investigate the deterioration of the PA12 powder properties in the LS process,

samples from several Sinterstation HiQ and EOSINT P700 builds were collected

and their MFR measured. One of these builds is shown in Figure 6.3. The

different parts size and shapes were built at 440 mm (maximum) height by using

the Sinterstation HiQ. Two powder collection methods were compared. The first

method is the new practice powder collection and second method is the current

practice loose powder collection.

Method 1 – Reuse the top and perimeter powder

The loose powder is collected at every 100 mm height from the top, middle and bottom of the central area and the periphery of the build. These powders are separated, sifted and the powder quality is tested.

Method 2- Mixing the overall loose powder

The loose powder from the whole build is mixed together. Then, the powder is sifted and the powder quality tested.
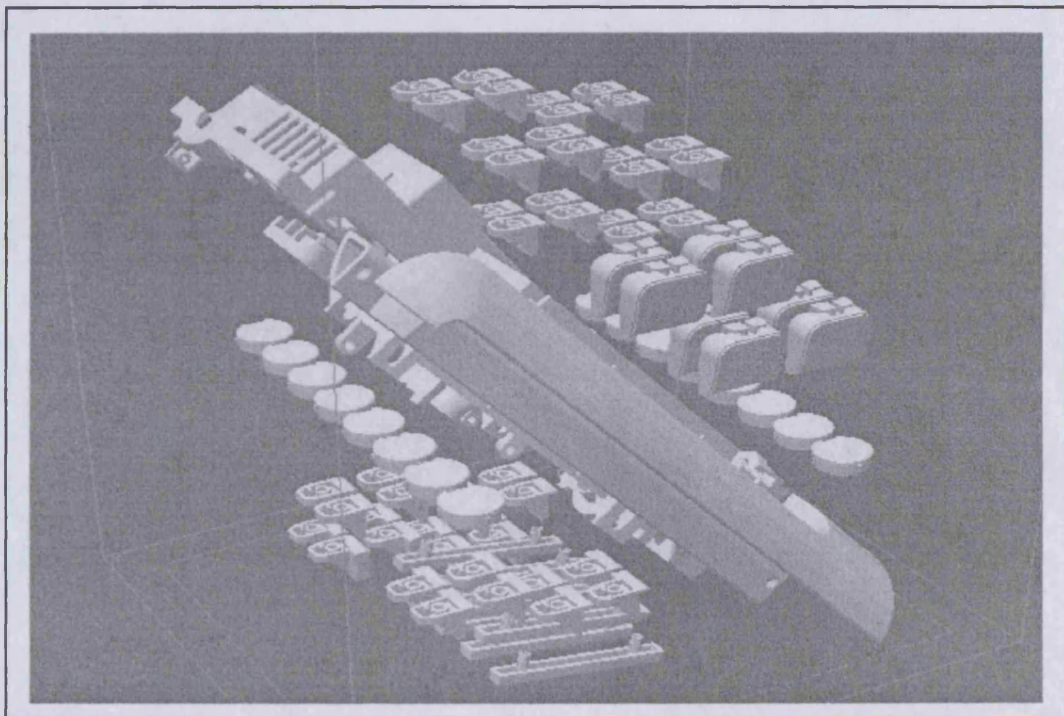
Figure 6.3 Parts orientation with different size and shapes in build cylinder
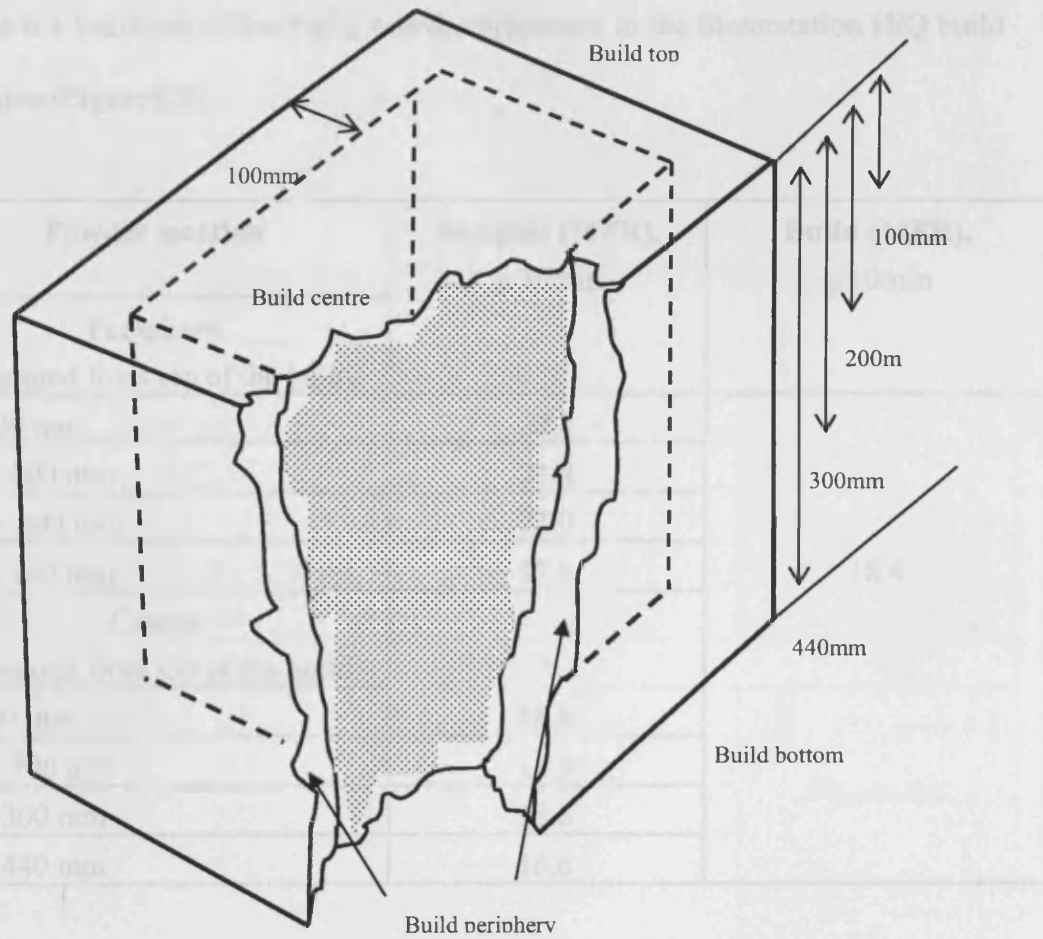
Figure 6.4 The LS build chamber (P700)

Table 6.3 Variation of the PA12 powder properties in the Sinterstation HiQ build

chamber (Figure 6.3)

Powder location	Samples (MFR), g/10min	Build (MFR), g/10min
Periphery (measured from top of the build)		
0 - 100 mm	22.4	
101 - 200 mm	21.4	
201 - 300 mm	21.0	
301 - 440 mm	17.6	18.4
Centre (measured from top of the build)		
0 -100 mm	19.6	
101 - 200 mm	18.3	
201- 300 mm	18.6	
301- 440 mm	16.6	

As shown in the Table 6.3, by employing the first method the loose powder from

the build periphery at 0 to 300 mm height has MFR 21-22 g/10min. compared to

the powder in the centre at 300-400 mm height with only MFR 17 g/min. In

contrast, by using the second method, when all powder from the build is mixed,

the average MFR is only 18 g/10min which is similar to the MFR of the "build

centre" powder and lower than "build periphery" powder MFR. These

experiments prove that the PRM approaches (first method) offer an effective

technique for loose powder collection.

In order to confirm these assumptions, and investigate the deterioration of PA12

powder properties in the LS process, samples from several other Sinterstation

2500 HiQ and EOSINT P700 builds were collected and their MFRs measured.

The samples were taken from the central and peripheral areas at every 100 mm

height of the build chamber as shown in Figure 6.4. The build height and total

build time are listed in Table 6.3 and 6.4.

Table 6.4 Sinterstation 2500HiQ and EOSINT P700 builds

Sinterstation 2500HiQ			
Build No	**Build height, mm**	**Total build time, hour**	
1	87.28	9.05	**Figure 6.5**
2	115.21	12.37	
3	129.75	13.56	
4	440	44.24	
EOSINT P700			
1	241	26.32	**Figure 6.6**
2	325	33.28	
3	372	39.27	
4	435	45.35	
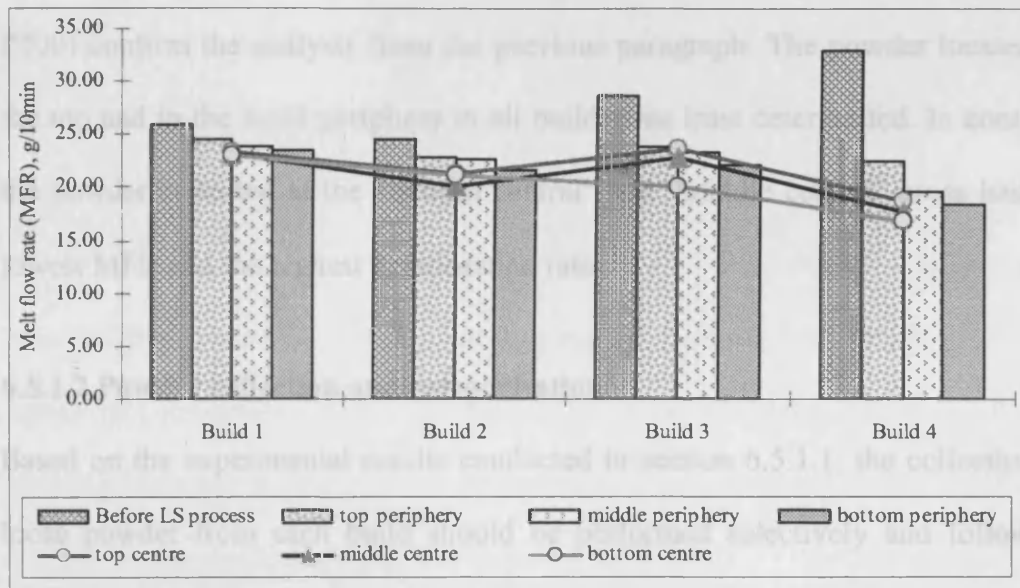
Figure 6.5 Loose powder deteriorated at different build heights (Sinterstation 2500 HiQ).
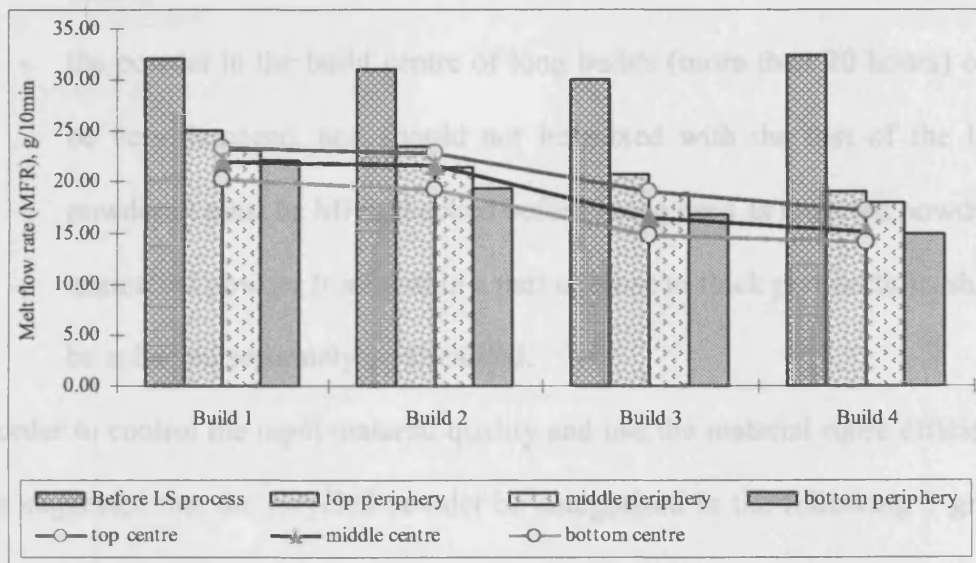
Figure 6.6 Loose powder deteriorated at different build heights (EOSINT P700).

The results shown in Figure 6.5 (Sinterstation 2500 HiQ) and Figure 6.6 (EOSINT P700) confirm the analysis from the previous paragraph. The powder located on the top and in the build periphery in all builds was least deteriorated. In contrast, the powder collected at the "bottom central" and "middle central" areas has the lowest MFR and the highest deterioration rate.

6.5.1.2 Powder collection and categorisation

Based on the experimental results conducted in section 6.5.1.1, the collection of loose powder from each build should be performed selectively and following some main rules such as:

- collect short builds separately from long builds;

- collect the peripheral build area separately from the material in the build centre;

- the powder in the build centre of long builds (more than 20 hours) could be very damaged, and should not be mixed with the rest of the loose powder. It must be MFR checked before being used as recycled powder;

- unsintered powder from within a part or close to thick part sections should be collected separately or discarded.

In order to control the input material quality and use the material more efficiently it is suggested that the recycled powder be categorised in the following 3 grades (Table 6.5).

Grade A

Only new PA12 powder falls into this category. It is the best powder having the highest melt viscosity (MFR higher that 50 g/10min.).

Grade B

It is PA12 powder that has been used in the LS process. Within this grade, the powder is categorised into six sub-grades, B1 to B6. The loose powder collected from the different builds in terms of locations and build heights has a different thermal history and therefore different properties.

Grade C

This is the worst grade PA12 powder quality. This powder has been used several times or has been collected from the centre of long builds. The MFR of this category is normally below 20 g/10min. It could be used for the fabrication of low quality parts or should be discarded.

Table 6.5 Un-sintered powder grades

PA2200 powder grades	MFR, g/10min
A (new powder)	More than 50
B1	49-45
B2	44-40
B3	39-35
B4	34-30
B5	29-25
B6	24-20
C	Less than 18-19

6.5.1.3 Variation of the new and once-used PA12 powder properties

The aim of this experiment is to determine the quality of fresh PA2200 powder

and once-recycled PA2200 grade supplied by EOS that has not been reportedly

tested.

Variations in the new and used powder quality that are currently employed were

investigated. A number of batches of new and recycled powder from various

builds were tested.
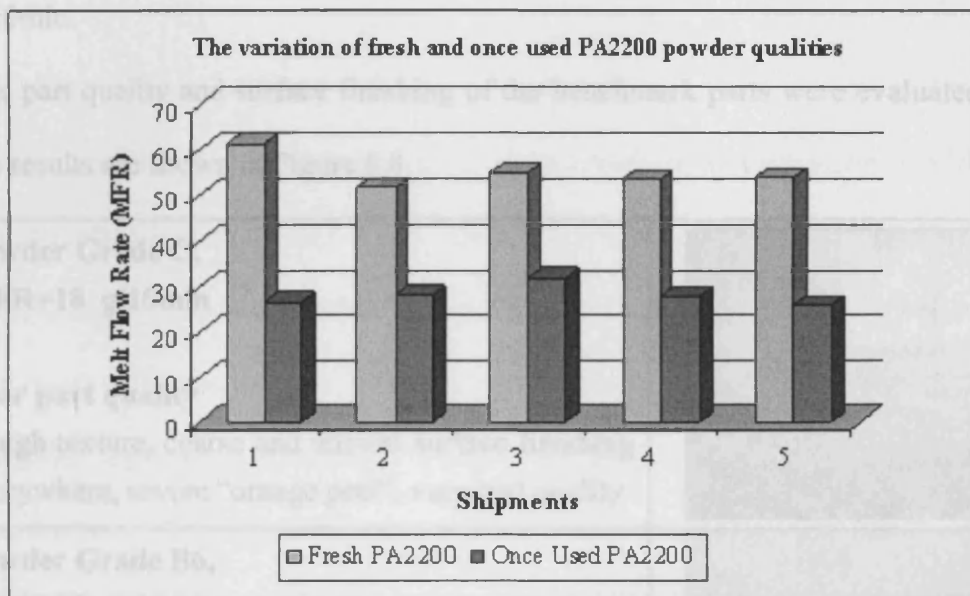
Figure 6.7 The MFR variation of "new" and "once used" PA2200 powder.
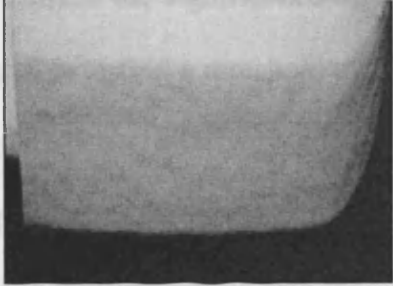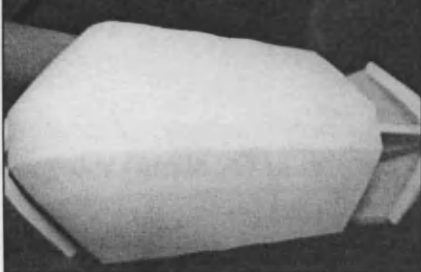
As shown in Figure 6.7, the MFR of "new PA2200" powder measured in five

random batches was found to be of between 50 to 60 g/10min (grade A). The

MFR of "once recycled PA2200" powder was in the range of 31 to 25 g/10min

(grade B4-B5). This example shows that the material properties of the new and

recycled powder could vary in a very wide range and as a result the properties of

the mixed material used in LS fabrication varies, which affects the final part

quality.

6.5.2 "Orange peel" texture and optimal PA12 powder quality

The objectives of these experiments were to find out the relationship between the PA12 powder MFR and the "orange peel" texture, and also to determine the minimum MFR required to maintain acceptable and consistent part quality.

Three different batches of PA12 powder were used to build the same design benchmark employed in Figure 3.6a and 3.6b on the Sinterstation 2500 HiQ LS machine. The MFRs of these batches were 28 g/10min., 23 g/10min., and 18 g/10min.

The part quality and surface finishing of the benchmark parts were evaluated and the results are shown in Figure 6.8.

Powder Grade C, **MFR=18 g/10min** **Poor part quality** Rough texture, coarse and uneven surface finishing everywhere, severe "orange peel", very bad quality	
Powder Grade B6, **MFR=23 g/10min** **Signs of "orange peel"** Some vertical surfaces have "orange peel" texture, uneven surface finishing, better than the previous part, unacceptable quality	
Powder Grade B5, **MFR=28 g/10min** **Good** No indication the presence of 'orange peel' texture, surfaces are smooth, even, acceptable quality	

Figure 6.8 Quality and surface finishing of the benchmark parts.

Employing less deteriorated powder (28 MFR) produced a good physical surface. In contrast, employing the lower MFR powders (23 MFR and 18 MFR) produced poorer results. In this case it was concluded that PA12 powder having an MFR of approximately 28 g/10min would produce the best results.

This relatively simple experiment could be performed on any LS machine in order to find out what is the optimum level of powder MFR for a given LS machine model with a particular setup of LS parameters.

6.5.3 Optimal refresh rates

As mentioned earlier the "orange peel" is an unwanted phenomenon resulting in rough surface texture of the LS parts and occurring when the portion of new PA12 powder is not sufficient or when too old powder is used in the input powder mix. The main questions are how to measure the powder age and what should be the minimum amount of new PA12 powder required to avoid the "orange peel" phenomenon. The purpose of this experiment is to investigate the significance of the PA12 powder age on the part surface quality. The goal is to find a threshold or a level of acceptable powder quality which would guarantee a relatively good surface finish and absence of "orange peel" for the LS process.

This section presents a series of experiments is to find the optimal refresh rate for a particular powder sub-grade within grade B when blending with new powder (grade A).

Samples from B1 to B6 grades were mixed with new powder (grade A) in ratios ranging from 10% to 50% new powder. The same ratio is used to mix among the B sub-grades powders. The MFR of the mixture was then measured and the results are shown in Figure 6.9 to Figure 6.13. In this way the user would be able

to control the input powder quality and therefore the final quality of the sintered parts. The proposed PRM is schematically explained in Figure 6.2.
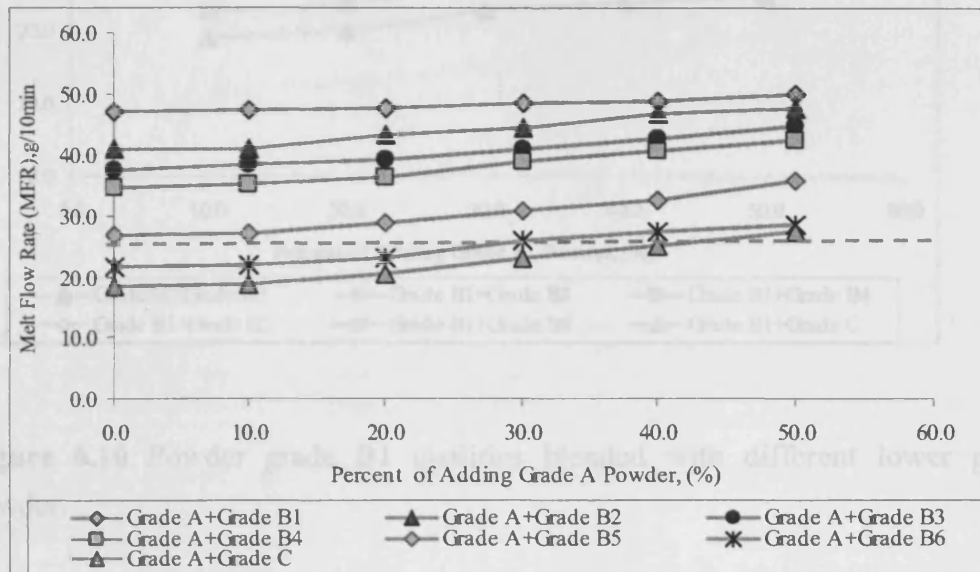
Figure 6.9 The MFR of B1 to B6 powder sub grades blended with new powder.

As shown in Figure 6.9, the first impression of these results is not very promising. One might expect that any recycled powder could be brought up to the required quality by blending it with a large quantity of new powder. The broken line indicates the minimum MFR required to avoid "orange peel", i.e. 25-28 g/10min., found from the previous experiments. From Figure 6.9 it may be seen that it is impossible to refresh the powder grade C and even grade B6 up to that minimum MFR of 25-28 g/10min. The powder grade C (MFR 18-19 g/10min.) must be mixed with 50% new material to be brought just to the minimal required level of 25-28 g/10min. This means that if the MFR is below the threshold of 18-19g/10min., the refresh rate must be higher than the recommended maximum of 50% or the manufactured parts could experience bad surface quality.
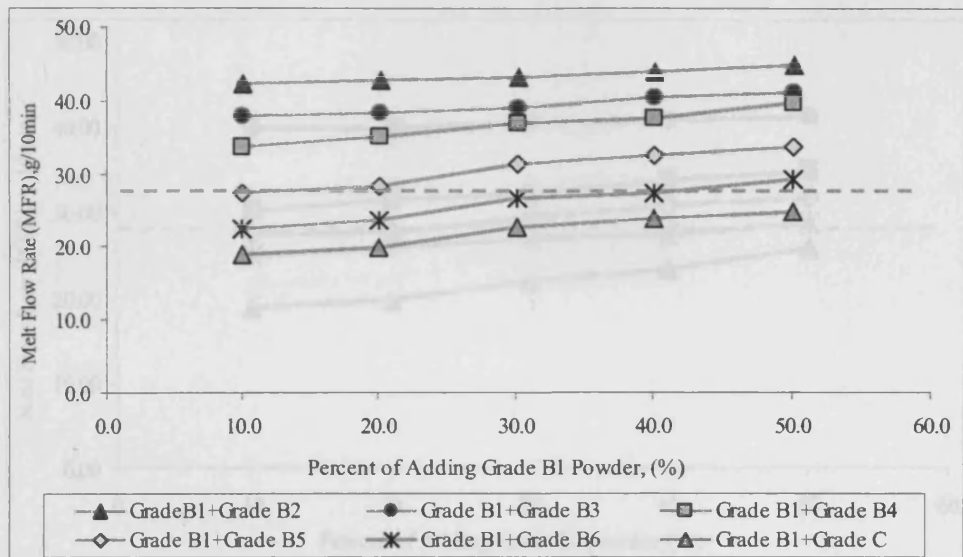
Figure 6.10 Powder grade B1 qualities blended with different lower grade powder.

In Figure 6.10, a straight line trend may be observed, which is not much different from the results as shown in Figure 6.9. This could be because the grade B1 powder is the second best quality after grade A.

The results suggest that the recycled powder grade B6 (20MFR-24MFR) requires approximately 40% of grade B1 powder to reach the refresh quality target. However, the worst powder grade (grade C) needs over 50% grade B1 powder to be refreshed to meet the target. This means the grade C powder requires greater amounts of better recycled powder than when blended with grade A powder.
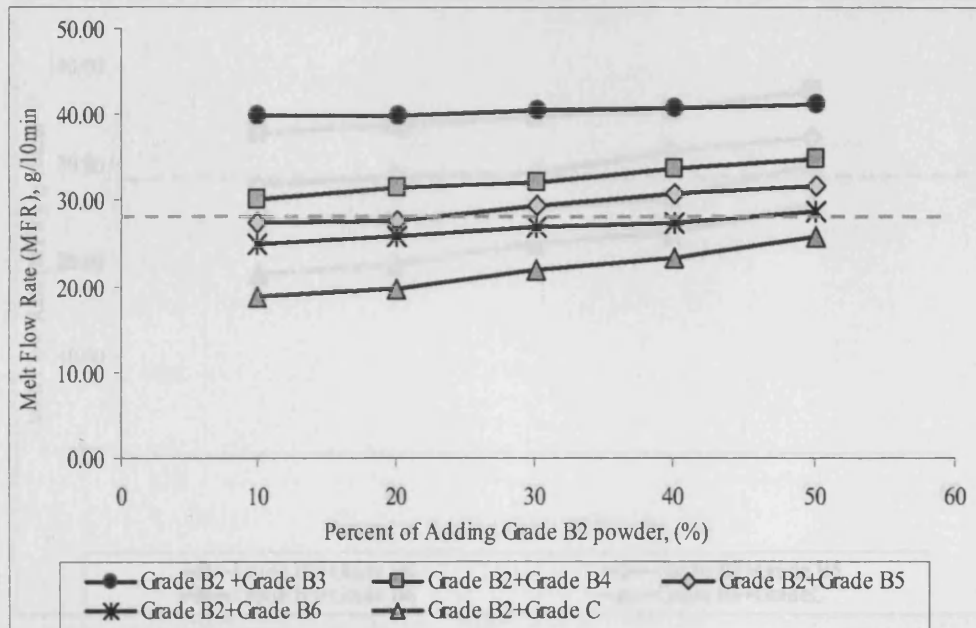
Figure 6.11 Powder grade B2 qualities blended with different lower powder grades.

As shown in Figure 6.11, there is not much MFR improvement from the results of blended grade B2 and B3 powders. This could be due to the only slightly different MFR range between these two powders. On the other hand, powder grade B6 requires approximately 41% to 43% of grade B2 to meet the refresh quality target, which is 1% to 2% higher than that needed by grade B1 powder. The grade B5 powder needs 10% to 12% ratio of grade B2 powder, which is the lowest ratio needed to meet the MFR target. It is estimated that the worst powder grades (grade C) needs at least 55% to 57% of grade B2 powder to achieve the MFR target.
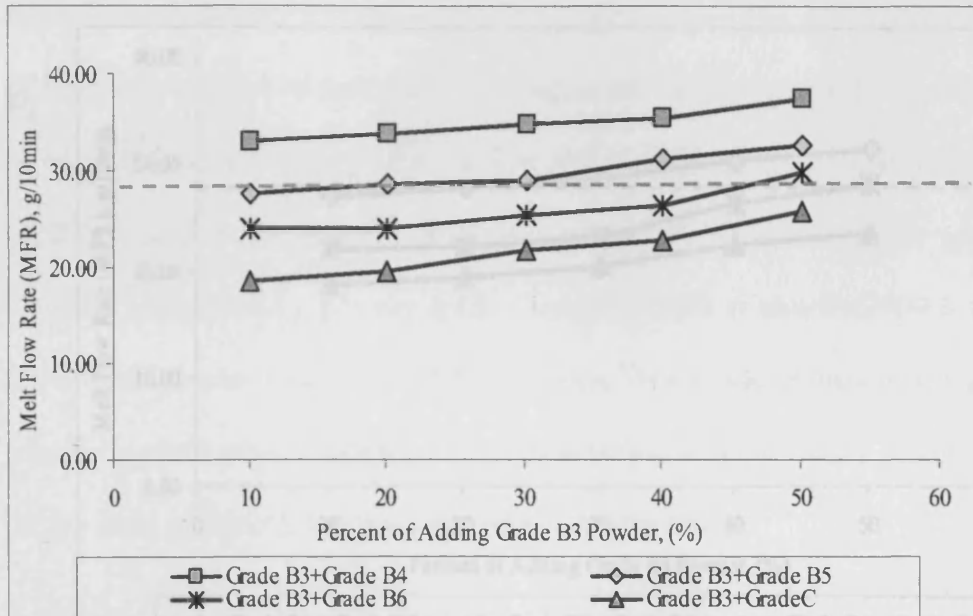
Figure 6.12 Powder grade B3 qualities blended with different lower powder grades.

As shown in Figure 6.12, grade B6 powder needs 44% to 46% of grade B3 powder to meet the refresh quality target. This ratio is slightly (2% to 3%) higher than when blended with powder grade B2. Grade B5 requires about 15% of grade B3 powder to meet the MFR target. The worst powder (grade C) needs about 60% of grade B3 powder to be refreshed.

Figure 6.13 Powder grade B4 qualities blended with different lower powder grades.

As shown in Figure 6.13, the results of blending 50% of powder grade B4 into grade B5 powders shows MFR increase of approximately 19%. In order to achieve the MFR target, grade B5 requires about 22% of grade B4 powder to be blended.

The grade B6 powder was observed to require 47% to 50% of grade B4 powder to reach the refresh MFR target. This is almost the same ratio as needed by grade B4 powder when blended with B3 to reach the MFR target. The lowest quality powder (grade C) needs over 60% grade B4 to attain the MFR target.

6.5.4 Case study:

The objective of this experiment is to implement the optimal refresh rate and to evaluate the surface quality of parts. For this reason, recycled loose powder 18.7 MFR (grade C) was employed in this experiment. As shown in Figure 6.9 (grade C mixed with grade A), powder grade C requires 50% of new PA2200 to achieve the refresh powder target (28MFR). However, the result of blending these two powder grades before loading into the LS machine was 26.4 MFR. This means a falling short of about 5.7% from the refresh quality target.
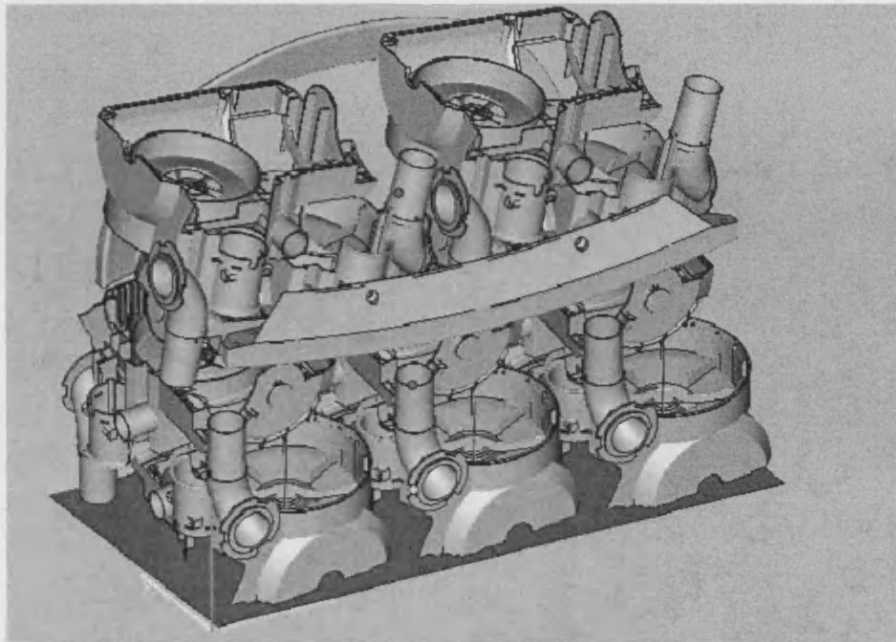
Figure 6.14 The parts orientation in the build.

The EOSINT P700 was employed to run the full build with over 450 mm build height which contains 10 large identical parts as shown in Figure 6.14. The LS machine was run over 45 hours to complete the build. The surface quality of the LS parts was evaluated through observation, feel, and touch on the part surface. It was found that two parts located at the bottom of the build were affected by light

"orange peel" texture; however other parts were classified as having acceptable

surface finish and no "orange peel" texture. This result proves that the PRM could

utilise the grade C (worst grade) powder and that it could be improved with

certain criteria in the future builds.

6.6 Discussion

This thesis suggests how to develop a methodology for improving the different Polyamide 12 (PA12) powder grades that will ensure consistent and good quality for the LS fabricated parts. The limitations of the current practice of collecting loose powder were discussed in section 6.3. A new powder recycling method (PRM) was developed to minimise the variations of the mixed PA12 powder properties. The PRM is based on the findings in the previous sections, and on the following strategies:

- the powder deteriorates at different rates in different areas of a build, so the powder at the periphery of the build cylinder is less damaged than the powder in the build centre;

- the loose powder in long builds, having more than 15-20 hours build time, is much more deteriorated than recycled powder from short builds;

- powder collected from each build should be tested and categorised;

- consistent and optimal recycled powder quality is the key to achieving consistent part quality and efficient use of the material;

- the proportion of new PA12 powder should be varied depending on the grade of the available recycled powder.

The LS part quality is significantly influenced by the PA12 powder properties. The tests performed in section 6.5.2 were aimed at investigating the significance of PA12 powder quality and its MFR on the surface quality. It has been found that the powder with a higher melt viscosity (lower MFR) produces a poor "orange peel" texture. An acceptable level of PA12 powder quality which would guarantee a relatively good surface finish and absence of "orange peel" is a powder blend with an MFR higher than 25-27. This could be used as a reference point when

mixing and blending used and new PA12 material in the LS process.

The results presented in sections 6.5.3 are a basis for the development of a strategy for systematic recycling and a set of rules for more efficient powder management. Considering the number of builds only [Gornet, 2002a,b] does not provide enough information for judging how to process the recycled material. The build time and the type of LS machine should be also taken into account. For instance, the recycled powder from a build of approximately 100 mm or less build height would have relatively good quality and will need a smaller amount of new material. On the other hand, powder collected from a 350mm to 400mm build height of EOSINT P700 build, which has 35 to 45 hours cooling down time, would be badly damaged and needs a lot of new material.

Also, the powder collected from the build periphery where the temperature was high only for a short period of time is less damaged than the material collected from the build centre.

The results of the case study parts build using (50%:50%) ratio of grade A and grade C powders in section 6.5.4 could still be employed in the future but with certain limitations. Below is a list of several factors that could influence the experimental result above:

- There is a possibility that that powder was not mixed thoroughly and/or needs longer mixing time;

- The part thickness, part geometry, and part orientation in the build should to be considered during the parts arrangement process. The reason for this is that if a low powder grade was employed to run the full build, the part with greater wall thickness should to be placed on the top and the thinner or smaller parts should be placed at the bottom of the build. This is

because the powder located at the bottom deteriorates at the highest rate due to expose to heat for the longest period through the LS process. This causes a higher chance that parts located at the bottom of the build might be affected by "orange peel" texture;

- The only way to employ grade C powder is it that it must be blended with new PA2200 at (50%:50%) ratio. In order to avoid having any parts affected by "orange peel" texture, it is recommended that this powder be used only for builds of less than 300 mm build height. Based on the experimental results (Figure 6.6 and Table 6.4), the deterioration rate in the build would range 35% to 38 % for 325mm.

However, if this powder is employed for a 440 mm build height, the powder located inside in the centre at the bottom will experience about a 50 % deterioration rate (Figure 6.5 and Table 6.4). Thus, there is a higher chance of the parts being affected by "orange peel" texture.

6.7 Summary

This chapter focuses on controlling and utilising the recycled powder. This can be achieved if a new recycling powder management practice is implemented. As a result, the manufacturing cost of LS parts can be reduced and the usage of new material can be optimised according to the properties of the recycled powder.

CHAPTER 7

CONCLUSION AND FURTHER WORK

7.1 Contributions

The "orange peel" phenomenon which affects fabricated LS parts has been investigated and experimental work related to the deterioration of PA2200 powder in the LS process has been undertaken.

Causes of the "orange peel" phenomenon related to changes in the properties of the LS material, in particular its melt viscosity, due to exposure to high process temperatures have been presented.

A new powder recycling method (PRM), which utilises the used powder and controls the powder quality, has been proposed.

An attempt has been successfully made to reduce occurrences of the "orange peel" texture by optimising the LS process parameters.

7.2 Conclusions

In chapter 2, the technology and applications of Selective Laser Sintering using a Sinterstation 2500 HiQ and an EOSINT P700 and their LS process parameters and materials are reviewed. This is followed by a description of the LS process and PA12 material deterioration.

There is very little information from previously published work on the "orange peel" phenomenon and how the "orange peel" texture affects the microstructure of the LS part. With this background in chapter 3, the effect of the properties of PA12 polymer-based powder such as molecular weight distribution, melting viscosity, and heat of fusion, on the quality of LS fabricated parts affected by the "orange peel" phenomenon is researched. The results of experimental work indicate that the polydispersity, melt viscosity, and part surface finish are correlated. The powder which has higher melt viscosity and lower melting heat becomes liquid more easily and therefore flows better during the sintering process due to a shorter chain molecular structure. SEM micrographs show that the morphology of the external surfaces and cross sections of parts affected by the "orange peel" texture exhibits a very inhomogeneous structure after laser sintering. On the basis of the experimental results, a qualitative LS mechanism has been proposed to describe the "orange peel" phenomenon.

Chapter 4 focuses on an experimental study of the deterioration or ageing of PA12 powder properties in the LS process. The influence of temperature, time, and the number of exposures on these properties is investigated. It has been found that the longer PA12 powder is exposed at higher temperature in the long heating period,

the longer a period of cooling is required. The longer cooling period leads to a longer period in which deterioration may take place. It has been found that PA12 samples with higher MFR experienced faster deterioration due to having a larger amorphous region. The MFR of the samples decreases when they are subjected to higher temperature and longer heating time. The deterioration speed is faster for the first 15 to 20 hours and then gradually decreases during the next 100 hours. The T_m, T_g and T_c temperatures slightly increase for samples subjected to higher temperature and longer heating time. MFR indexing is the recommended method for determining the polymer powder quality due to it effectiveness. Based on the results from the experiments explained in the previous sections, the MFR index was selected as a criterion for the powder "age" evaluation for the following reasons:

- MFR testing is a relatively cheap, quick and efficient way of measuring PA12 powder properties;

- MFR is very sensitive to powder deterioration;

- MFR is directly correlated with the PA12 material morphology and other thermal properties.

However, skills are needed to conduct the test and time is required for the cleaning process. DSC is useful for thermal analysis to study the thermal behaviour of the polymer samples in determining T_m, T_g and T_c. The limitation of DSC is that T_g is not clearly apparent from the DSC curve if the polymer sample is highly crystalline.

Gel Permutation Chromatography (GPC) is one of the common methods that can be used to determine the M_w and M_n of a semi-crystalline polymer. This method

separates the molecules based on their size. A higher $M_{\overline{w}}$ and $M_{\overline{n}}$ means shorter chain segments with lower viscosity. A challenging aspect of determining powder deterioration in the LS process is that the different LS machines have different process capabilities and the different LS powder materials may have different properties, affecting deterioration rate.

Chapter 5 furthers understanding of how the LS process parameters, together with the powder quality, determine the final quality of the produced parts. The DOE approach has been applied successfully in determining the optimum LS process parameters by using deteriorated recycled PA2200 powder. The "orange peel" surface texture is influenced by the variable scan spacing (*SCSP*), as well as by interactions between laser power (*LP*) and laser scan speed (*LSp*); laser power (*LP*) and scanning strategy (*SSt*); and laser scan speed (*LSp*) and scan spacing (*SCSP*). Optimisation of the LS process parameters could improve the part surface quality if the MFR of the recycled powder is 18g/10min-19g/10min or higher. The proposed method does not lead to improvement of the surface quality once the PA2200 powder has badly deteriorated (18-19 MFR or lower). Adding more parameters, including other process parameters such as powder layer thickness and laser scanning patterns, would result in an accurate and useful model for predicting the part surface quality. An increase in the number of levels could be helpful. The effects plots are also useful in obtaining an understanding of surface finish quality in relation to process setting parameter variation. Therefore, the DOE method which has been applied to the PA2200 powder could also be applicable to the DF™ powder.

The advantage of DOE is that it could be used to improve the part surface finish by analysing the effects and interaction of the selected factors. The disadvantage is that it is relatively slow and expensive because it requires the performance of many tests.

Chapter 6 concentrates on the question of maintaining consistent materials quality as a main requirement for achieving consistent part quality and increasing LS process reliability and efficiency. This chapter presents a methodology for improving the different PA2200 powder grades that will ensure consistent and good quality of the LS fabricated parts. A powder recycling method (PRM) is developed to improve on the limitations of current powder recycling practice. It introduces the loose powder collection method from the build; the classification of PA12 powder qualities; a method of utilising used powder to gain better control of used powder quality. For instance, refreshed powder quality after the deteriorated PA12 powder is blended results in a 10% to 50% better powder quality. However, not all grades of powder can be recycled. The results from recycled powder quality consistency graphs suggested that badly deteriorated powder (grade C or < 18 MFR) needed the highest ratio of added better quality powder to achieve the refresh powder target of 28MFR (grade B5). The eventual benefit of this study is to utilise the deteriorated recycled PA12 so as to reduce the material cost and produce a better part surface quality. The RPM method which was applied to the PA2200 powder could also be used for the DF™ powder.

7.3 Future work

It is important to predict the temperature distribution and its effects on powder deterioration in the LS process by using a simulation model. It is useful to collect loose powder of acceptable quality from different positions in the build chamber as proposed in chapter 6. The PRM will be more efficient and practical if LS machine users could determine regions of the build chamber with less powder deterioration. As a result, powder of acceptable quality would be more fully utilised due to the fact that its location is known. This can be achieved by developing a Finite Element simulation model. The method undertaken in model development might be mainly focused on specifying temperature changes expected to reflect those experienced during LS processing. Mathematical equations could be developed in order to predict temperature changes experienced at different points in a build during processing. This takes into consideration the fact that temperature distribution in both liquid and solid phase through the LS process causes the powder deterioration which leads to the "orange peel" phenomenon. Once the model has been developed, the density of solid parts could also be predicted.

It is suggested that properties of the used powder (grade B and grade C) may be improved by using special additives and plasticisers. As described in chapter 4, the results of this research show that the more badly deteriorated is the powder the higher is the degree of chain entanglement due to the longer molecular chains. This significantly increases the melt viscosity, leading to the "orange peel" phenomenon. For this reason, it is suggested that special additives are mixed into used powder. This would shorten the molecular chains which could reduce the

degree of chain molecular entanglement, in turn lowering the melt viscosity and

giving the desired high MFR values.

Appendix 1

Polymers and polyamides

3.1 Preliminaries

Polymers are important engineering materials for many reasons. One of the most popular, high demanding and widely used polymer is polyamide. It was originally the name given and discovered by Carothers W.H of Du Pont Co. in 1934 [Kohen, 1995]. Nowadays, there are many types of PA group of polymers available in the market under the heading of "Nylon". They become the key component of current polymer research and technology, because of the diversities of properties and their applications. The variations in properties are largely associated with the chain flexibility, the interchain attraction, and the regularity of the molecular chain factors which determine whether a polymer is glassy, rubbery, or liquid. This makes thermoplastic material can be heated to a soft condition and then reshaped before cooling.

The work presented in this thesis focuses on polyamide 12 based material known as PA2200 of EOS. In the LS process, the PA2200 polymer powder in the bed part cylinder goes through extreme changes temperature causes its transform phase transitions results in changes physical and thermal properties of the polymer. In following sections, brief descriptions of thermal properties are presented. In addition, an attempt is made to show how such properties are influenced when the temperature of the polymer is changed.

The classification of polymers

Polymer builds up from numerous smaller molecules or monomers through the polymerisation process. There are many types of polymers with the different properties and applications. In general polymers can be categorised into three main groups namely as thermoplastics, thermoset and elastomers is illustrated in Figure A1.1[Belofsky, 1995 and Callister, 2005].

```
          ┌─────────────────────────────┐
          │  Classification of Polymers │
          └─────────────────────────────┘
     ┌──────────────┼──────────────┐
┌──────────────┐ ┌──────────────┐ ┌──────────────┐
│Thermoplastics│ │  Thermosets  │ │  Elastomers  │
└──────────────┘ └──────────────┘ └──────────────┘
```
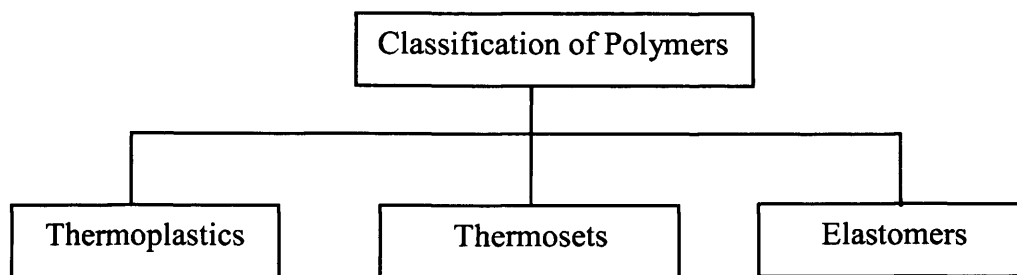
Figure A1.1 Classification of polymers

Chain structure of polymers consists of branch, liner and cross link. Branch polymers have long chain polymers could have similar type A monomer, different types of AB monomers, block AABB or draft liner ABBBABAA. Polymer with similar of monomer known as homopolymer and polymer with different types of monomers or repeating units identified as copolymer.

Thermoplastics refer those polymers, which melt when heated, and resolidify when cooled for examples polyamides (PA), polypropylene (PE), and PVC. They are various types of polyamides, but they tend to have similar physical properties. These include high impact strength, toughness, flexibility, and abrasion resistance due to the linear molecular chain structure [Crawford, 1990].

On the other hand, thermosets refer to polymers which have an extensive three-dimensional network of covalent chemical bonding for example melamine and epoxy. Elastomers refer to cross link chain structure for example rubber.

The structure of polyamides molecules

PA is an important group of thermoplastic polycondensates. The amide group (-NHCO-) can be obtained by polymerization of lactams (polylactams) or by condensation of diamines with dicarboxilic acides. All PA group is semi-crystalline thermoplastics. PA consists of repeating unit or mer are joined end to end in single flexible long chain by the additional polymerisation process. It has a very long main chains of carbon covalently bonded together. Chemical structure of polyamides and bonding consists of the amide group CONH, hydrogen bond, covalent bond (primary), van der wall (secondary) [Kohan ,1995]. The existing of (carbon) amide groups (-CO-NH-) in polyamides are responsible for the formation of hydrogen bonds between molecular chains (primary) and van der wall (secondary). The hydrogen bonds contribute to the crystalline region polymers which influence the strength and melting temperature of polyamides.
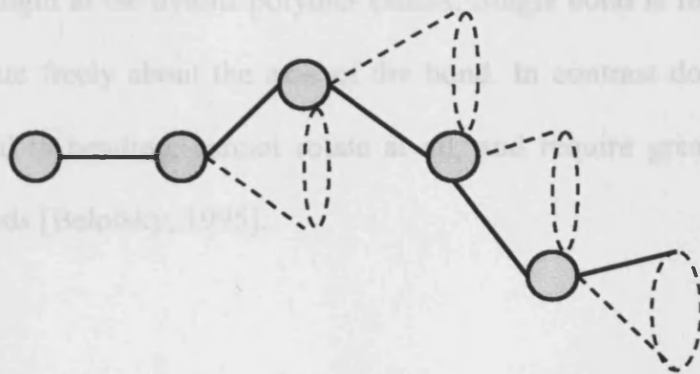
Figure A1.2 The molecules orientation influence by the thermal vibration [Callister, 2005]
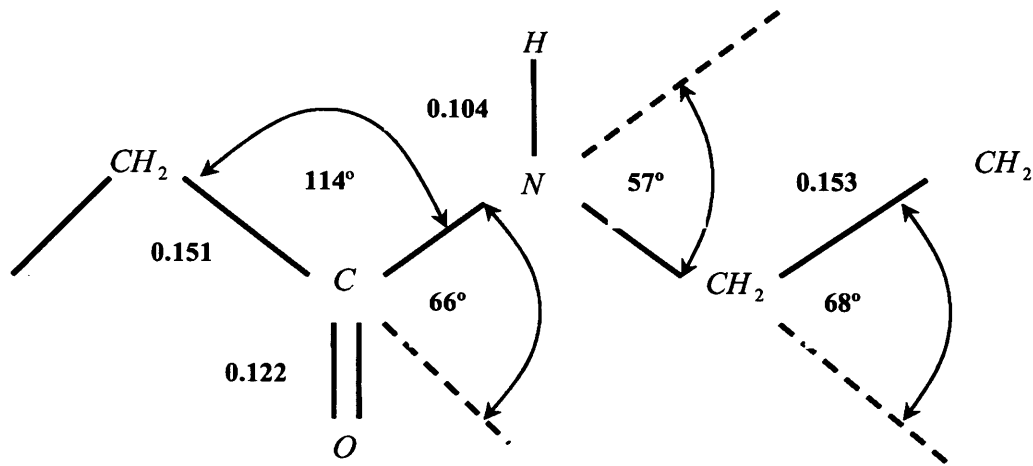
Figure A1.3 The structure of amide group in PA [Kohen, 1995]

The molecules chains orientations are subject to heat. At higher temperature above the glass transition temperature (T_g), it becomes higher mobility in brown motion due to kinetic energy of thermal vibration. The single chain bonds are capable to rotate, twist, and bend in the manner as illustrated in Figure A1.2 and Figure A1.3.

As shown in Table A1.1 show the carbon-carbon bonds are the primary source of strength in the nylons polymer chains. Single bond is flexible in bending and can rotate freely about the axis of the bond. In contrast double bonds are relatively rigid in bending, cannot rotate at all, and require greater energy to disrupt the bonds [Belofsky, 1995].

Table A1.1 Lengths and dissociation energies for primary and secondary bonds

Bonding elements	Bond length (Å)	Bond energy (kJ/mol)
C-C	1.54	348
C=C	1.35	611
N-H	1.01	368
C-O	1.43	360

The flexibility and the chemical molecules structures are the key factors of the ability molecules to orientate. This leads to change the polymer characteristics, for example some of the mechanical and thermal properties of the PA12.

Thermal properties of the semi crystalline polymers

Each polymer displays unique thermal behaviour, the most important characteristics that determine the application of thermoplastic polymers in the LS process are T_g, T_m and T_c [Gibson and Shi, 1997]. This due to the polymer powder experience changes transition phases through the LS process cause changes its properties. This section describes the thermal behaviour of semi crystalline polymers which is commonly used to determine and to investigate the thermal history of materials. This can be done by monitoring the heat flow as a function of temperature phase transitions.
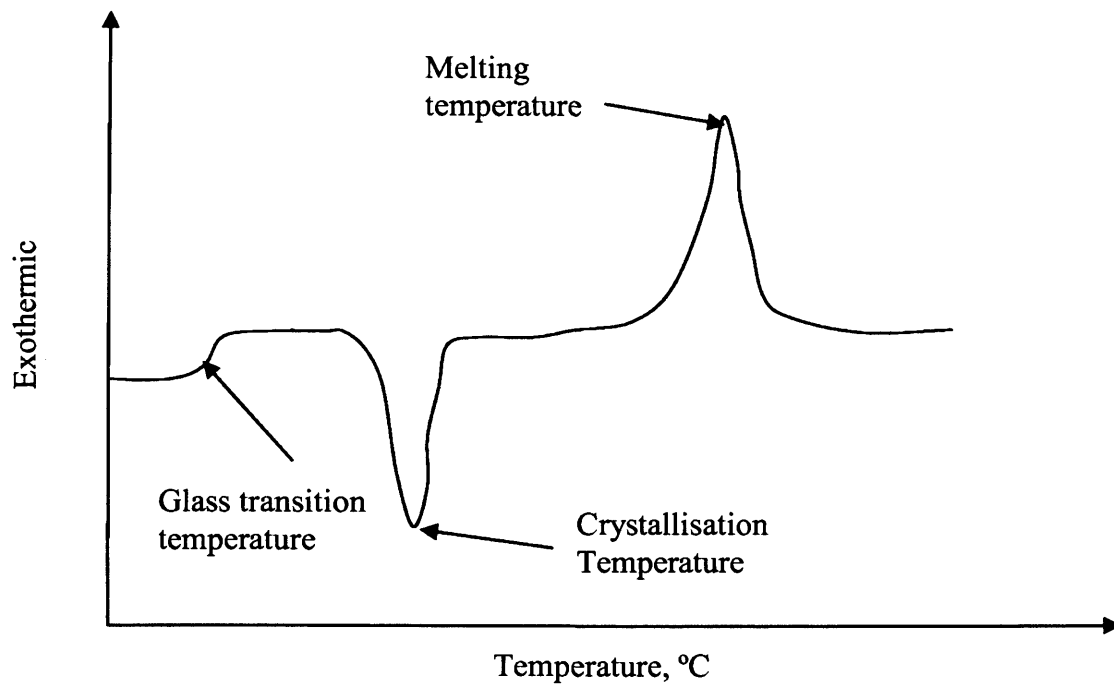
Figure A1.4 Phase transformation of semi-crystalline PA [Salmoria et.al., 2007]

Glass transition temperature (T_g)

At the ambient temperature, the amorphous regions are solid, the polymer is in a glassy state which causes it is very hard and brittle where the modulus remains high [Van Vlack, 1989]. T_g takes place in amorphous region of semi-crystalline polymers [Mangonon, 1999]. It occurs due to increase the motion of large segment motion of molecular chains as it is being slowly heated from below T_g.

As shown in Figure A1.4, when certain amount of heat is applied causes the temperature increase, there will be a point where the behaviour of the polymer rapidly changes due to broken of van der wall bonds. At this point, the mechanical behaviour of the polymer changes from glassy and brittle becomes less rigid and rubbery [Ian Gibson et al., 1997]. However the crystalline regions are maintained due to stronger covalence bonds which gives the polymer adequate strength and softened amorphous regions provide it with toughness [Potsch and Micheali, 1995

and Crawford, 1990]. This sequent of events occurs in the reverse order when a reduction of temperature or upon cooling from leathery to rubbery then to solid material.

Melting temperature (T_m)

As illustrated in Figure A1.4 if the polymer sample is keep heated thus allowing for significant increases in chain mobility as temperature above T_g, it will reach to another thermal transition know as melting point (T_m). At this point a polymer crystal corresponds to the transformation state from solid to liquid the due to polymer crystals melt and flow under very low pressure. The DSC yields important information about the transition such as latent heat or a relatively abrupt change in heat capacity. This can be seen the peak breadth is primarily related to the size and degree of perfection of the polymer crystals [Cogswell, 1981]. In case of LS process, sintering occurs when the powder is heated above the T_m. To large extent the factors which determine the T_g also determine the T_m. These two temperatures takes place over a range of temperatures and their behavior depends on the following factors [Callister, 2005 and Brydson, 1999];

- Thermal history of the powder- the longer the PA12 expose at high temperature, the longer cooling time, this significantly influence the formation of highly ordered molecular structure.

- Group attached to the backbones which increase the energy required for rotation.

- Chain stiffness- the presence of the NH group to form strong hydrogen bonds (H-bonds) with the CO group leads to significant intermolecular bonding forces an relatively high T_m

- Lamellae thickness-the thickness of chain-folded lamellae will depend on T_c, the thicker the lamellae the higher T_m

- Molecular weight (M_w)- The higher M_w, the less ease of movement and more restriction in overall molecular freedom

Crystallisation Temperature (T_c)

The crystallisation of a polymer crystal corresponds to the transformation of a viscous liquid to solid phase. At T_c the polymer starts to solidify in which no order molecule chains becomes the ordered structure of aligned molecular chains in highly random then the crystal structural is formed due to heat given off. The ability of a material to crystallise depends on the regularity of its molecular structure. The longer cooling rate causes the more efficient packing of the polymer chins leads to significant shrinkage and degree of crystallinity. This influences the mechanical and thermal properties of this material. For this reason the structure and properties of a given polymer will very much depend on the way crystallisation has taken place [Potsch and Michaeli, 1995].

Polymer crystallinity

PA12 crystalline region is form due to the presence of spherulites or high degree entanglement of the molecular chains. It may vary in size from frictions of a micron to several millimetres in diameter, depending on the cooling rate from the melt [Crawford, 1990]. If the polymer melt is cooled very quickly it may undercool, for instance remain molten at melting point. This result a plenty of nucleation sites becoming available. The solid polymer will then consist of a large number of small spherulites. The feature of long chain molecules as described in section 4.2.

Effects of molecular factors in viscous flow properties

The properties of polymers are strongly dependent on their temperatures. During the LS process molecules in the melted polymer flow in a non-Newtonian manner and tend to line up in the direction of flow [Van Wazer et al., 1963; Shearman, 1970 and Barnes, et al., 1998].

Viscous flows

A further important property of polymers, also strongly dependent on their temperatures, is their response to the application of a force, as indicated by two main types of behaviour: elastic and plastic. In polymer materials, flowing is takes place, much like viscous liquid. The viscous flow behaviour of the polymer plays a key feature in the LS process. This because the powder experience the phase transition by laser beam scanning. The viscosity of the fluid can be measured by the ratio of the shearing stress to the velocity gradient [Bourell and Beaman, 2005].

$$\eta = \frac{\tau}{\gamma}$$

Where η is the viscosity, τ - a shear stress and γ - a shear strain.

The study of deformation and flow of molten polymer under the influence of an applied stress can be measured using a kind of viscometer known as melt flow indexer device [Rides 2002.; Potsch and Micheali, 1995]

Appendix 2

Publications

D.T.Pham , K.D.Dotchev , W.A.Y Yusoff, Explanations of the "orange peel" phenomenon in the laser sintering process (LS), **Proceedings of the Institution of Mechanical Engineers**, Part B: Journal of Engineering Manufacture.

(Final preparation for submission)

D.T.Pham , K.D.Dotchev , W.A.Y Yusoff, Deterioration of Polyamide Powder Properties in the Laser Sintering Process, **Proceedings of the Institution of Mechanical Engineers**, Part B: Journal of Engineering Manufacture.

(Final preparation for submission)

D.T.Pham , K.D.Dotchev , W.A.Y Yusoff, Improvement of powder management and recycling in laser sintering (LS), **Proceedings of the Institution of Mechanical Engineers**, Part B: Journal of Engineering Manufacture.

(Final preparation for submission)

D.T.Pham , K.D.Dotchev , W.A.Y Yusoff, Improvement of part surface finishing in Laser Sintering by experimental design optimisation (DOE), **3rd Virtual International Conference on Innovative Production Machines and Systems (I*PROMPS)**, 2nd-13th July 2007, Cardiff, United Kingdom.

(Accepted)

K.D.Dotchev , D.T.Pham , W.A.Y Yusoff , S.Soe, Investigation on polyamide powder properties deterioration and efficient powder recycling in Laser Sintering, **3rd International Conference on Advanced Research in Virtual and Rapid Prototyping**, $24^{th} - 29^{th}$ September 2007, Leira, Portugal.

(Accepted)

References

Ajoku U, Saleh N, Hopkinson N, Hague R and Erasenthiran (2006) Investigating mechanical anisotropy and end-of-vector effect on laser-sintered nylon parts, **Proceedings of the Institution of Mechanical Engineers**, Part B: Journal of Engineering Manufacture, Vol.220, No.7, pp 1077-1086.

Badrinarayan B and Barlow J W (1995) Effect of processing parameters in SLS of Metal-Polymers, **Proceedings of Solid Freeform Fabrication Symposium**, Austin, Texas, pp 55-63.

Barnes H A, Hutton J F and Walters K W (1998) **An introduction to Rheology**, Elsevier, ISBN 0-444-87140-3.

Beaman J J, Barlow J W, Bourell D L, Crawford R H, Marcus H L and Mc Alea K P (1997) **Solid Freeform Fabrication**: A New Direction in Manufacturing, Kluwer Academic Publishers, Dordrecht, The Netherlands, ISBN 0 7923 9834 3.

Badrinayaran and Barlow J W (1995) Effects of Processing Parameters in SLS of metal-polymer powders, **Proceedings of Solid Freeform Fabrication**, Austin, Texas, pp 55-63.

Belofsky.H (1995) **Plastics: Product Design and Process Engineering**, Hanser. ISBN 3-446-17417-6.

Bourell D L and Beaman J J (2005) 2nd **International Conference on Advanced Research in Virtual Research and Rapid Prototyping**, Portugal

Bower D I.(2002) **An Introduction to Polymer Physics**, Cambridge University Press, ISBN 0-521-63721-X.

Brydson J (1999) **Plastics Material**, Butterworth Heinemann, 7th editions, United Kindom. ISBN-10: 0750641320

Callister W D (2005) **Fundamentals of Materials Science and Engineering**, 2nd, John Wiley & Sons Inc. ISBN 978-0-471-74477-1

Caulfield B, McHuge P E and Lohfeld S (2007) Dependence of mechanical properties of polyamide components on build parameters in the SLS process, **Journal of Materials Processing Technology**, Vol.182, Issues 1-3, pp 477-488.

Choren J , Gervasi V, Herman T, Kamara S and Mitchell J (2001) Selective Laser Sintering (SLS) powder life, **Proceedings of Solid Freeform Fabrication**, Austin, Texas, pp 39-45..

Chua C K and Fai L K (1997) **Rapid Prototyping**: Principles and applications in manufacturing, John Wiley & Sons. Inc,ISBN 0-471-19004-7.

Cogswell F N (1981) **Polymer Melt Rheology**, A Guide for Industrial Practice, John Wiley&Sons. ISBN 0-470-27102-7.

Coleman E D ,Montgomery C D (1993) A Systematic Approach to Planning for a Design Industrial Experiment, **Technometrics Journal**, Vol.35, No.1, pp 1-26.

Cooper K G, **Rapid Prototyping Technology, Selection and Application**, Marcle Dekker, Inc, 2001.0-8247-0261-1.

Crawford R J (1990) **Plastics Engineering**, 2nd editions, Pergamon Press. ISBN 0-08-032626-9.

Das S B, Wohlert M, and Bourell D (1998) Direct Laser Freeform Fabrication of High Performance Metal Components, **Rapid Prototyping Journal**, Vol 4, No 3, pp 112-117.

David A (2001) The use of statistical experimental design for PCB process optimisation, **Circuit World**, Volume 27, No 4, pp 12-15.

Dean A (2005) EOSINT P Series, **Prototype**, The dedicated Journal for Prototyping and direct manufacturing.

Dean Y (1995) **Materials Technology**, Longman, pp 151-158. ISBN 0-582-21259-6

Deng X, Zong G, and Beaman J J (1992) Parametric analysis for the Selective Laser Sintering of a sample polymer system, **Proceedings of Solid Freeform Fabrication**, Austin, Texas, pp 102-109.

Determination of the melt flow rate (MFR) and the melt volume rate (MVR) of Thermoplastics, **ISO1133 Standard**.

Desktop Engineering, http://www.deskeng.com/Articles/Hardware-Review/Parts-from-Powder-200612121522.html, Parts from Powder [Accessed 15th February 2006].

Determination of average molecular mass and molecular mass distribution of polymers using Gel Permeation Chromatography (GPC), **ISO16014 Standard**.

Dewidar M and Dalgarno K W (2001) Direct selective laser sintering of high-speed steel, **17th National Conference on Manufacturing Research**, pp 181-186.

Dimov S S, Pham D T, Lancan F and Dotchev K.D (2001) Rapid tooling applications of the laser sintering process, **Rapid Prototyping Journal**, Vol.4, No.4, pp 296-302.

Dickens P M and Keane J N (1998) Rapid manufacturing, **Prototyping Technology International '98,** pp 209-212.

Dochev K and Soe S (2006) Rapid Manufacturing of patterns for investment casting: improvement of quality and success rate, **Rapid Prototyping Journal,** Vol 12, Issue.3, pp 156-164.

DTM (1996a) **The Sinterstation$^@$ System 2500,** Guide to Materials for Nylon Compounds; DTM Corporation. DCN:8001-10003.

DTM (1998b) **DTM 2nd European User Group Meeting** Leuven, Belgium, Rapid Steel 2.0, 7-8 October 1998.

DTM Product information-Rapid Tool 2.0 Material (1998c) **DTM GmbH,** OttoHahn –Str.6, D-40721 Hilden.

DTM Product information (1998d) Copper Polyamide Mold Insets for Plastic Injection Moulding, **DTM Corporation,** June, 81611 Headway Circle, Building 2, Austin, TX.

DTM SandForm material fuels development of new aircraft engine part for Woodward Governor company (1998e) **Horizons,** newsletter published by DTM.

3D System Corporation, www.3dsystems.com, [Accessed 15th February 2007].

Effier P Jand Saal J D (1997) Prototyping: a design chain integration perspective, **Prototyping Technology International '97,** The International Review of Simulations-Based, Rapid Prototyping & Manufacturing, UK& International Press, United Kingdom, pp 23-25.

EOS, Electro Optical Systems GmbH, www.eos-gmbh.de, [Accessed 15th February 2007.]

Ellekjaer M.R, (1998) The use of experimental design in the development of new products, **International Journal of Quality Science**, Vol 3, No 3, pp 254-274.

Forderhase P, Mc Alea K, Michelewicz M, Ganninger M, and Firestone K(1992) SLS prototypes from nylon, **Proceedings of Solid Freeform Fabrication Symposium**, Austin, Texas pp 102-109.

Fritz F (1998) Laser sintering on its way up, **Prototyping Technology International '98,** pp 186-189.

Gale L (1997) RP past and present, **Prototyping Technology International '97,** The International Review of Simulations-Based, Rapid Prototyping & Manufacturing, UK& International Press, United Kingdom, pp 12-14

Ghanekar A and Crawford (2003) Optimisation of SLS Process Parameters using D-Optimality, **Proceedings of Solid Freeform Fabrication**, Austin, Texas, pp 348-361.

Gololewski E, Czerniawska K, Gasiorek M (1980) **Colloid Polymer Science,** Vol.258, pp 1130-1136.

Gornet T J (2002) Characterisation of Selective Laser sintering TM to Determine Process Stability, **Proceedings of Solid Freeform Fabrication,** Austin, Texas, pp 546-553.

Gornet T J (2002) Improving Selective Laser Sintering Consistency, **CAD/CAM Publishing,** pp-1-3 .

Ghany K A and Moustafa S F (2006) Comparison between the products of four RPM systems for metals. **Rapid Prototyping Journal,** Vol.12, Issue 2, pp 86-94.

Gibson,I. and Shi (1997) Material Properties and Fabrication Parameters in SLS, Process, **Rapid Prototyping Journal**, Vol 3, No 4, pp 129-136.

Guo and Suiyan (1996) Optimizing of Selective Laser Sintering; Laser Processing of Materials and Industrial Applications. **Proceedings of SPIE The International Society for Optical Engineering**, Beijing. Vol 2888, pp 389-391.

Hatakeyama T and Liu Z (1999) **Handbook of Thermal Analysis**, John Wiley & Sons, ISBN 1418-2874.

Hardro P J, Wang J H, and Stucker B E (2004) A design of experiment approach to determine the optimal process parameters for rapid prototyping machines, **Proceedings of Solid Freeform Fabrication**, Austin, Texas, pp 1-20.

Hedge R R., Kamath M G. and Dahiya A. Polymer Crystallinity, **Material Science** Lecture Notes, pp 1-17.

http://www.engr.utk.edu/mse/pages/Textiles/Polymer%20Crystallinity.htm-last [Accessed on 22nd April 2006].

Ho H C, Gibson I and Cheung, L W (1999) Effects of energy density on morphology and properties of selective laser sintered polycarbonate, **Journal of Materials Processing Technology**, Vol.89, pp 204-210.

Ho H C, Gibson I and Cheung W L (2000) Effects of Energy density on Bonus Z , surface roughness and warpage of SLS sintered Polycarbonate, **Rapid Prototyping, 9th International Conference**, Tokyo Japan, June 12-13, pp 99-103.

Hopkinson N, Hauge R and Dickens P (2006) **Introduction to Rapid Manufacturing**, an industrial revolution for the digital age. ISBN 13 978-0-470-01613-8.

Jiji A (1998) Some key things industrial engineers should know about experimental design, **Journal of Logistics Information Management**, Vol 11, pp 386-392.

Kai C C, Chou S M and Wong T S (1998) A study of the state of the Art Rapid Prototyping Technologies, **The International Journal of Advanced Manufacturing Technology**, Vol 14, pp 146-152.

Kimble. L.L (1992) The materials advantage of the Selective Laser Sintering process, **Proceedings of Solid Freeform Fabrication Symposium**, Austin, Texas, pp 212-219.

King D and Tansey T (2003) Rapid Tooling: selective laser sintering injection tooling, **Journal of Materials Processing Technology**, pp 42-48.

King D and Tansey T (2002) Alternative for Rapid Tooling, **Journal of Materials Processing Technology**, Vol 121, pp 313-317.

Kohan MI (1995) **Nylon Plastics Handbook**, Hanser. ISBN 3-446-17048-0

Kruth J P, Wang X, Laoui T, and Froyen L (2003) Laser and materials in selective laser sintering, **Rapid Prototyping Journal**, Vol 23, No 4, pp 357-371.

Lacan F (2000) Capabilities of the RapidTool process, **PhD thesis**, Cardiff University.

Lauwers B, Kruth J P, Froyen L, Bonse J and Morren B(1998) Hard metal parts by SLS, **Prototyping Technology International '98**, pp 124-126.

Levy G N and Schindel (2002) Overview of layer manufacturing technologies, opportunities, options and applications for rapid tooling, **Proceedings of the Institution of Mechanical Engineers**, Part B: Journal of Engineering Manufacture, Vol 216, pp 1621-1634

Mangonon P.L (1999) **The principles of materials selection for engineering design**, Prentice Hall. ISBN 0-13-242595-5.

Mantia F L (2002) **Handbook of Plastic Recycling**, Rapra Technology Limited, ISBN 1-85957-325

Marit R E (1998) The use of experimental design in the development of new products, **International Journal of Quality Science**, Vol 3, No 3, pp 254-274.

Martin J (2006) **Materials for engineering**, 3rd editions, Woodhead publishing in materials, pp159-184, ISBN10-0-84938780-9

Martin R, Crispin A and Angela D (2001) Multi-rate and Extensional Flow Measurements using the Melt Flow Rate Instrument: Measurement Good Practice Guide, **National Physical Laboratory**.

Martin R, Crispin A and Angela D (2002) Improved melt flow rate measurements: an industrial case study, Measurement note, **National Physical Laboratory**.

Materialise Belgium, www.materialise.com, New EOSINT P700 machine and Alumide material [Accessed 18th September 2006].

Mc Alea K, Booth R, Foderhase P, and Lackminarayan U (1995) Materials for Selective Laser Sintering Process, **International SAMPE technical conference**, Vol 27, pp 949-961.

Mazzoli A, Moriconi G, and Pauri M G (2006) Characterisation of an aluminium-filled polyamide powder for applications in selective laser sintering, **Journal of Materials and Design**, pp1-8.

Metalworking Production magazine, http://www.mwponline.com, Laser-sintering for series production [Accessed 11th September 2006].

Michael S (1998) New RP Material from EOS Rapid Prototyping, **Electronic Mailing List**, http://rapid.lpt.fi/rp-ml-1998/2284.html [Accessed 11th September 2006]

Moen D R, Norlan W T and Provost P L (1991) **Improving Quality Through Planned Experimentation**, McGraw-Hill, ISBN 0-07-100837-3.

Montgomery C D (2000) **Design and Analysis of Experiments**, Wiley,5th edition, ISBN 0471316490.

Murphy J, Lappo K, Wood K, Beaman J J (2002) Statistical Model of Laser Surface Finishing using Design of Experiments, **Proceedings of Solid Freeform Fabrication**, Austin, Texas, pp 585-593.

Naim J (2001)**Phd thesis**, Finite Element Analysis of Curl Development in the SLS process, Leeds University.

Neal P J (1994) Rapid Prototyping Using the Selective Laser Sintering Process, **Rapid Prototyping Journal**, Vol 14, No 2, pp 14-17.

Nelson J C and Barlow J W (1992) Relating operating parameters between SLS machines which have different scanner geometries and laser spot sizes, **Proceedings of Solid Freeform Fabrication**, Austin, Texas, pp 228-235.

Odonnchadha B and Tansey A (2004) A note on rapid composite tooling by selective laser sintering, **Journal of Materials Processing Technology**, pp 28-34.

Pham D T, Dimov S.S and Gault R.S (1997) RP past and present, **Prototyping Technology International '97**, The International Review of Simulations-Based, Rapid Prototyping & Manufacturing, UK& International Press, United Kingdom, pp 15-19.

Pham D.T, Dimov S.S and Gault R.S (1998) Laser sintering on its way up, **Prototyping Technology International '98**, pp 196-202.

Pham D.T, Dimov S.S and Lacan F (1999) The RapidTool process: Selective Laser Sintering: Applications and Technological Capabilities, **Proceedings of the Institution of Mechanical Engineers**, Part B: Journal of Engineering Manufacture, Vol. 213, No 5, pp 435-449.

Pham D T, and Dimov S S, (2000) **Rapid Manufacturing**, The Technologies & Applications of Rapid Prototyping & Rapid Tooling, Springer, ISBN 1-85233-360-X.

Pham D T, and Dimov S S, (2003) **Rapid Prototyping and rapid tooling – the key enablers for rapid manufacturing, Proceedings of the Institution of Mechanical Engineers**, Part B: Journal of Engineering Manufacture, Vol. 217, No 1, pp 1-24.

Plastics- Differential Scanning Calorimetry (DSC), **ISO 11357 Standard.**

Potsch G and Micheali W (1995) **Injection Moulding**, Hanser publishers, ISBN: 1-56990-193-7.

Potts A (1998) Real prototypes at realistic cost, **Prototyping Technology International '98**, pp 204-208.

Salmoria G V, Leite J L, Ahrens C H, Lago A and Pires A T N (2007) Rapid manufacturing of PA/HDPE blend specimens by selective laser sintering : Microstructural characterisation, **Journal of Polymer Testing**, pp1-8

Shearman P (1970) **Industrial Rheology**, Academic Press, pp 33-40, ISBN:12-639950-6

Stephen Z D, Christopher Y L, Bret H C. Lei Z and William W Z (2000) Thermal analysis: the next two decades, **Thermochimica Acta**, Vol 355, pp 59-68.

Shi Y, Li Z, Huang S and Zeng F (2004) Effects of the properties of the polymer materials on the quality of selective laser sintering parts, **Proceedings of the Institution of Mechanical Engineers**, Part B: Journal of Engineering Manufacture, Vol 214, No 6, pp 247-249.

Shi Y, Li Z, Sun H, Huang S and Zeng F (2004) Development of a polymer alloy of polystyrene (PS) and polyamide (PA) for building functional part based on selective laser sintering (SLS), , **Proceedings of the Institution of Mechanical Engineers**, Part B: Journal of Engineering Manufacture, Vol.218, No.5, pp 299-306.

Stacey Au and Paul K.Wright (1993) A Comparative study of Rapid Prototyping Technology, **Proceedings of Solid Freeform Fabrication**, Austin, Texas ,pp 73-82.

Stierlen P, Keller B, Shen J and Eyerer P (1997) Developments in SLS technology, **Prototyping Technology International '97**, The International Review of Simulations-based, Rapid Prototyping & Manufacturing, UK& International Press, United Kingdom, pp 153-155.

Ryan A Y, Fairclough P A, Terril N J, Olmsted P D and Pooh W C K (1999)

Scattering study of nucleation phenomenon in polymer crystallisation, **Royal Society of Chemistry**, No 112, pp 13-29.

Steve U and Richard F (2003) Rapid prototyping technologies, **Journal of Rapid Prototyping**, Vol 23, No 4, pp 318-330.

Theodore L, Bergman, and David L B (1996) Materials and Materials Processing, **WTEC Rapid Prototyping Report**.

Thermo Haake (2000) Meltflow Indexer 2000, Thermo Haake Scientific.

Tontowi A E and Childs T H (2001) Scanning Electron Microscope of a Glass-Filled Crystalline polymer sintered part, ISTECS Europe, **Proceedings 6th ISSM**, pp 1-4.

Usher S J and Srinivasan K M (2000) Quality improvement of Selective Laser Sintering process, **Journal of Quality Engineering**, pp 161-168.

Van Wazer J R, Lyons J W, Kim K Y, Colwell R E (1963) **Viscosity and Flow Measurement**, Interscience publishers.

Wahab M S, Dalgarno K W and Cochrane (2006) Processing of A Polyamide/Yttrium stabilised Zirconia nanocomposite using the Selective Laser Sintering, **7th conference on Rapid Design, Prototyping and Manufacture**, pp 21-28.

Walter K, Bart V, Hessel M and Nico K (2006) Design for Rapid Manufacturing functional SLS parts, **Innovative Production Machines and Systems Conference**, pp 389-394.

William F S (1993) **Foundations of Materials Science and Engineering**, 2nd editions, ISBN 0-07059202.

Wohlers Report (2005) An in-depth worldwide progress report on the Rapid

Prototyping, tooling, and manufacturing state of the industry, **Annual**

Worldwide Progress Report, Wohlers Associates Inc.

Wholers T (2000) Executive Summary, **Worldwide Progress Report**,

Wohlers Associates Inc.

Wholers T (1999) Rapid Prototyping & Tooling State of the Industry,

Executive Summary, **Worldwide Progress Report,** Wohlers Associates Inc.

Vinay S, Kristin W, Davis B, Beaman J J (2003) Selective Laser Sintering of

Duraform Polyamide™ with small-scale features, **Proceedings of Solid**

Freeform Fabrication, Austin, Texas, pp 585-605.

Young R J (1983) **Introduction to Polymers**, Chapman and Hall, pp185,

ISBN 0-412-221802.

Zarringhalam H, Hopkinson N, Kamperman N F, and Vlieger. D J J (2006)

Effects of processing on microstructure and properties of SLS Nylon 12,

Journal of Materials Science & Engineering, pp 172-180.